ELECTRONIC SURVEYING INSTRUMENTS

A Review of Principles, Problems and Procedures

J. M. RÜEGER

MONOGRAPH 18

SCHOOL OF SURVEYING AND SPATIAL INFORMATION SYSTEMS

THE UNIVERSITY OF NEW SOUTH WALES UNSW SYDNEY NSW 2052 AUSTRALIA

J. M. Rüeger

Electronic Surveying Instruments

A Review of Principles, Problems and Procedures

First Edition

Reprint 2010

With 81 Figures and 6 Tables

Monograph 18
School of Surveying and Spatial Information Systems
The University of New South Wales
UNSW SYDNEY NSW 2052
Australia

Published by
School of Surveying and Spatial Information Systems
The University of New South Wales
UNSW SYDNEY NSW 2052
Australia

Received October 2003

First published: November 2003
Reprinted with corrections: October 2010

National Library of Australia
Card Number and ISBN
0-7334-2083-4

Preface

The field equipment used in daily surveying practice has changed considerably over the last 15 to 20 years of the 20th century. The traditional optical-mechanical instruments gave way to the newer electro-optical-mechanical devices. The new technology was not always understood nor were the field procedures always amended to suit it. Sometimes, field procedures were changed incorrectly because of a lack of understanding of the new instrumentation. It is hoped that this text will improve the understanding and use of the electronic equipment that is used today.

This text evolved from more advanced undergraduate and postgraduate courses taught by the author at the University of New South Wales (UNSW, Sydney, Australia) as well as from continuing professional development courses on electronic theodolites and digital (bar code) levels. It covers theoretical and practical aspects of modern field surveying instruments, their operating principles and their differences from traditional (non-electronic) field surveying equipment. Not discussed are methods involving the Global Positioning System (GPS), photogrammetry and remote sensing and the details of electronic data recording and coding. The reader is referred to other textbooks on these topics. The principles of electronic distance measurement (EDM) are not covered either as a modern and detailed textbook is available (Rüeger 1990 1996). Some specialised instruments using EDM, however, are discussed, as is reflectorless distance measurement.

This text was written for readers that had some previous exposure to field surveying. In particular, it is assumed that the reader is familiar with the basic principles and operation of optical theodolites and spirit levels. If not, the reader should consult a standard textbook on surveying and read the chapters on theodolites, levels and on the field operations with such before reading this text. This book suits professionals, who went through tertiary courses before the widespread introduction of electronic surveying instruments, current students who wish to broaden their understanding of

field instruments, and readers of standard textbooks on 'surveying', who are not satisfied with the, usually very limited, information on instruments and procedures provided by these texts.

After an introduction, Chapter 2 introduces a number of hand-held instruments, such as hand-held distance meters, compasses, clinometers (and combinations thereof) as well as different types of electronic barometers. The latter double as altimeters and can be used for heighting.

Chapter 3 discusses digital (bar code) levelling instruments and rotating laser levels. Particular emphasis is placed on the various errors that may occur in levelling with digital levels and laser levels. This chapter also contains useful advice for all professionals involved in precise levelling with digital levels.

Chapter 4 introduces the different types of electronic theodolites and tacheometers, including gyro, laser, tracking, scanning and reflectorless instruments. Electronic circle reading systems and electronic level sensors are discussed in some detail, as are their inherent errors. Some notes on the practical use of these instruments follow.

Chapter 5 presents a number of dedicated instruments or techniques that were developped for specific tasks. Reflectorless EDM is discussed in some detail, highlighting some of the problems that can occur and giving some advice on its use. Laser scanners are mentioned as is the often ignored technique of motorised levelling. The chapter concludes with sections on airborne laser profilers, laser trackers and a laser measurement system. The latter two are employed in metrology.

Exercises are given at the end of each chapter. These exercises are designed to further the understanding of the principles and concepts discussed in the text. The solutions are not provided; they can be worked out from the information given in the text.

Sydney, Spring 2003 J. M. Rüeger

Reprint 2010

The author is greatly indebted to the readers that have communicated errors in the first editions, in particular A. Young. All known errors have been corrected in this reprint of the first edition.

Sydney, Spring 2010 J. M. Rüeger

Contents

1.	**Introduction**	**1**
2.	**Hand-Held Equipment**	**5**
2.1	Electronic Pocket Tapes	5
2.1.1	Ultrasound Sensor	6
2.1.2	Electro-Optical Sensor	7
2.2	Hand-Held Angle-Angle-Distance Devices	8
2.2.1	Fluxgate Compass	10
2.2.2	Clinometers	12
2.2.3	Use of Hand-Held Angle-Angle-Range Devices	13
2.3	Electronic Barometers (and Altimeters)	15
2.3.1	Working Principles	15
2.3.1.1	Vibration Pressure Sensor	15
2.3.1.2	Capacitive Pressure Sensor	17
2.3.1.3	Piezo-Resistive Pressure Sensor	18
2.3.2	Performance of Digital Barometers	19
2.3.3	Heighting with Digital Barometers/Altimeters	20
2.4	Exercises	22
3.	**Levelling Equipment**	**27**
3.1	Digital (Bar Code) Levelling Instruments	27
3.1.1	Introduction	27
3.1.2	How do Digital Levels Differ from Conventional Automatic Levels?	29

3.1.2.1	DC Power	29
3.1.2.2	Staffs	30
3.1.2.3	Electronic Staff Reading and Distance Measurement	30
3.1.2.4	Illumination of Staff	30
3.1.2.5	Compensator	30
3.1.2.6	Optical or Electronic Horizontal Circle	30
3.1.2.7	Electronic Data Recording	31
3.1.2.8	Computer Interface	31
3.1.2.9	Real-Time Correction of Instrument Errors	31
3.1.2.10	On-Board Computing	31
3.1.3	Principle of the Wild NA2000	32
3.1.3.1	Basic Design and Working Principle	32
3.1.3.2	Measuring Sequence	34
3.1.3.3	Signal Processing	35
3.1.3.4	Accuracy of Bar Code Levels	37
3.1.4	Bar Code Staffs	39
3.1.4.1	Leica Normal Bar Code Staffs	39
3.1.4.2	Leica Invar Bar Code Staffs	40
3.1.4.3	Errors of Normal Bar Code Staffs	40
3.1.4.4	Errors of Invar Bar Code Staffs	40
3.1.5	Errors in Precise Levelling with Bar Code (Digital) Levels	40
3.1.5.1	Errors in Bar Code (Digital) Levels	41
3.1.5.2	Errors of Invar Bar Code Staffs	46
3.1.5.3	External Influences on Line of Sight	47
3.1.5.4	Errors of the Observer	48
3.2	Laser Levels	49
3.2.1	Construction of a Rotating Laser Level	50
3.2.2	Design of a Two-Axis Compensator of a Rotating Laser Level	53
3.2.3	Major Errors of Rotating Laser Levels	53
3.2.3.1	Compensation Error	53
3.2.3.2	Adjustment Conditions of Rotating Laser Levels	54
3.2.3.3	Misalignment of Rotating Mirror	55
3.2.3.4	Secondary Height Error	56
3.2.4	Calibration of Rotating Laser Levels	56
3.2.5	Computation of Heights, Earth Curvature and Refraction	57
3.3	Exercises	59
4.	**Electronic Theodolites and Tacheometers**	**65**
4.1	Types of Electronic Theodolites and Tacheometers	65

4.1.1	Electronic Theodolites	65
4.1.2	Electronic Tacheometers	66
4.1.3	Gyro-Theodolites	67
4.1.4	Motorised Electronic Tacheometers	68
4.1.4.1	One-Person-Survey-Systems	70
4.1.4.2	Automatic Monitoring Systems	71
4.1.5	Motorised Electronic Video Theodolites	73
4.1.6	Laser Theodolites	75
4.1.7	Tracking Electronic Tacheometers	76
4.1.8	Reflectorless Electronic Tacheometers	76
4.1.9	Scanning Electronic Tacheometers	77
4.2	Features of Electronic Theodolites and Tacheometers	78
4.2.1	Circle Types	78
4.2.1.1	Incremental Circles	79
4.2.1.2	Quasi-Absolute Circles	80
4.2.1.3	Absolute Circles	80
4.2.2	Diametrical Circle Reading	81
4.2.3	Electronic Level Sensors versus Vertical Circle Compensators	82
4.2.3.1	Definition of an Electronic Level Sensor	82
4.2.3.2	Definition of a Vertical Circle Compensator	82
4.2.4	Data Recording	83
4.2.5	On-Board Computing	84
4.2.6	Power Supply	84
4.2.7	Communication with Personal Computers	85
4.2.8	Automatic Focussing, Searching and Pointing	86
4.2.8.1	Automatic Focussing	86
4.2.8.2	Automatic Searching	86
4.2.8.3	Automatic Pointing	87
4.2.9	Computer Assisted Instrument Calibration	89
4.2.10	Modern Vertical Axis Systems	90
4.3	Circle Reading System of the Electronic Tacheometer Nikon DTM-1	91
4.3.1	Coarse Measurement	92
4.3.2	Fine Measurement	93
4.3.3	Sensing of the Direction of Rotation	95
4.4	Electro-Optical Level Sensors	95
4.4.1	Nikon DTM-1 Single-Axis Level Sensor	97
4.4.2	Leica TPS1100 Series Dual-Axis Level Sensor	97
4.4.3	Kern E2 Dual-Axis Level Sensor	98
4.4.4	Principle of the Determination of the Theodolite's Dislevelment	100

4.5	Properties of Electronic Level Sensors	102
4.5.1	Compensation Error	103
4.5.2	Scale Factor Error	103
4.5.3	Setting Error	104
4.5.3.1	Random Component	104
4.5.3.2	Systematic Component	105
4.5.4	Vertical Circle Index Error and Correction	105
4.6	Circle Graduation Errors	106
4.6.1	Periodic Errors	107
4.6.2	Interpolation Errors	107
4.7	Some Notes on the Use of Electronic Theodolites and Tacheometers	109
4.7.1	Levelling of Electronic Theodolites and Tacheometers	110
4.7.2	Selection of Measuring Unit	110
4.7.3	Use of Umbrella	111
4.7.3.1	Electronic Theodolites	111
4.7.3.2	Electronic Tacheometers	112
4.7.4	Automatic Power-Off	112
4.7.5	Two-Way Radios and Cellular (Mobile) Phones	112
4.7.6	Real-Time Corrections to Measured Data	112
4.7.7	Direction Measurements	113
4.7.7.1	Single-Face versus Dual-Face Measurements	114
4.7.7.2	Sequence of Direction Measurements	115
4.7.7.3	Elimination of Periodic Errors	115
4.7.7.4	Circle Setting	115
4.7.8	Zenith Angle Measurements	116
4.7.9	Simultaneous Direction, Zenith Angle and Distance Measurements	116
4.7.10	Plumbing of Structures	117
4.7.10.1	Plumbing Shafts and Wells	117
4.7.10.2	Plumbing a Building	118
4.8	Exercises	118

5.	**Specialised Equipment**	**121**
5.1	Reflectorless Electronic Distance Measurement	121
5.1.1	Basic Properties	122
5.1.2	Beam Size and Shape	123
5.1.3	Multiple Target Problem	125
5.1.3.1	Pulse Distance Meters	125
5.1.3.2	Phase Measuring Distance Meters	127

5.1.4	Influence of the Material and Colour of Target	128
5.1.5	Target Orientation	128
5.1.6	Measurement to Corners	129
5.1.7	Some Notes on the Use of Reflectorless EDM	130
5.2	Laser Scanners	132
5.3	Motorised Levelling	134
5.4	Laser Profiling and Laser Altimeters	137
5.4.1	Laser Profiling on Land	137
5.4.2	Depth Sounders	139
5.5	Single Beam Laser Trackers for Metrology	140
5.6	Reflectorless Single Station Laser Measurement System	143
5.7	Exercises	144

References **147**

Subject Index **153**

1. Introduction

Surveying technology did change considerably during the last 30 years due to developments in computers, electro-optics and satellite technology, to name just the major influences. It has been stated (Rüeger 1995b) that surveying practice does not make full use of the new (and more efficient and cheaper) opportunities. For reasons of efficiency and economics, electronic data recording and electronic post-processing will be mandatory in any large scale survey such as setting-out, detail and contour surveys. In consequence, a number of field techniques and surveying instruments have become obsolete over the last decades. Rüeger (1995b) discussed these aspects in more detail.

The changes in the surveying instrument market indicate the new technology bought by geomatic engineers and surveyors. For simplicity, the periodical instrument surveys published by the American journal Point of Beginning (POB) are used to show the trends in the purchasing of instruments. Although these surveys reflect the US market, the detected changes would be similar to those in South-East Asia (apart of vernier theodolites, naturally).

In 1982, the journal POB reported 46 optical theodolites and 3 electronic theodolites on the market. Ten years later, POB listed 18 optical theodolites and 16 electronic theodolites. It is unlikely, that optical theodolites will be manufactured very much longer, considering that an increasing number of second hand optical theodolites becomes available.

The journal POB reported 24 electronic distance meters in 1981 and 25 in 1993. Although the number of models did not change in the 12 years, one would expect a significant drop in the numbers sold. POB listed 11 fully electronic tacheometers ('total stations') in 1983 whilst listing 68 different models in 1994. It is obvious that the electronic tacheometers slowly replace stand-alone theodolites and stand-alone distance meters.

As far as tilting and automatic levelling instruments are concerned, 27 were reported by POB in 1984 and 37 in 1994. Six digital (bar code) levels were reported for the first time in 1994. Most noticeable are the 51 different models of rotating laser levels listed in 1994. Although some rotating laser levels did exist in 1984 (but were not included in the POB survey in that year), the number of models has certainly grown significantly over the last ten years. New is that all traditional surveying instrument manufacturers now cater for this market.

The above market surveys demonstrate that the electronic tacheometer has become a universal surveying instrument, replacing theodolites, distance meters and levels. The dumpy levels on building sites are clearly being replaced by the rotating laser levels. Where levelling instruments are still required for special applications, digital (bar code) levels are being used. The market for GPS receivers will grow further once millimetre accuracy can be achieved at the same price, with the same ease and with the same speed as with electronic tacheometers. GPS receivers, however, will never work in buildings, underground and under trees, to give a few examples.

Another trend in instrumentation, which could be documented with the aid of surveys on the purchase of data recorders, is electronic data recording. This goes hand-in-hand with the other trend of using personal computers for the processing of all field data and the production of plans, maps and data bases. In the opposite sense, set-out data are pre-computed in the office and transferred in electronic form to the field instrument for the setting-out. Electronic data capture is essential if data are to be transferred in electronic form from the field to the office or if they are to be processed in the field.

The trend towards one-person-survey-systems should also be noted. For example, the rotating laser levels on building sites are very powerful one-person levelling systems. Robotic electronic tacheometers can find and track (moving) reflectors and can be operated remotely by the surveyor at the reflector. They provide efficient one-person-systems for detail and contour surveys as well as setting-out work. They are also ideally suited for repeated surveys of the same network as, for example, in around-the-clock deformation measurements of unstable terrain and structures.

Electronic distance measurement (EDM) to passive targets (now referred to as 'reflectorless' EDM) has been possible for quite some time. Stand-alone distance meters, able to measure to non-cooperative targets, became available in 1986. Zeiss released the first 'reflectorless' electronic tacheometer ('total station') in 1993. Broad acceptance by the surveying profession followed once Leica, Topcon and Trimble released their reflectorless instruments in 1998, followed by Nikon in 1999. The range of reflectorless EDM depends heavily on the type of surface that is measured to and its orientation to the measuring beam. At the time of writing, 50 - 100 m seem to be typical maximum distances to 'natural' targets.

Laser scanners are another type of instrument that measure distances to passive targets. In this case, the laser beam is deviated vertically and horizontally to scan the surrounding space in a grid pattern. The step interval can be selected. Some instruments can scan around the full circle (360°), others only in a limited sector. The typical results of a laser scan are the x, y, z coordinates of a large number of points 'seen' by the scanner. The precision of these coordinates depends on the precision of the angular measurements (directions, zenith angles) and the precision of the distance measurements. The range and accuracy specifications vary greatly between the different products, from ±0.5 mm at 5 m to ±50 mm at 1000 m at the time of writing.

Geomatic engineers and surveyors must consider the above trends and check if their current operations make the best use of current technology. If not, they may provide slower, more expensive or less sophisticated services to their customers. Also, geomatic engineers and surveyors must ensure that their personnel is competent in the use of the new technology. Although some basic principles of traditional instruments also apply to modern instruments, some new aspects arise. For example, do you know how to calibrate a rotating laser level or the electronic level sensor of an electronic tacheometer? Do you know why it is better to have diametrical circle reading on the vertical circle (rather than on the horizontal circle) of electronic tacheometers or on what kind of survey jobs the dual-axis level sensors (of electronic tacheometers) are most useful? Do you know the properties of the compensators used in automatic levels, digital levels and rotating laser levels? The answer to these and other questions can be found in this text.

2. Hand-Held Equipment

Hand-held instruments are used in many ways in geomatic engineering and surveying. For example, they may provide the traditional angle-angle-distance data with lesser accuracy but faster than electronic tacheometers. Such applications include reconnaissance surveys and surveys in support of land information systems or geographic information systems. On other occasions, a geomatic engineer or surveyor needs to measure short distances fast, such as in the case of building surveys. Finally, the ambient temperature, pressure and humidity is required in the connection with all electronic distance measurements. Electronic instruments are available for all these and other applications. Some types of instruments are briefly reviewed below.

2.1 Electronic 'Pocket Tapes'

The 'electronic pocket tapes' may replace the traditional steel pocket tapes and 30 m steel tapes. They do require a surface for the (passive) reflection of the transmitted beam. Because they measure the average distance to the 'foot print' at the target surface, they work best, if the entire area 'illuminated' by the beam (the 'foot print') is flat and at a right angle to the beam. Measuring to concave or convex corners of walls will not give the true distance. Also, any other objects in the beam between the instrument and the reflecting surface can cause a false reading (too short).

Two types are discussed further, one based on an ultrasound sensor, the other one based on the well-known principle of electronic distance measurement.

2.1.1 Ultrasound Sensor

The *Accutape-S ultrasonic distance estimator* (see Figure 2.1, on left) is one example of an ultrasound sensor. It can measure distances from 0.6 m to 13 m with a resolution of 1 cm or 1 inch. The precision is quoted as ±1% + 1 digit which is equivalent to ±(10 mm + 1000 ppm). It operates between 4°C and 38°C and weighs 57 g. The instruments uses an electro-acoustic transducer (made by Polaroid) to transmit and receive sound waves. The 'flight time' for a pulse to travel to the reflecting surface and back is measured. Knowledge of the speed of sound c permits to compute the distance d as follows:

$$d = \frac{(c \times \text{flight time})}{2} \qquad (2.1)$$

Schwarz (1985) did derive the following equation for the speed of sound c (in m/s):

$$c = 20.0533 \sqrt{\frac{T}{1 - 0.3780\,(e/p)}} \qquad (2.1a)$$

where T is the atmospheric temperature (in kelvin; = 273.15 + t), t is the atmospheric temperature in degrees Celsius (°C), e is the atmospheric partial water vapour pressure (in hPa) and p the atmospheric pressure (in hPa). The speed of sound is 325.30 m/s at –10°C and 354.86 m/s at +40°C, for example.

Figure 2.1: *Accutape-S* ultrasonic distance estimator (on left) and hand-held (electro-optical) laser meter *DISTO* by Leica (on right).

As the speed of sound depends greatly on the density of the medium (air), the *Accutape-S* is temperature compensated. Some systematic errors occur, however, with changes in pressure (altitude) and humidity. Sonic signals are

not reflected by absorbing materials such as curtains, upholstery and carpets. Rough surfaces return an average distance. Because of the internal measurement of temperature (for the computation of the most appropriate speed of sound), the device must be given enough time to settle at the ambient temperature and should not be exposed to the sun or other heat sources.

2.1.2 Electro-Optical Sensor

As an example of an electro-optical sensor, the Leica hand-held laser meter 'DISTO' is discussed (see Figure 2.1, on right). The first DISTO model was released in 1994. The instrument is 235 mm long. That is much longer than the ultrasound device discussed above. It uses an visible laser diode distance meter to measure the distance to surfaces. This distance meter uses the same phase-measurement principle as most other electronic distance meters. (The unit length of the original DISTO is 3 m.) The range is quoted as 0.2 m to 30 m, without reflector. The resolution is 1 mm. Test measurements have established that all systematic errors (additive constant, periodic errors, scale errors) of the particular DISTO tested were well below the 2 mm level (Witte & Yang 1994). The fifth DISTO series was released in 2002. For the DISTO *lite*[5] and the *classic*[5], the operating range is listed as 0.2-200 m and the accuracy as ±3 mm at 2σ (±1.5 mm at 1σ). The display resolution is 1 mm below 100 m and 10 mm above 100 m. (Tests have shown that these two models are programmed not to measure distances longer than 200 m. Special target plates are required to achieve the maximum distance.)

The DISTO does not have an input facility for the atmospheric parameters. Like with all other electro-optical distance meters, the scale of the measurements does change at a rate of about 1 mm/100 m per 10°C change in atmospheric temperature and per 33 hPa change in atmospheric pressure. Whilst this might be ignored for distances of 0.2 m to 30 m, corrections might be appropriate for distances of 100 m. At temperatures higher than the reference ('standard') temperature of the instrument, distances are measured too short; a positive correction has to be applied. At pressures lower than the reference ('standard') pressure of the instrument, distances are also measured too short; a positive correction is required.

According to the manufacturer, the Leica DISTO measures the correct distance at 23°C, 953 hPa and 60% relative humidity. When ignoring the influence of humidity, the following correction equation can be derived from the standard conditions and the carrier wavelength of 635 nm given by the manufacturer:

$$d_{corr} = d_{meas} + \{(259.7 - \frac{80.91\ p}{T}) (10^{-6})\ d_{meas}\} \qquad (2.2)$$

where T is the atmospheric temperature (in kelvin; = 273.15 + t), t is the atmospheric temperature in degrees Celsius (°C), and p the atmospheric pressure (in hPa).

The visible laser diode projects a red dot onto the reflecting surface, so that the user knows exactly to what point the distance is being measured to. The range can be extended to 100 m (or 200 m for newer models) by using a (brown) target plate (made of reflective sheeting). As the laser dot cannot be seen by eye at longer distances, Leica sells a telescope attachment, which clips onto the DISTO and is held in place by magnets. Also, freehand operation may not provide a stable pointing at longer distances. DISTOs can be screwed onto camera tripods if better beam stability is required.

Since 1995, the instrument is available in some specialised versions, such as the Data DISTO RS232 for operation from computers for control measurements and as Data DISTO GSI for the attachment to the Leica electronic theodolites. In 1996, DISOFTmini followed. This data acquisition system links a DISTO to a penpad computer for the computer-assisted survey of buildings. A data transfer to CAD systems is possible.

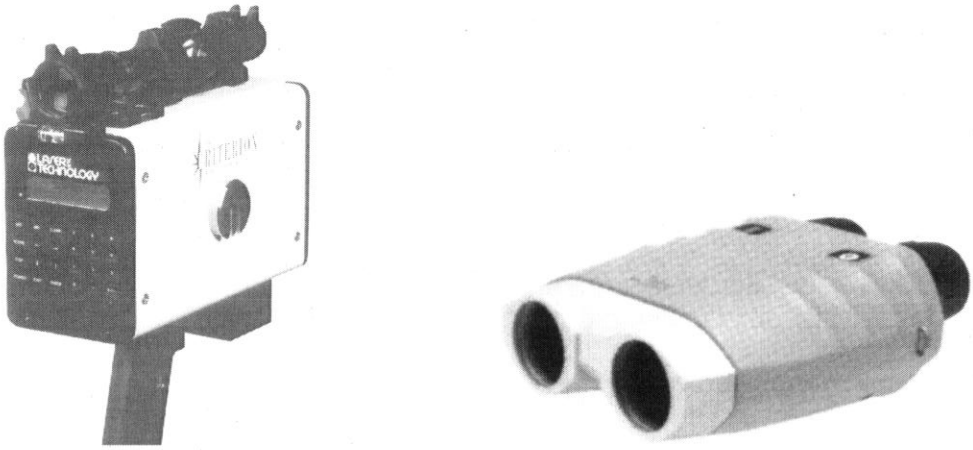

Figure 2.2: Criterion hand-held Survey Laser by Laser Technology (on left) and Leica Locator (on right)

2.2 Hand-Held Angle-Angle-Distance Devices

A number of manufacturers provide binocular-type systems, that can measure the distance to a point as well as the magnetic bearing and the inclination of the corresponding line of sight. Such systems provide data similar to those of the electronic tacheometers, namely a slope distance, a horizontal angle (referenced against magnetic north in this case) and a vertical angle. In consequence, the horizontal distance and the height difference to a point can be calculated on-board. Together with the magnetic

bearing, a three-dimensional positioning is possible. An RS-232 interface for the external storage and processing of the data is usually available.

Instrument	Criterion 300	LEM 300-W Laser Meter	Leica Locator	Laser Scout 1000-C
Distance				
Accuracy	±100 mm	±100 mm	±1 m	±200 mm
Minimum Distance	6 m		25 m	2 m
Range to Poles	275 m	<100 m		1200 m
Range to Buildings	455 m	300 m	1500 m	1500 m
Range to Triple Prism	12200 m	3000 m		3500 m
Measuring Time	0.3 s	???	0.3 s	0.5 s
Azimuth				
Accuracy	±0.3°	???	0.6°	0.2°
Measuring Time	1.0 s	???	0.2 s	???
Stabilisation	±15°(floating)	???	3-D sensor	±20°(gimbals)
Inclination				
Range	1x±60°	1x±65 grads	2x±45°	1x±60°
Accuracy	±0.2°	±0.1 grad	0.2°	0.1°
Measuring Time	0.75 s	???	???	???
RS-232 Port	yes	yes	yes	yes
Manufacturer	Laser Technology 7399 S Tucson Way Englewood Co 80112 USA	Jenoptik GmbH D-07739 Jena Germany	Leica Geosystems CH-9435 Heerbrugg Switzerland	Dr. Johannes Riegl Wiener Strasse 2 A-3580 Horn Austria

Table 2.1: Technical data of a selection of laser range finders

These hand-held instruments have many uses for mapping, profiling, estimating, sampling, volume, inventory, topographic, relocation and GIS/LIS measurements. They are often used to connect additional features to points which were coordinated by GPS techniques. Because the instruments measure bearings directly, no other points need to be visible, at least in principle. Specialised instruments have been designed for the timber industry. Having measured the distance to a tree, the instruments can easily determine the height (measure elevation angle to the top and the bottom) and the diameter (measure azimuth to left and right edge), after some trigonometric computations. Some application aspects are discussed by Carr (1992). Other versions of the same type of instruments permit the measurement of the velocity of objects, such as cars. Jenoptik, for example,

supplies an instrument (Video-LAVEG Laser Velocity Guard) that measures speeds of 0 to 320 km/h (to 1 km/h) at distances up to 350 m and more. All particulars are overlaid on a video image of the scene for documentation purposes.

The key data of a selection of typical instruments is given in Table 2.1. Two specific instruments are depicted in Figure 2.2. All instruments use pulsed diode lasers for the distance measurements, usually operating in the near infrared (wavelengths of about 900 nm). The distance is derived from the flight time of the pulses to and from the reflecting surface (see Eq. (2.1)). The quoted distance range is for daylight measurements. At night, like with all other electro-optical distance meters, the range can be extended up to the double of the daytime range. Further information on pulse distance meters may be found in Rüeger (1990 1996). It should be noted that freehand operation of these devices may not be able to sufficiently stabilyse the beam on a distant target. In these cases, some support may be required to keep the beam on the target. The components used for the azimuth and the tilt measurements are discussed below in more detail.

2.2.1 Fluxgate Compass

All hand-held angle-angle-distance devices described above use so-called flux-gate compasses for the measurement of the magnetic bearing. This technology is not new; it has been used for many years in aircraft navigation. However, the flux-gate compasses have only recently become sufficiently small for inclusion in surveying instrumentation.

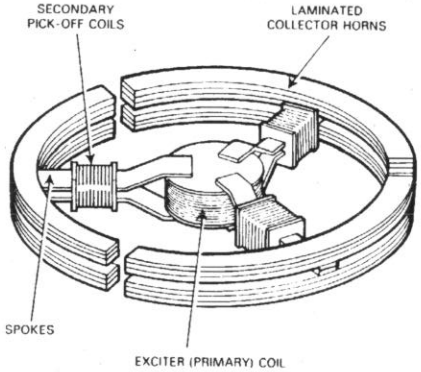

Figure 2.3: General construction of a flux detector (after Pallett 1972)

The flux-gate compass is a magnetometer which has been designed to determine the direction of the horizontal component of the vector of the earth's magnetic field. The design shown in Figure 2.3 has been the primary sensor design for more than 30 years. The flux sensor is usually gimballed so that it remains horizontal even if the host (or host vehicle) is tilted forwards and/or sideways. Naturally, the sensor has no degree of freedom about its vertical axis. To damp the vibrations induced by the host (or host

vehicle), the sensor module is usually surrounded by a fluid ('floated'). The accuracy is typically 0.1°.

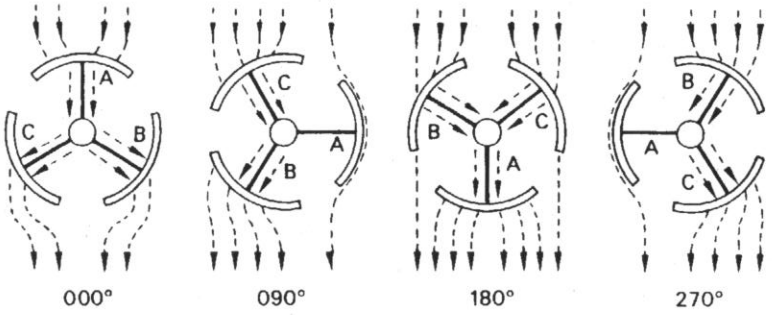

Figure 2.4: Path of the Earth's magnetic field through a flux detector and the signals induced in the pick-off coils on the three spokes (after Pallett 1972)

The primary coil generates an magnetic field (e.g. at 400 Hz) in the three spokes. The magnetic flux is carried by the upper and the lower part of the spokes. As the secondary (pick-off) coils include the forward and return paths of the induced magnetic flux, the total flux measured by the pick-off (at 800 Hz) will be zero in the absence of the Earth's magnetic field. As soon as the Earth magnetic field adds to the induced magnetic flux, the total flux through the secondary coil becomes non-zero and a voltage is generated in the pick-off coil due to electro-magnetic induction. The voltages from the three pick-offs are then combined to give the angle of the Earth's magnetic field with respected to the coordinate system defined by the three spokes. Figure 2.4 shows how the orientation of the flux gate sensor in the Earth's magnetic field changes the flux in the three spokes. A pick-off generates a maximum signal, when its measuring axis (spoke) is parallel to the Earth's field, and a minimum signal, when it is at right angle to it. In aircrafts, the flux detector elements were connected to the heading indicator in the cockpit. For hand-held instruments, the pick-off voltages have to be digitised and processed further by the on-board computer.

The traditional flux gate compasses are relatively large and heavy and must be stabilised in a horizontal plane. The gimbals or pivots used for the latter purpose restrict the allowable along- and across-tilts of the device. Rather than stabilise the traditional two-dimensional sensor in a horizontal position, it is possible to use a triad of three orthogonal single-axis flux gate sensors. Such a triad can measure the three components of the Earth's magnetic field in the case coordinate system. To derive the bearing of the sensor's case in a horizontal plane, the along- and across-sensor tilts must be measured. (The traditional flux-gate compass does not require this additional information as such. But in combination with the distance meter, at least the tilt in the forward direction must be measured anyway.)

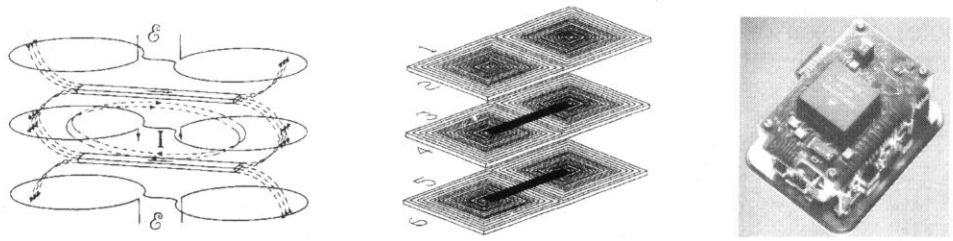

Figure 2.5: Principle (on left) and possible design (in middle) of a planar parallel-gated fluxgate sensor (after Vincueria et al. 1994). On the right, the three-dimensional digital magnetic compass (DMC) designed by Leica for their 'Vector' and 'Geovid' hand-held devices (after Leica 1995).

Figure 2.5 shows the basic principle a possible design on the left (Vincueria et al 1994). The (planar) induction coil is sandwiched between two (planar) exciting coils. Two cores made from amorphous low magnetostrictive ribbons are placed between the layers with the coils. In the absence of an external magnetic field, the induction coil would register a total flux of zero, which means that no induction would occur. The diagram in the middle of Figure 2.5 shows a practical design with four exciting coils (Numbers 2 to 5) and two secondary (pick-off) coils (Numbers 1 and 6) (Vincueria et al 1994). Leica does manufacture a three-axis flux-gate sensor (Digital Magnetic Compass, DMC) triad for their binocular based measuring systems. The device is specified to operate at along- and across-tilts of ±35°. Two integrated inclination sensors determine the two components of the dislevelment of the sensor and correct the sensor reading in real-time.

2.2.2 Clinometers

Most manufacturers of hand-held angle-angle-distance devices are not specific about the tilt sensors used. All instruments require a clinometer reading in direction to the target for the reduction of the measured slope distances to horizontal. The instruments which use a triad of single-axis flux sensors require an additional tilt sensor for the measurement of the cross tilt for the correction of the azimuth readout.

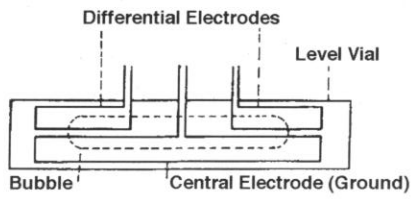

Figure 2.6: Plan view of an electrolytic level sensor.

Only Riegl quotes a 'high-quality electrolytic level sensor' with a measuring range of ±60° and a resolution of 0.1°. Figure 2.6 shows the basic design of such a sensor. The electrolytic level sensors resemble the plate levels in theodolites. The glass vials are filled with an electrolyte, which is conductive. If the air bubble is centred, both differential electrodes will be covered equally by the liquid. This means that the current in both leads will be the same. If the bubble moves to one side, one differential electrode will carry a larger current than the other. The difference between the two currents is a measure of the tilt. As an alternative, the readout electronic can be based on the differential change of the capacitance.

All tiltmeters and clinometers have a number of errors requiring calibration or adjustment. The most important corrections are the additive constant (for the zero error) and the scale correction (for the vertical-angle-dependent (linear) error). The former can be easily tested by the user through the measurement of the *same* slope, forward and backward. The latter requires a comparison against true slopes and is less easily established. Errors in the additive constant of the clinometer can be eliminated in the field by measuring the *same physical slopes* (or height differences) in both directions and by taking the mean.

2.2.3 Use of Hand-Held Angle-Angle-Range Devices

The hand-held angle-angle-distance devices are promoted for the measurement to non-cooperative targets such as poles, trees, bushes, houses etc. It is clear that the measurement accuracy of the devices cannot be realised if the dimensions of the object are larger than the measurement accuracy. All distances are measured to the closest surface (on the object), and not to the centre of the object. Also, one has to make sure that the foot print of the laser beam falls fully onto the object. If a number of objects are 'hit' by the beam, the instrument may display an average distance.

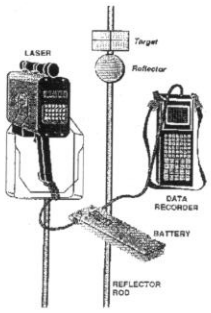

Figure 2.7: Equipment used by the Forest Service of the US Department of Agriculture for the reconnaissance surveys of single lane, low-use roads. (after Moll 1993)

The fluxgate instruments can be used to build up survey networks as it was done in the past with magnetic compasses. The compass traverses are well known. The definition of the forward, backward and instrument stations becomes very important, if measurements from different stations are to be linked. Figure 2.7 shows some ancillary equipment trialed by the Forest Service of the US Department of Agriculture for the survey of forest roads. The use of (supporting) poles at the instrument and the target stations, and the use of (plastic) reflectors, ensures that the marked points can be re-occupied with an accuracy that is better than that of the final product. The data are recorded for later processing on a personal computer. The reflector rod carries a target plate at the same offset as the telescope above the distance meter. Equal instrument heights and reflector heights ensure that the forward and backward elevation differences are compatible. Having an 'active' reflector and a well defined instrument station (on rod) and target (on rod) delivers the best accuracy in all three components.

All types of flux-gate compasses make use of the Earth's magnetic field to obtain orientations (magnetic bearings). In consequence, they are subject to the same effects as the older magnetic compasses. If the measured orientations are to be referenced against true north (geographic north), then the value for the *magnetic declination* (the angle between the true north (TN) and the magnetic north MN) must be considered. The declination value must be current for the time and location of the measurement site. Most instruments have a facility to enter this value. The problem is that the Earth's magnetic field is not constant. It is well known that the magnetic declination is subject to a secular (long-term) variation, a diurnal variation (periodic error over one day) of about 8 minutes of arc, an annual variation (periodic error of less than one minute of arc) and to irregular variations due to magnetic storms. The latter can reach one degree or more. In 1970, the magnetic declination was 11.50 degrees in Newcastle (NSW) and the secular variation +1.7 minutes of arc per year (Finlayson 1973). In Carnarvon (WA) and again for 1970, the values were –1.15 degrees and –1.1 minutes per year, respectively.

If the measured orientations are to be referenced against the grid north (GN) of a map projection, then the *grid convergence* (the angle between the true north (TN) and the grid north, GN) has to be considered in addition. In practice, it might be easier to calibrate an angle-angle-distance device on a few lines of known azimuth or bearing, depending on requirements.

Less predictable are local disturbances of the magnetic field. These 'local attractions' fall into two categories, namely those due to the station environment and those introduced by the observer. The magnetic field at a particular set-up is affected by metallic objects in close proximity (such as passing or stationary cars, transmission line towers, steel street light poles, steel structures, reinforced concrete structures, to give just a few examples), mineral deposits and direct currents. The errors caused by these objects are not predictable, but are constant at a particular point. Measuring bearings

forward and backwards on lines allows to detect station specific errors, unless both end points are affected. The interference caused by the observer, such as from the metal frame of glasses, the watch, the buckle of a belt, the keys and/or the pocket knife will be constant for a particular observer (if the readings are always taken the same way). The measuring devices can compensate for these errors, either as part of the declination or as a separate entry.

The problem of local disturbances should not be underestimated. In urban areas, for example, it would be extremely difficult to obtain correct magnetic bearings. In these cases, where local disturbances are unavoidable, the measured bearings can be processed as measured directions, as all bearings observed from one station would be wrong by the same amount.

2.3 Electronic Barometers (and Altimeters)

Electronic (or 'digital') barometers have two main uses in geomatic engineering. Firstly, they can be used to measure the atmospheric pressure required for the reduction of electronic distance measurements. In this case, a read-out in hectopascal (hPa, previously known as millibar, mb) or in another pressure unit is required. Secondly, barometers double as altimeters, in which case a read-out in metres (or in another length unit) is required.

2.3.1 Working Principles

All electronic barometers are built around a pressure sensor with its associated analogue and digital circuits. The devices feature on-board computers for the conversion between different units, the corrections for the calibration values and the computation of the elevations from the measured absolute pressure. The most common sensor principles are now outlined.

2.3.1.1 Vibration Pressure Sensor

Vibration pressure sensors make use of the change in the resonance frequency of, typically, a quartz beam or a metallic cylinder under varying load. They are the most accurate of the three sensor types discussed here. Figure 2.8 shows one implementation of each type. In the vibrating quartz sensor, a quartz beam is placed in an oscillator circuit and is made to oscillate at its fundamental resonance frequency by piezoelectric means. This quartz beam is compressed by a lever arm which moves with the pressure in the steel bellows. The changing force on the vibrating beam causes a change in the resonance frequency. The frequency of the oscillator circuit follows this varying resonance frequency. In consequence, the changes in the oscillator frequency become a measure for the changes in the

atmospheric pressure in the bellows. The frequency can be measured as in frequency counters.

Vibrating beam pressure sensors show a good repeatability and very small hysteresis effects. (Hysteresis is present if the pressure reading at a particular pressure is different depending on the pressure being reached by a pressure reduction or by a pressure increase. In the presence of hysteresis, the pressure reading is, slightly, dependent on the preceding pressure trend.) As with frequency counters, the resolution can be increased by increasing the length of the counting interval. Because quartz crystals change their resonance frequency also with temperature, the resonance frequency of a second (equivalent) quartz is monitored for temperature compensation purposes. The long-term stability is quite good. The vibrating quartz beam pressure sensors can be classified as precision pressure sensors (Sudau 1994).

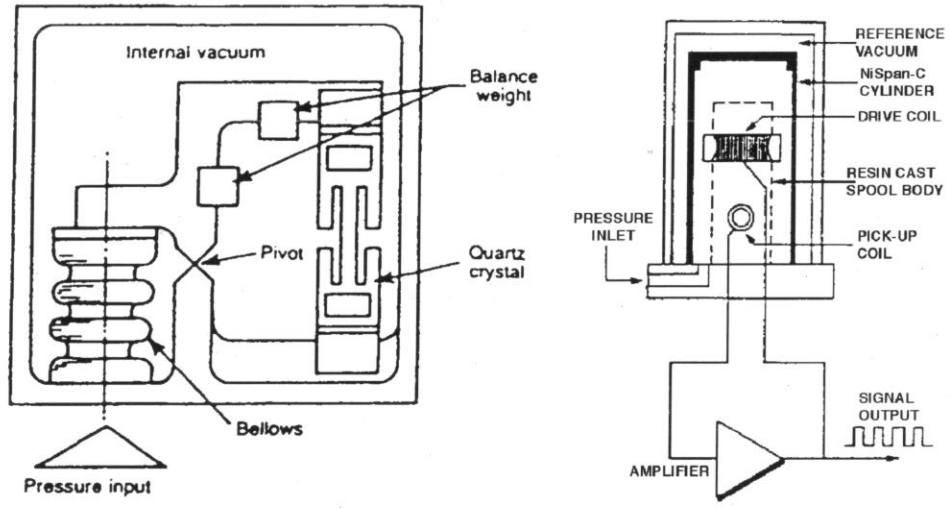

Figure 2.8: Two vibration pressure sensors. An oscillating quartz sensor (made by Paroscientific) is shown on the left and a oscillating cylinder sensor (made by Solartron) on the right. (after Sudau 1994)

The vibrating cylinder pressure sensor has a NiFe cylinder as a sensor element. A vacuum is present between the outer shell and the metallic cylinder. The drive coil causes the cylinder to vibrate at its resonance frequency. The pick-off coil is used to monitor the vibrations of the cylinder wall and to synchronise the frequency of the drive coil (in a feed-back loop). The inside of the cylinder is exposed to the pressure to be measured. As with the quartz sensor, the resonance frequency is measured and converted to the corresponding pressure by the on-board computer. The vibrating cylinder devices feature a very good repeatability, a small hysteresis and small long-term drifts. They are basically insensitive to accelerations but are susceptible to humidity (Sudau 1994). As the humidity enters into the

cylinder, it is in contact with the inside of the cylinder and the drive and pick-off coils and, thus, may alter the readings.

2.3.1.2 Capacitive Pressure Sensor

The capacitive sensors are based on the principle of a capacitor, where a change in the width of the gap between the two electrodes causes a change in capacitance. Capacitive sensors are, typically, less accurate than the vibration sensors. In the case of a pressure sensor, one electrode is fixed whereas the other one is exposed to the pressure to be measured. Figures 2.9 and 2.10 show the arrangement used in the AIR-HB-1A hand-held digital barometer/altimeter. The device uses a dual-diaphragm, aneroid pressure sensor. It is highly sensitive to pressure changes and has a low susceptibility to shock and vibration. The dependence on temperature is small, almost linear and, thus, easily calibrated.

Figure 2.9 shows the two NiSpan-C diaphragms on opposite sides of a ceramic disk. The inside of the sensor is in vacuum. The two capacitors are electrically in parallel. Mechanically, they are differential. This back-to-back arrangement provides large capacitance changes in function of pressure and low susceptibility to vibrations and shocks. The sensor is placed in an oscillator circuit, the frequency of which varies with the applied pressure. For error compensation purposes, a high and a low reference capacitor and a temperature sensitive capacitor are also switched sequentially into the oscillator circuit. The frequency measured with each of the four elements is then used by the microprocessor to derive the pressure reading. The transfer function, calibrated during manufacturing, provides the temperature compensated pressure and the elevation reading (Whitaker & Call 1987; Pike & Bargen 1976; Pike et al. 1983; Whitaker & Call 1986; Pascoe & Rüeger 1989).

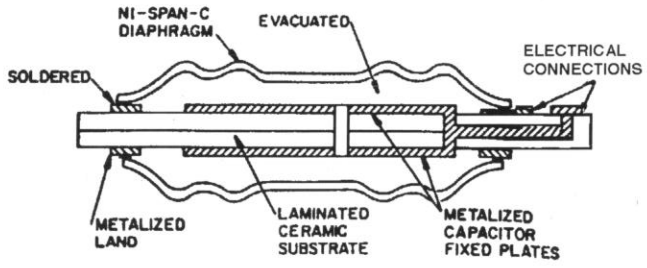

Figure 2.9: Capacitive pressure transducer of the AIR-HB-1A hand-held digital barometer/altimeter (after Pike et al. 1983)

According to Sudau (1994), capacitive pressure sensors feature a good resolution, a good repeatability, a good long-term stability and a good dynamic behaviour. The non-linearity between pressure change and capacitance change can be compensated by the microprocessor. The

susceptibility to temperature can be calibrated and corrected for by the on-board microprocessor. See Pascoe & Rüeger (1989) for some test data.

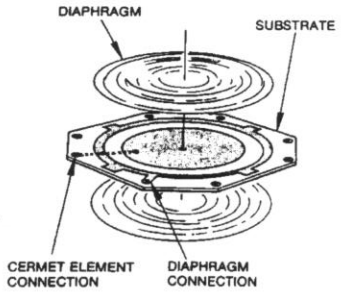

Figure 2.10: Dual-diaphragm, capacitance, aneroid pressure sensor of the AIR-HB-1A hand-held digital barometer/altimeter (after Whitaker & Call, 1987)

2.3.1.3 Piezo-Resistive Pressure Sensor

The piezoresistive sensors are the least accurate of the three types of sensors discussed here. They consist of a silicon membrane on a silicon substrate. A vacuum exists between the membrane and substrate. On top of the silicon membrane, four resistance sensors (strain gauges), in cardinal directions, are implanted. The strain gauges are connected in a Wheatstone bridge circuit. A change in the pressure causes a strain in the silicon membrane. This changes the resistance of the four gauges through changes in the specific resistance of the semiconductor material and yields a bridge voltage which is proportional to the applied pressure.

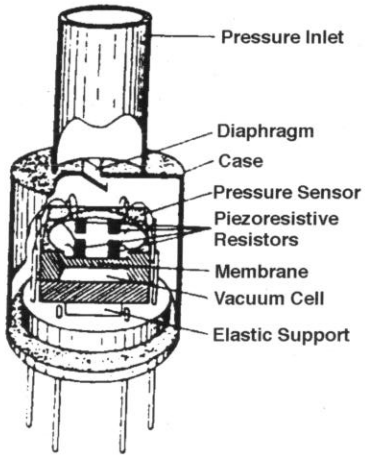

Figure 2.11: Construction of a piezoresistive pressure sensor (after Sudau 1994)

The silicon chips can be as small as 4 x 4 mm, with a membrane thickness of 25 micrometres and a membrane diameter of 3 mm. As shown in Figure 2.11, the measuring chip is not directly exposed to the pressure to be measured. The external pressure is applied to an outer membrane ('diaphragm' in Fig. 2.11), which pressurises the oil inside the device. The oil applies the pressure to the silicon chip. The simple construction of piezoresistive sensor, together with their long service life and their miniaturisation, have lead to a multitude of applications in a number of fields. The temperature sensitivity of the resistance measurement is largely eliminated by the bridge circuit with the four strain gauges. The temperature dependence of the pressure reading must be compensated by other means.

2.3.2 Performance of Digital Barometers

Sudau (1994) summarised the performance of the three types of sensors discussed earlier. Sudau's table is reproduced in Table 2.2 in modified form. Rather than give the performance data in percent of the full scale (measuring range) of the devices, they have been converted to hPa by assuming a range from 600 to 1100 hPa (full scale = 500 hPa) for the devices. The performance as an altimeter can be estimated from the vertical lapse rate of the atmospheric pressure of about 1 hPa per 10 m.

The vibration sensors are intrinsically digital devices (frequency output) whereas the other two types are analogue devices, which require analogue to digital conversion. Most devices designed for outdoor use and having a display for the pressure (and elevation) readings seem to be of the piezoresistive and capacitive kind. Other devices provide the data only through a serial (RS232) computer interface and, thus, must be connected to a personal computer for the readout of the pressure or altitude.

Specification	Type of Sensor		
	piezoresistive	capacitive	vibration
Resolution (hPa)	~0.1	<0.03	>0.000025
Linearity (hPa)	<2.5	<0.25	0.03
Repeatability (hPa)	0.15–2.0	<0.10	<0.03
Hysteresis (hPa)	0.15–0.5	<0.10	<0.03
Overall Accuracy (hPa)	~2.5	0.10	0.05
Long-term Stability (hPa/year)	2.5-8.5	0.25-0.50	<0.05

Table 2.2: Performance data of three types of pressure sensors (after Sudau 1994)

The specifications of some self-contained hand-held barometer/altimeter devices are given in Table 2.3. The data have been taken from the respective instrument brochures. Prices start from about AUS $350 and are, typically, lower than the prices of a mechanical aneroid barometer/altimeter of equal precision.

Manu-facturer	Eschenbach Optic Germany	Atmospheric Instrument Research (AIR) USA	Thommen Switzerland	Väisälä Finland
Model	6941 Alpin EL	HB-1A	Altitronic Professional	PA 11
Range (m)	-500 to 10000	-700 to 4200	-700 to 10000	
(hPa)		600 to 1100	250 to 1100	800 to 1050
Resolution (m)	0.5	0.1	1	
(hPa)	0.1	0.1	0.1	0.1
Tolerance		±0.5 hPa	±1.0 hPa	±0.3 hPa
			±10m (>500m)	
	±8 m		±2m (<500m)	
Temperature Range (°C)	-20 to +50	5 to 40 (Option: -25 to +50)	-30 to +60	+5 to +55
Temperature output	no	no	yes (Pt-1000) ±0.3°C	no
Sensor	?	1x capacitive	1x piezoresistive	3x capacitive
Weight (g)	?	280	170	1700
Size (mm)	?	30x91x145	131x68x25	72x144x250
Supply Voltage (V)	?	9	9	4.8

Table 2.3: Specification of some commercial hand-held barometers and altimeters

2.3.3 Heighting with Digital Barometers/Altimeters

Based on the height formula for a standard atmosphere, the microprocessors of digital barometers can easily compute and display elevations. Kahmen & Faig (1988, Eq. 11.7.2) give the following formula for the height H (in metres) in a standard atmosphere:

$$H\,(m) = \frac{T_o}{a}\left(1 - (p/p_o)^{1/n}\right) \qquad (2.3)$$

where
$n = 5.256$
p_o = mean sea level pressure = 1013.25 hPa
T_o = mean air temperature at sea level = 288 K (~15°C)
a = vertical lapse rate of temperature = 0.0065°C/m

Substitution in Eq. (2.3) of $T_o = 288.15$ K and other numerical values as given above leads to the following equation used by Atmospheric Instrument Research (AIR) for their HB-1A barometer/altimeter:

$$H\,(m) = 44330.77\,(1.0 - (\frac{p}{p_o})^{0.19026}) \qquad (2.4)$$

where p (in hPa) is the pressure measured at the elevation H. The above equation is based on many assumptions, namely that the temperature at the mean height (H/2) is $\{T_o - a\,(H/2)\}$, the humidity is zero, the mean gravity is equal to g_o and that the sea level pressure is indeed p_o. These conditions are usually not fulfilled. In consequence, correction formulæ have been used in the past to compensate for the deviation of the real atmosphere from the standard one in the computation of barometric height differences. Details on these formulae may be found in sections on barometric heighting in surveying textbooks. (See Kahmen & Faig, 1988, Sect. 11, for example.)

Practical tests have shown that a simple interpolation (proportional to the height difference) of the barometric heights between the points of given elevation can provide quite accurate elevations when using electronic barometers. The interpolation formula is given by Kahmen & Faig (1988, Eq. 11.7.7) as follows;

$$H_i - H_A = (H_E - H_A)\,\frac{h_i - h_A}{h_E - h_A} = \Delta H_{A->E}\,\frac{\Sigma\Delta h_{A->i}}{\Sigma\Delta h_{A->E}} \qquad (2.5)$$

where $\Sigma\Delta h_{A->i}$ is the measured elevation difference from the starting Point A to a Point i, $\Sigma h_{A->E}$ the measured total elevation difference between the fixed Points A and E and ΔH the given elevation difference between the fixed Points A and E.

Lechner el al. (1987) reported on a test of motorised levelling with three different electronic barometers/altimeters (two types of piezoresistive devices) in two networks. (The speed of travel was about 30 km/h between set-ups.) The first network featured height differences of 20 to 80 m over 5 to 12 km, the second one a height difference of 250 m over 6 km. The root mean square error of the interpolated barometric heights were, on average, ±0.4 m and ±1.0 in the first and second network, respectively. The worst errors in the interpolated heights did not exceed 1.1 m and 2.8 m in the first

and second network. Sudau (1994) quoted results of the interpolation method in barometric heighting with the more precise vibrating quartz beam instruments. A height precision of ±0.06 m was achieved between bench marks 450 m apart and over a height difference of 43 m. It follows that barometric levelling (motorised or otherwise) with digital barometers is a powerful and simple method, particularly if points of given heights are available at the edge of the area to be surveyed.

The interpolation method is based on the assumption that the atmospheric pressure does not change with time. Unfortunately, this is usually not the case. Even in stable weather conditions, the pressure falls by about 3 hPa between 9 h and 15 h and rises a similar amount between 15 h and 9 h on the next day. A smaller rise and fall occurs during the night and early in the morning (Bureau of Meteorology 1990). Considering a pressure change of 1.145 hPa per 10 m height difference (at 500 m above sea level), this diurnal pressure change translates into a 'change' of 26 m in the altimeter reading. (At 2500 m above sea level, the lapse rate of pressure is 0.9428 hPa per 10 m.)

Larger pressure changes occur during weather changes. When a high is moving away or a depression is approaching, the pressure can easily drop by more than 7 hPa over 24 h (Bureau of Meteorology 1990). This is equivalent to a change in the altimeter reading of 74 m (at 500 m above sea level). The interpolation method with a single altimeter is therefore only appropriate during stable weather conditions and over short periods of time. Best results are achieved on uniform slopes and when starting and finishing on points with given heights at the highest and lowest points of the height 'traverse'. Naturally, changes of pressure due to weather can be monitored by a second, stationary barometer if the barometric levelling extends over a longer period of time.

If given elevations are not available at both ends of a barometric heighting run, then the normal formula of barometric heighting and the normal observation procedures should be employed. The latter includes the use of a stationary barometer to monitor the changes, due to weather, of the atmospheric pressure with time. Refer to textbooks (e.g. Kahmen & Faig 1988) for full details.

2.4 Exercises

2.1 The measurements taken with the Accutape-S ultrasonic distance 'Estimator' are corrected internally for temperature. It is assumed that these devices are calibrated for 20°C, sea level pressure (1013.25 hPa) and zero humidity.

(a) Investigate the error in a 30 m distance measured at +35°C and 100% relative humidity (56 hPa partial water vapour pressure).

(b) What is the error in a distance of 100 m measured at 20°C at an altitude of 3000 m?
Hint: Consider Eqs. (2.1), (2.2) and (2.4).

2.2 Discuss the relative merits of ultrasonic, electro-optical and steel 'pocket tapes' for the three-dimensional (length, width, height) measurement of the internal size of rooms and buildings.

2.3 The Leica 'DISTO' *classic*[5] measures distances correctly at 23°C and 953 hPa. The instrument is accurate to ±3 mm at these conditions.
(a) What error would you expect in a 100 m distance measured at +30°C and 890 hPa?
(b) Would you correct the instrument reading in any way? Why?

2.4 The manufacturer of the Criterion 300 hand-held 'Survey Laser' (angle-angle-range device) specifies the distance accuracy as ±100 mm, the bearing accuracy as ±0.3° and the vertical angle (inclination) accuracy as ±0.2°.
(a) At what range does the accuracy of the computed height difference reach ±100 mm? (Assume a horizontal line of sight.)
(b) At what range does the accuracy of both components (Easting and Northing) of the horizontal coordinates (computed from bearing and horizontal distance) of a target point attain ±100 mm? (Assume a point due East or due North from the instrument station.)

2.5 You have been asked to map (in the Map Grid of Australia 1994, MGA94) a stand of old trees on a development site. Four survey marks with given MGA94 eastings and northings are available on the site. You are using a hand-held angle-angle-range device with a flux gate compass for the purpose. How do you get the MGA94 bearings (required for the calculation of the coordinates) from the measured magnetic bearings?

2.6 You have been asked to determine the height and the diameters of the stem and spread of some trees with a hand-held angle-angle-range device.
(a) What do you measure, exactly, to each tree?
(b) How do you calculate the required tree dimensions? Derive the necessary formulae!
(c) What precision of the three elements would you expect when using a Leica Geovid at 50 m from the tree?

2.7 Standing on a survey mark, *you* measure the height difference to the top of a power line pole with a hand-held binocular based angle-angle-range device similar to the one shown in Figure 2.2 (on right). The height of the survey mark is 238.44 m above sea level (Australian Height Datum 1971, AHD71). The height difference between the device and the top of the pole is displayed as –45.6 m. What is the AHD71 height of the top of the pole?

2.8 You have mounted a reflector on a ranging rod at a height above ground which corresponds to your eyelevel. You stand on a Mark A. Your assistant holds the ranging rod on Mark B. You read a vertical angle of +10.8° with a binocular based angle-angle-range device. You then move to Mark B and your assistant to Mark A. From B, you measure the vertical angle from B to A as –12.2°C.

(a) What do you conclude?

(b) What would you do next?

2.9 List and discuss those variations of the magnetic field of the Earth which affect the magnetic bearings measured with flux-gate compasses.

2.10 The vibrating cylinder pressure sensors are said to be susceptible to humidity, whereas the vibrating quartz beam sensors (of equal precision) are not. Based on the Figures 2.8, explain the reason for this difference.

2.11 Compare the practical results of the interpolation method in barometric levelling with digital barometers/altimeters reported by Lechner (1987) and Suday (1994) with the performance parameters of the respective devices. What performance parameter corresponds best with the test results?

2.12 The motorised barometric levelling with one digital altimeter was used to determine the elevations of a number of points along a road. Given the 'true' heights of the Point 40 and the Point 51, compute the elevations of the Points 41 to 50.

Point	Given (m)	Measured (m)	Adjusted (m)	Point	Given (m)	Measured (m)	Adjusted (m)
40	256.85	251.7	256.85	46		456.7	_____
41		292.6	_____	47		484.3	_____
42		327.3	_____	48		513.9	_____
43		351.8	_____	49		545.2	_____
44		390.1	_____	50		561.5	_____
45		421.4	_____	51	586.28	573.3	586.28

2.13 Barometric levelling was executed with a digital barometer along a forest road. Compute the elevations of the Stations 61 to 65 based on the given elevations of Stations 60 and 66.

Point	Given Elevation (AHD) (m)	Measured Pressure (hPa)	_____ ___	Adjusted Elevation (AHD) (m)
60	1946.75	799.2	_____	1946.75
61		789.7	_____	_____
62		785.2	_____	_____
63		780.8	_____	_____
64		774.9	_____	_____
65		770.1	_____	_____
66	2339.42	760.5	_____	2339.42

3. Levelling Equipment

3.1 Digital Levelling Instruments

3.1.1 Introduction

Digital levelling instruments ('bar code levels') were introduced in 1990 by the surveying equipment manufacturer Wild (now Leica) of Switzerland. Two other manufacturers (Topcon and Zeiss) released digital levels in 1994. Sokkia followed in 1998. Each of the manufacturers uses a proprietary design of the bar code graduations on the respective staff, so that staffs cannot be interchanged between instruments of different manufacturers. Digital levels simplify the traditional levelling by not having to read the levelling staff through the telescope and permit electronic data recording. In consequence and because larger sighting distances can be used in non-precise levelling applications, digital levelling instruments have made levelling faster. However, levelling with digital levels is still labour intensive as somebody has to operate the instrument and somebody has to hold the staff.

Considering the wide-spread use of one-person rotating laser levels on building and construction sites (discussed in the next section) and the replacement of line levelling by EDM-Height Traversing (Rüeger 1995, Rüeger & Brunner 1981) with electronic tacheometers in all but high precision 'levelling' applications, the traditional use of levelling instruments is likely to decline. The largest use of digital levels may well be in precise levelling applications in geodesy and engineering (e.g. monitoring of structures and machines) as the other possible applications are likely to be taken over by more efficient techniques.

In 2003, one manufacturer (Topcon Japan) offers three models of digital levels, two manufacturers (Leica (Wild) Switzerland, Trimble (Zeiss)

USA/Germany) offer two instruments each, and one manufacturer (Sokkia Japan) offers one. The manufacturers that sell at least two models, provide one or more for normal levelling (with fibre glass, aluminium or wooden staffs) and one for precise levelling (with invar staffs).

Figure 3.1: Zeiss (Trimble) DiNi10 digital levelling instrument (on left) and Zeiss bar code (on right)

Figure 3.2: Topcon DL-102 digital levelling instrument (on left) and Topcon bar code (on right)

The precision listed by manufacturers for 1 km double run levelling (after the German DIN Standard 18723) with the less accurate instruments (and the corresponding (normal) bar code staffs) is as follows:

Leica DNA10 $s_{1km\ double\ run} = \pm 1.5$ mm

Sokkia SDL30 $s_{1km\ double\ run} = \pm 1.0$ mm

Topcon DL-102	$s_{1km\ double\ run}$	=	±1.0 mm	
Topcon DL-103	$s_{1km\ double\ run}$	=	±1.8 mm	
Wild NA2002	$s_{1km\ double\ run}$	=	±1.5 mm	(now Leica)
Zeiss DiNi20/21	$s_{1km\ double\ run}$	=	±1.3 mm	(now Trimble)

The precision listed by manufacturers for 1 km double run levelling (after the German DIN Standard 18723) with the more accurate instruments (and the corresponding invar bar code staffs) is as follows:

Leica DNA03	$s_{1km\ double\ run}$	=	±0.3 mm	
Topcon DL-101/C	$s_{1km\ double\ run}$	=	±0.4 mm	
Wild NA3003	$s_{1km\ double\ run}$	=	±0.4 mm	(now Leica)
Zeiss DiNi10/11	$s_{1km\ double\ run}$	=	±0.3 mm	(now Trimble)

3.1.2 How do Digital Levels Differ from Conventional Automatic Levels?

3.1.2.1 DC Power

When using invar staffs, having no power means that no readings can be taken. When using non-invar staffs (like sectional fibre glass staffs), the digital levels can still be used as a normal level as the non-invar bar code staffs have a normal graduation on the back.

Having no power also means that no data recording is possible. It is evident that enough charged batteries must be taken into the field if no loss of time is to take place because of a lack of power.

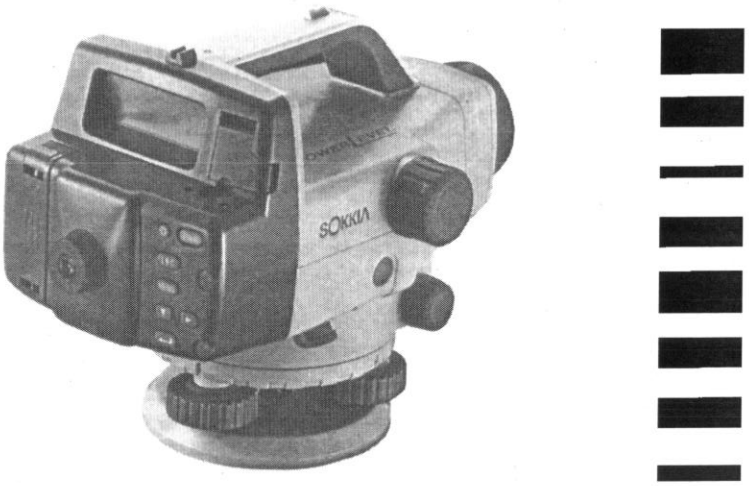

Figure 3.3: Sokkia SDL30 digital levelling instrument (on left) and Sokkia bar code (on right)

3.1.2.2 Staffs

Digital levels require special bar code staffs, which are make specific. The staff and the digital level must be of the same make. Normal bar code staffs are made from fibreglass, aluminium or wood and have normal graduations on the back face. They are usually sectional or folding staffs. Invar bar code staffs do not have a normal staff face on the back. The invar ribbon is typically mounted inside an aluminium frame which has a steel base plate at the bottom.

3.1.2.3 Electronic Staff Reading and Distance Measurement

Digital levels not only measure the staff reading but also the distance between the instrument and the face of the staff. The latter is measured with an accuracy of a few centimetres. Both values are displayed on the read-out screen.

The electronic reading is non-personal and faster and allows to change the units of measurement between metres and feet very easily (No need to change the staff as in the past!) and the resolution of the readings can be selected.

3.1.2.4 Illumination of the Staff

The illumination of the staff is more important than in the past, as the electronic measurement requires a good contrast. An artificial (warm) light source is required for indoor or poor light conditions. (The early Wild (Leica) and the Sokkia instruments use only the infrared image of the staff for the processing.) It has been found that problems occur when observing against a bright background, against the sun and in the case of shadow patterns on the staff.

3.1.2.5 Compensator

In 1995, all digital levels are equipped with compensators similar to those in the classic automatic levels where the entire optical path of the telescope is deviated. Electronic level sensors (similar to those in electronic theodolites) could be used, but this would no longer permit the use of the instrument as a normal automatic level.

3.1.2.6 Optical or Electronic Horizontal Circle

Most bar code levels have an internal or external circle for rough angular measurements. This circle is typically read by eye as in traditional automatic levels.

In 1995, Zeiss did release a digital level with an electronic horizontal circle reading ('*Total Level Station*' DiNi10T) where the directions are measured to 6" and the distances to 1 cm/10 m. In this case, the instrument can be used for detail and contour surveys like electronic tacheometers, as long as the ground is reasonably level. It is to be noted that correct pointing to the centre of the staff is then essential as is the set-up of the staff exactly in the

centre of the staffs base plate. Strictly speaking, the distance is measured to the front of the staff whereas the (fibreglass) staff is usually set-up in the centre of its cross-section.

3.1.2.7 Electronic Data Recording

This is the most important advantage of digital levels. Electronic booking speeds up the measuring process and avoids booking errors. Also, no additional person is required as 'booker'. The electronic data can be recorded on the following media, depending on instrument:

Removable memory cards: These cards may be make specific or may be PC cards, formerly known as PCMCIA-cards (**P**ersonal **C**omputer **M**emory **C**ard **I**nternational **A**ssociation). The latter may be read by inserting them into a PCMCIA port of a computer. The former need an additional memory card reader for the up or down loading of the data.

Internal (RAM) Memory: with RS-232 port for the up and down loading of data.

Hard Disk of External Notebook Computer: linked to the instrument via a RS-232 port.

3.1.2.8 Computer Interface

All digital levels feature an two-way RS-232 port for the up and down loading of data and/or the remote operation of the digital level from a computer.

3.1.2.9 Real-Time Correction of Instrument Errors

Having the measurements in electronic form and a computer on board makes it possible to correct instrumental errors by (real-time) computation rather than by physical adjustment. This requires that the instrumental errors be determined by the manufacturer and/or the user, stored in a non-volatile memory on board the instrument and removed from the raw observations by computation, prior to displaying and recording the measurements.

The manufacturers provide on-board program routines which guide the user through the determination and storage of user accessible instrument corrections, such as the (vertical) collimation error. Other on-line error corrections are only accessible to the manufacturer. This may include corrections for temperature dependent effects, which are corrected on the basis of an internally measured temperature.

3.1.2.10 On-Board Computing

The powerful computers on-board digital levels can be programmed to assist with some calculations which were previously done by hand. Manufacturers may provide on-board programs in support of:

Line Levelling: For example, carrying forward of elevations from a starting point, summation of backsight and foresight distances, height transfer to intermediate sights.

Two-Peg Test: Calibration, storage and correction for the vertical collimation error.

Users should note, that **it is impossible to adjust or calibrate the collimation error of digital and other automatic levels without error**. The two-peg test gives the collimation error at a particular instant and temperature only. The collimation error changes all the time. Experiments have shown changes of 8" between two set-ups and changes of 1" per °C! Digital levels were found to be more sensitive to temperature changes than optical automatic levels.

3.1.3 Principle of the Wild (Leica) NA200x/300x Instruments

As the WILD NA2000 was the first digital levelling instrument (released in 1990), it will be used to introduce the principle of operation of such instruments. Other makes of digital levels do employ slightly different procedures for the decoding of the bar code staffs. Most operational aspects are the same, however. The principle of the Topcon digital levels is explained in Rüeger (2000) and that of the Zeiss (Trimble) digital levels in Feist et al. (1995), for example.

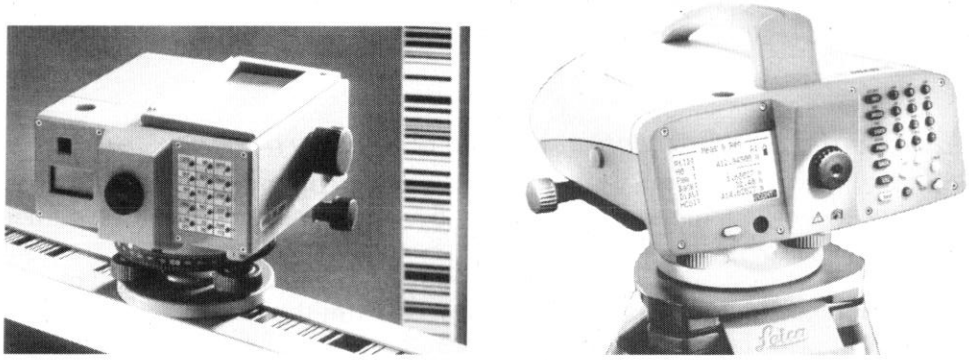

Figure 3.4: Wild NA2002 digital level (on left), Leica DNA03 precision digital level (on right), Leica fibre glass staff (in middle) and Leica invar staff (under the instrument on the left)

3.1.3.1 Basic Design and Working Principle

The digital level Wild NA2000 by Leica uses the same optical and mechanical components as a traditional automatic level. (For example, the compensator is the same as in the Wild NA2 and NA24 automatic levels.) In consequence it can also be used like a conventional automatic level. Figure 3.5 shows the main components of this digital level. The image of the staff's bar code is deviated onto the detector array by the beam splitter. The beam splitter doubles as an optical filter which deviates the infrared part of the spectrum onto the detector. The maximum sensitivity of the Silicon

detector is in the near infrared. The visible part of the spectrum proceeds to the reticule of the level.

The linear detector array is 6.5 mm long and features 256 pixels. The spacing and the size of the pixels is 25 μm. The viewing angle of the telescope is about 2 degrees. At the shortest measuring distance of 1.8 m, a 70 mm long staff section is projected onto the array. At the maximum measuring distance of 100 m, the detector array sees a staff section of 3.5 m length. (This arrangement is quite different from that in the Zeiss DiNi10/20 levels, where only 15 cm above and 15 cm below the line of sight are used for the measurement.) It should be noted that the *white code elements* are detected and used in the processing. They produce a light pattern on the photodiode array; the black lines become the gaps between recorded signals.

The focussing and pointing to the staff is manual. The position of the focussing lens is a measure of the distance to the staff and is recorded by a linear encoder. The focussing lens travels about 14 mm within the focussing range from 1.8 m to 100 m. The position of the compensator is checked by a monitoring system. This compensator monitor generates an error message whenever the compensator is outside its specified operating range. This check ensures that the instrument is levelled with the spot bubble before measurements are taken. The linear photodiode (CCD) array converts the received bar code image into an analogue video signal.

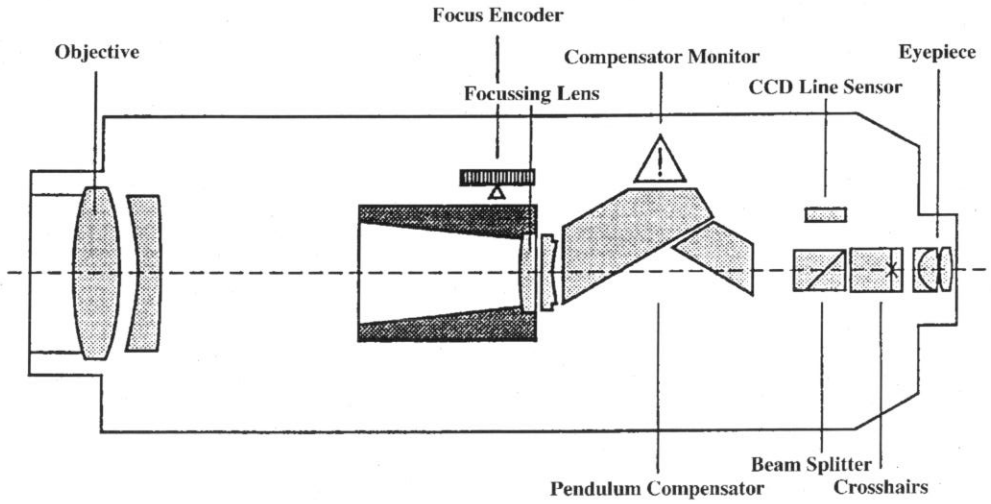

Figure 3.5: Schematic cross section through the Wild NA2000 digital level. The parts are described in the text. (after Ingensand 1990)

A block diagram of the electronics of the instrument is shown in Figure 3.6. A micro-processor performs the real-time image processing required. For the computation of the correlations the processor is supported by a gate array. The read-out electronic amplifies and digitises the video signal. It

uses an 8-bit analogue-to-digital converter which provides 256 grey values for each of the 256 pixels.

3.1.3.2 Measuring Sequence

After pressing the measuring button, the position of the focussing lens is read and the proper functioning of the compensator is checked. The integration time for the image recording is selected according to the measured signal intensity. The image of the bar code on the photo diode array is then measured and stored. This takes 0.004 to 1.0 seconds.

The *coarse measurement* follows. Starting with the recorded position of the focussing lens (see d_f in Fi. 3.8), an approximate value for the staff reading and the image scale (distance) is determined. This is basically done by trial-and-error, namely by comparing the recorded image pattern with the simulated image pattern, which is calculated by the computer for a large number of different distances and staff readings. To assess the goodness of fit of the real and the simulated patterns for the different distance and staff readings, the correlation coefficient is computed. This (1-bit) correlation process takes 0.3 to 1.0 seconds.

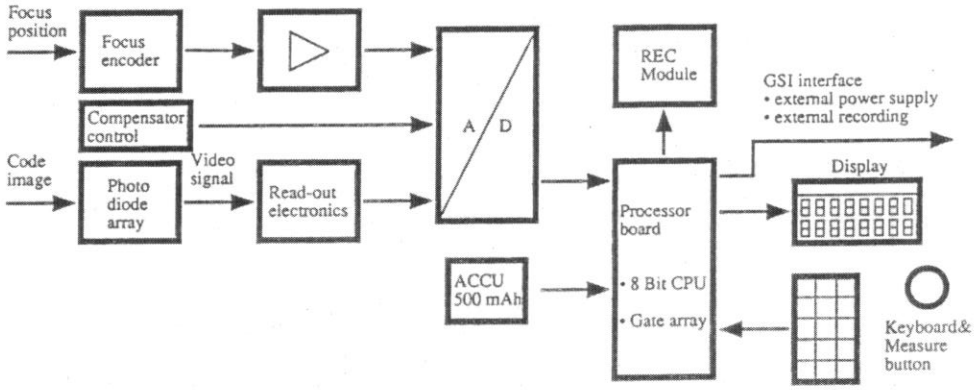

Figure 3.6: Block diagram of the electronic section of the Wild NA2000 digital level (after Ingensand 1990)

During the final *fine measurement*, the staff reading and the image scale (distance) are determined with full 8-bit correlation between measured and simulated readings of the 256 pixels. The final staff reading and distance are obtained through the application of stored calibration values. The time required for the fine optimisation depends on distance and the quality of the optical signal. The time varies from 0.5 to 1.0 seconds. Depending on the selected measuring mode, the measurements are then processed further and/or displayed and/or stored.

3.1.3.3 *Signal Processing*

The digital level compares the measured grey values of the 256 pixels of the photo detector with the simulated values computed from the known code pattern. Two parameters must be optimised through the correlation process, namely the *staff reading* and the *scale of the staff image*. Changes in the height difference h lead to a *shift of the bar code* image on the photo detector array. Changes in the distance d between the instrument and the staff change the *scale of the bar code* on the photo detector array.

To optimise the two unknown parameters, a two-dimensional correlation function has to be used. In the Wild NA2000, the following correlation function ρ_{PQ} (d,h) is computed between the measured signal Q(y) and the reference signal P(d,y+h) for all 256 pixel values of the array (Ingensand 1990):

$$\rho_{PQ}(d,h) = \frac{1}{N} \sum_{i=0}^{N} Q_i(y) \times P_i(d,y+h) \qquad (3.1)$$

Figure 3.7 shows a typical result of the correlation result over the measuring range of d = 1.8 – 100 m and h = 0.0 – 4.05 m. (The position of the code relative to the detector is denoted by y.) The distance (d_0 in Fig. 3.7) and staff reading (h_0 in Fig. 3.7) corresponding to the peak of the correlation function are the solutions for the unknown parameters d and h.

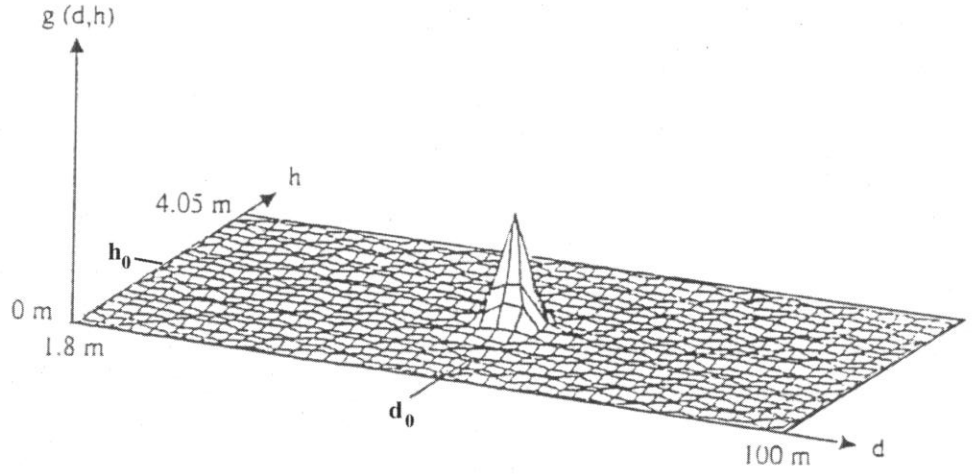

Figure 3.7: Plot of a typical result of the image correlation (ρ) in function of the distance (d) and the staff reading (h) (after Ingensand 1990)

In principle, the entire measuring range of d from 1.8 m to 100 m and of h from 0.0 m to 4.05 m must be checked to find the maximum of the correlation function. To scan the entire measuring range, the correlation coefficient would have to be computed about 50 000 times. To reduce the

amount of computing (and measuring time), the search for the maximum correlation is divided in two stages.

The *coarse search* covers a band of about 80% of the total search area. The search band covers the total range of staff readings and is centred about the distance value d_f derived from the linear encoder on the focussing lens. To further reduce the amount of computing, the coarse search is carried out with a 1-bit signal of each pixel only. The original 8-bit signal of each pixel is reduced to 1-bit on the basis of a computed threshold level. In consequence, the multiplications in the above formula can be replaced by an equivalent exclusive-not-or-logic.

The correlation coefficient is computed for each intersection of the distance-height grid within the search band. A peak appears where the reference signal coincides with the measurement signal. This correlation peak is significantly above the noise level.

The *fine search* is used to find the correlation peak with the highest resolution. Within the square fine search area the correlation coefficient is computed with the full 8-bit signal values of each pixel. As the signal levels in the measurement and reference signal are different, the correlation function is normalised as follows (Ingensand 1990):

$$\rho_{PQ}(d,h) = \frac{\frac{1}{N}\sum_{i=0}^{N-1} Q_i \times P_i - \bar{Q} \times \bar{P}}{\sqrt{\frac{1}{N}\sum_{i=0}^{N-1} Q_i^2 - \bar{Q}}\ \sqrt{\frac{1}{N}\sum_{i=0}^{N-1} P_i^2 - \bar{P}}} \qquad (3.2)$$

The normalisation through Eq. (3.2) has the added advantage that the correlation coefficient ρ will be in the usual range, that is between –1.0 and +1.0, and that the quality of the measurements can be assessed.

A few other aspects must be considered during the image processing:
(1) The inhomogeneous light intensity of the bar code image must be analysed and taken into account.
(2) Missing code elements have to be detected and omitted from the subsequent correlation computations. (Partial coverage of the staff can lead to missing elements.) Tests have shown that, for sighting distances longer than 5 m, up to 30% of the staff image can be missing without loss of accuracy and reliability. It does not matter where on the image the obstruction occurs.

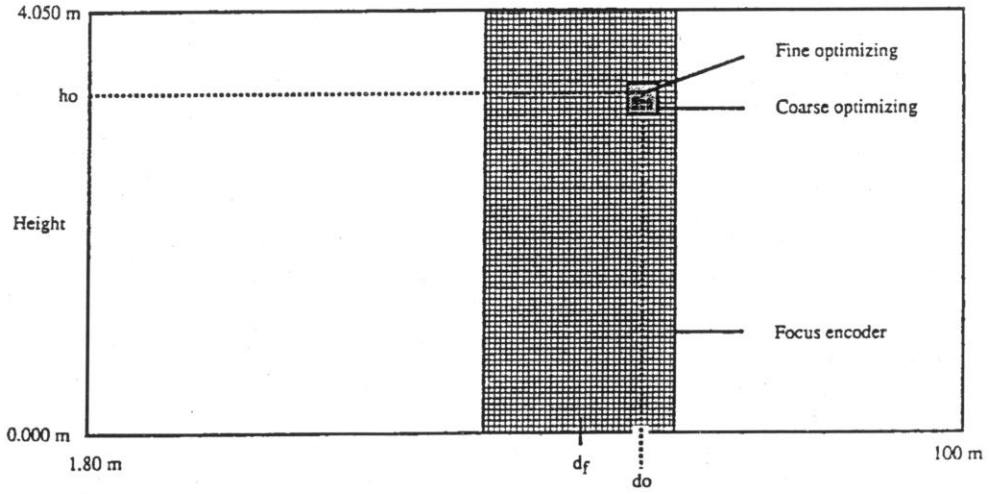

Figure 3.8: Definition of the coarse and fine search areas for the correlation maximum about the coarse distance d_f measured by the focus lens encoder. The final estimates of d and h are denoted by h_o and d_o. (after Ingensand 1990)

3.1.3.4 Accuracy of Bar Code Levels

The accuracy of the measurements depends on the following *internal* aspects of the measuring system (instrument and staff):

- accuracy of the code on the staff
- quantisation/sampling errors/noise
- quality of the optics
- quality and stability of the linear CCD array

The following *external* aspects also affect the accuracy of the system:

- Accuracy of the *Focussing*: Factory tests with the Wild NA2000 have shown that the accuracy of the staff reading is largely independent from the accuracy of the manual focussing. Proper focussing, however, leads to faster measurements. Since other makes of digital levels are more susceptible to poor focussing, it is advisable to properly focus at all times. One of the Topcon digital levels can be bought with an autofocus system.

- The *pointing* of the vertical hair to the centre of the staff is not critical for the reading of the staff. (Pointing becomes important, however, as soon as directions are also measured.) Over 100 m, the photo diode array views only 14.0 mm of the total width of 50 mm of the bar code pattern. Over 2 m, the photodiode array sees only 0.3 mm of the total bar code width of 50 mm. The correct orientation of the staff is also not critical. Even at an erroneous staff orientation of 45°, the apparent width of the graduation still exceed the width of the pixels.

• *Atmospheric Turbulence*: Heat shimmer reduces the contrast of the image of the bar code pattern and distorts the code pattern. Because of the averaging over a large number of graduations, the influence of turbulence is less than in conventional instruments.

• *Tripod Vibrations:* Image vibrations can be caused by the vibrations of the compensator (e.g. due to a set-up near a busy road). The effect of vibrations on measurements depends on the amplitude and the frequency of the vibrations and the speed of the readout of the photodiode array. As the whole image oscillates as a block, averaging over a large number of graduations does not help. (However, increasing the number of measurements does!)

Like other automatic levels, there are occasions when digital levels cannot be used on vibrating platforms or ground. This case arises when the frequency of the vibrations is close to the resonance frequency of the level's pendulum compensator.

• *Staff Graduation Errors:* The errors of the individual bars are averaged because of the large number of graduations processed. However, the scale error of the staff is not eliminated!

• *Illumination* of the staff is critical. When levelling in the open air, the 'colour' of the light reflected of the staff cannot be influenced. When using artificial lighting, the spectrum of the light source should be similar to that of the sun.

The intensity variation between full sun exposure, overcast conditions and dusk and dawn must be compensated by a variable integration time of the sensor array. The integration time is varied between 4 ms in full sun and 1 second in poor light. Inhomogeneous illumination of the staff (caused by partial shadowing) is also considered in the processing.

• *Partial Covering* of the bar code is a particular challenge to the processing software: There is no prior knowledge of where, how and how much of the code is blocked out. The software has to recognise missing patterns and ignores those sections in the correlation process. For reasons of reliability, a block out percentage of 30% has been selected as a maximum (above 5 m sighting distance). At least 30 elements (70 mm) of the bar code must be projected onto the sensor array to permit a unique height determination. At sighting distances below 5 m, no block out is acceptable.

• The *repeatability of the staff reading* is distance dependent. A number of tests have been carried out to establish the precision of staff readings. The table below gives the peak-to-peak variation of 20 observations with a Wild NA2000 (Müller 1990). The table shows that sighting distances should not exceed 50-60 m in sunny conditions.

Sighting Distance	10 m	30 m	60 m	80m
peak-to-peak variation				
at +18°C, overcast	0.0 mm	0.2 mm	0.4 mm	0.8 mm
at +27°C, heat shimmer	0.2 mm	0.5 mm	2.8 mm	not possible

Schauerte (1992) established the precision (in millimetres) of the staff reading with a Wild NA2000 digital level as ±(0.021 + 0.012 D[m]), where D is the sighting distance (in metres, not exceeding 35 m).

- The *repeatability of the distance measurement* is also distance dependent.

For the Wild NA2000 the repeatability of the distance measurements to the staff was once reported as <±3 mm for distances below 20 m, <±10 mm for sighting distances less than 40 m and ±10-30 mm for distances between 50 m and 100 m. These values give an indication of the trend with distance.

3.1.4 Bar Code Staffs

Originally, only glass fibre staffs (Wild GKNLE4) were available for the Wild NA2000. These staffs come in three sections of 1.35 m length each. The three plug-in sections give a total length of 4.05 m. Later, Leica added the invar staffs Wild GPCL3 and GPCL2 as options for the more accurate versions of the Wild NA2000 (e.g. Wild NA3000) and aluminium and wooden staffs for normal levelling. (Zeiss offers folding bar code staffs for their digital levels.)

3.1.4.1 Leica Normal Bar Code Staffs

The basic bar code element is 2.025 mm wide. The 4 m fibre glass staff features 2000 elements over 4050 mm. Leica uses a pseudo-stochastic code for their staffs. (Topcon and Zeiss use different coding principles.) On the reverse side, standard metric (10 mm) or imperial (0.1 feet) faces are available. The Wild instruments and staffs permit unique measurements for sighting distances between 1.8 m and 100 m. The manufacturer claims a coefficient of expansion of less than 10 ppm/°C for the fibre glass staffs. Based on practical measurements, the manufacturer reported coefficients of expansions of <8 ppm/°C and <0.2 ppm / (percent relative humidity).

The temperature coefficient of the fibre glass staff is worse than that of the traditional wooden staffs but better than that of aluminium staffs. On the other hand, the humidity coefficient of (poorly painted) wooden staffs can be much worse. Leica also sells 4 m wooden and aluminium staffs. The manufacturer quotes a coefficient of expansion of 10-20 ppm/°C for the former (depending on humidity) and 24 ppm/°C for the latter.

3.1.4.2 Leica Invar Bar Code Staffs

The bar code invar staffs are constructed in the same way as all modern invar staffs, namely with an invar ribbon recessed in an aluminium housing and a hardened and rust-free base plate. The usual length of the invar staffs supplied by Leica is 3.0 m or 2.0 m. (For industrial surveys, thin staffs of 60 cm, 92 cm and 182 cm length are also supplied.) The coefficient of expansion of these staffs is less than 1 ppm/°C. The errors of the individual bar code graduations (the basic interval is again 2.025 mm) are less than 10 μm because the bar code is manufactured with the aid of laser interferometry.

3.1.4.3 Errors of Normal Bar Code Staffs

The errors of the bar code staffs are no different from those of the traditional levelling staffs. These errors are listed for convenience. See surveying textbooks for a detailed discussion.

- Zero error
- Random errors of individual graduations
- Systematic graduation errors, e.g. scale errors in function of humidity, temperature and time
- Junction errors (of sectional, telescopic and folding staffs)
  Practical investigations have found errors of 0.1 mm to 1.0 mm across junctions of the Wild fibre glass sectional staff (!!!)
- Maladjustment of spot bubble
- Other errors such as bending, kinks

3.1.4.4 Errors of Invar Bar Code Staffs

The errors of invar bar code staffs are similar to those of classical invar staffs, which are also produced by modern manufacturing techniques (laser engraving under control of a laser interferometer). The support structure of modern invar staffs is made from aluminium and, thus, not sensitive to humidity changes.

It is expected that the coefficient of expansion is below the 1 ppm/°C level and the random graduation errors at the 10 μm level. Maurer & Schnädelbach (1995) quote an average coefficient of expansion of 0.75 ppm/°C for invar staffs manufactured after 1992. Although the coefficient of expansion is small, it varies from one staff to the next and needs to be calibrated for high precision levelling over large height differences.

3.1.5 Errors in Levelling with Digital Levels

The errors of digital levels are similar to those of automatic levels. Only a listing of most errors is given below. The readers are referred to textbooks for a complete discussion. The following books are suggested for further reading on this topic: Cooper, M. A. R. 1982, Modern Theodolites and

Levels, Granada, London, ISBN 0-246-11502-5, Sections 9.6 and 10, pp. 216-234 and Deumlich, F. 1982. Surveying Instruments, Walter de Gruyter, Berlin, ISBN 3-11-007765-5, pp. 179-211. The listing of the errors in levelling is based on the tables published by Schauerte (1993).

For general purpose levelling most errors of automatic and digital levelling instruments can be ignored. The collimation error must be considered, however, if the sighting distances in the foresight and backsight are not strictly the same. The scale errors of staffs and the refraction errors must be considered if large height differences are levelled. When using automatic and digital levels for precise levelling, all error sources must be considered. In consequence, the operator should be familiar with the properties of such levelling instruments.

3.1.5.1 Errors of Bar Code (Digital) Levels

• *Electronic Collimation Error*

Remedy: Observe strictly from the middle between the two adjacent staff set-ups (or determine the collimation error before and after the measurements and post-correct all measurements using the recorded sighting distances.) Note that this error is temperature and time dependent!

There is only one sure way of eliminating the effect of the collimation error on the height difference measured from one set-up: **set up in the middle**! This allows to use the same focus in BS and FS and avoids mechanical shocks between BS and FS.

Furthermore, the measuring procedures must be selected so that temperature changes at one set-up are minimised. If the **instrument is kept in the shade** at all times, there should not be any temperature induced changes of the collimation error between BS and FS.

• *Maladjustment of the Spot Bubble*

Remedy: At the beginning of a levelling run, **adjust the circular bubble** if it moves relative to its case when the instrument is turned around its vertical axis.

• *Compensation and Height Error* (leads to the 'obliquity of horizon')

Remedy: Observe in such a way that the error generates a systematic effect and eliminate it through an appropriate observation techniques such as the 'red trousers' method

BFFB (odd numbered set-ups)

FBBF (even numbered set-ups)

or the modified classical 'Wild-Zeiss' method

BFFB (at all set-ups)

(underlined = *level the spot bubble whilst the instrument is pointing to this staff*, B = *backsight*, F = *foresight*)

• *Measurements near the Top and Bottom of Staffs*

Digital levels are programmed to be able to measure near the bottom and top end of staffs since ordinary levels can measure to any graduation on a levelling staff. Users have found that digital levels can measure to a staff, even if the line of sight is slightly above the top end (or slightly below the bottom end) of a staff. Since the digital levels can use only half the measuring sector when measuring to the ends of staffs, the precision of staff readings near the ends of staffs may be reduced and systematic errors may occur.

Figure 3.9a shows some experimental results with a Leica NA3003 near the bottom end of a Leica invar staff. At 10 m sighting distance, the maximum error is about 0.4 mm and at 30 m, the error may be as large as 1.2 mm (even though the instrument displays staff readings to 0.01 mm). Figure 3.9b shows the field of view of the level should extend to a maximum of 20% (of the field of view diameter) above the highest useable staff graduation.

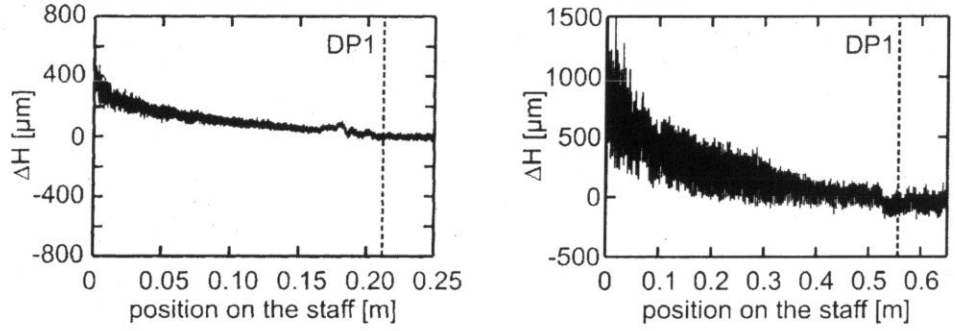

Figure 3.9a: Errors when measuring to the bottom end of a Leica invar staff with a digital level Leica NA3003 at a sighting distance of 10 m (left) and 30 m (right). For measurements to the right of the DP1 line, the full measuring sector falls on the staff. (after Woschitz 2003)

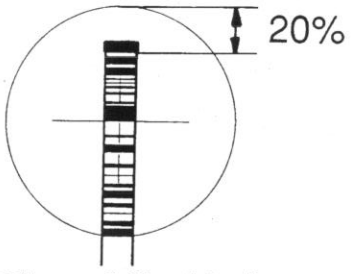

Figure 3.9b: Maximum reading on staffs as suggested by Leica for precise levelling with the NA2000/3000 series of digital levels (Leica 1996)

Figure 3.9c shows some experimental results with a Topcon DL-101C near the top end of a Topcon invar staff. At 10 m sighting distance, the maximum error is about 0.8 mm and at 30 m, the error may be as large as 0.7 mm. Note that, at 10 m, the staff readings are too small near the top end of the

staff and, at 30 m, too large. Woschitz (2003) recorded a gross error of more than 2 metres during a similar test at the bottom end of the Topcon staff. Figure 3.9c (after Woschitz 2003) indicates what range of staff readings should be avoided with Topcon digital levels near the top of 3 m Topcon digital levelling staffs.

Similar tests by Woschitz (2003) with a Zeiss(Trimble) DiNi11 digital level showed a maximum error of about 0.2 mm at 10 m and no errors at 30 m. Ingensand (2001) reported additional errors (to 0.2 mm) of Zeiss (Trimble) DiNi levels near the top end of staffs caused by artificial lighting in tunnels.

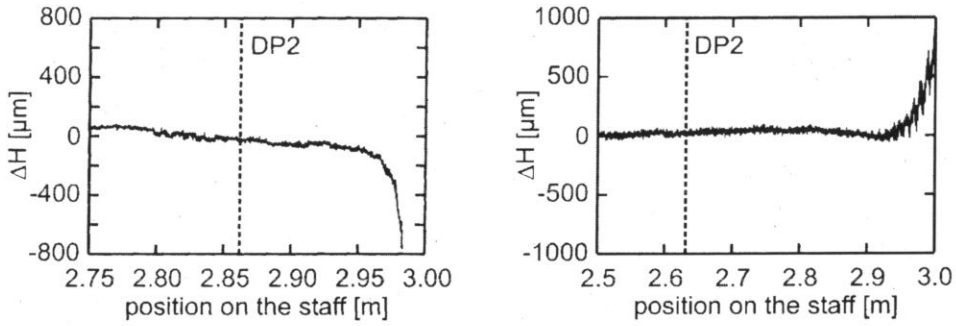

Figure 3.9c: Errors when measuring to the bottom end of a Topcon invar staff with a digital level Topcon DL-101C at a sighting distance of 10 m (left) and 30 m (right). For measurements to the left of the DP2 line, the full measuring sector falls on the staff. (after Woschitz 2003)

• *Systematic Staff Reading Errors*

Soon after the release of the first digital levels, periodic staff reading errors were noted at sighting distances of 15 m and 7.5 m. The effect was thoroughly investigated later by Woschitz (2003). Figure 3.9d shows how the errors of the staff reading change with height in line with the projected pixel size on the staff. The largest errors occur when the fundamental staff interval coincides with the (projected) pixel interval. The largest peak-to-peak variation of 0.81 mm occurs at 14.98 m. Similar effects are found at sighting distances of around 30 m and around 7.5 m. Equivalent tests in the 'extended system accuracy mode' showed reduced peak-to-peak variations of 0.30 mm (at 15 m). At other sighting distances, the peak-to-peak variation is much less, namely 0.1 to 0.2 mm in 'standard system accuracy mode'. Clearly, these sighting distances should be avoided when using the Wild/Leica NA200x/NA300x series of instruments for precise levelling.

Woschitz (2003) also investigated the systematic errors in Topcon digital levels. Some experimental results are shown in Fig. 3.9e. The error patterns at 5 m (and below) and 11 m (and above) are quite different. It is known that the Topcon digital levels change the way they derive the staff reading at about 9 m (Rüeger 2000).

Figure 3.9e seems to indicate that the short range measuring mode is free of systematic errors. At 7.0 m, the Topcon level seems to switch occasionally to the long range measuring mode. At 9.0 m, the level seems to switch continuously between short and long range mode. Woschitz determined a mean staff reading offset between the two modes of 0.19 mm. At sighting distances of 11 m and more, the Topcon levels show a periodic error pattern with a period of 300 mm and a peak-to-peak variation of 0.18 mm.

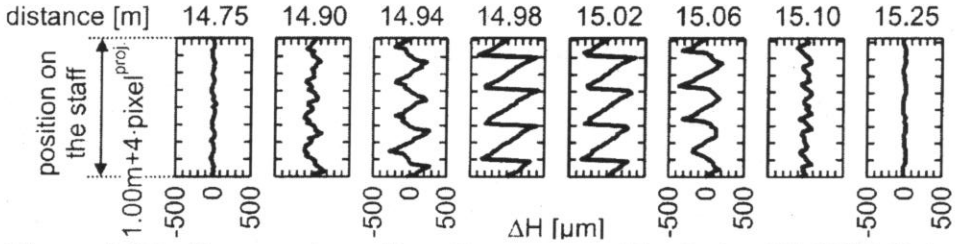

Figure 3.9d: Systematic staff reading errors with a Leica NA3003 digital level in 'standard system accuracy mode', at sighting distances near 15 m. (after Woschitz 2003)

The amplitude of the sine pattern decreases with distance and cannot be distinguished any more at about 30 m. In practice, sighting distances between, say, 7 m and 11 m should be avoided in precise levelling since one measurement may differ from another by 0.36 mm because of the switching between the two processing modes and the 'cyclic error' of the long range mode.

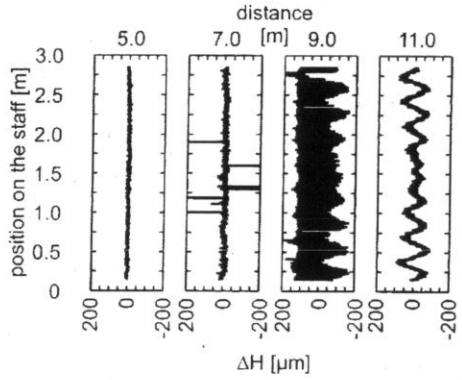

Figure 3.9e: Systematic staff reading errors with a Topcon DL-101C digital level at sighting distances from 5 m to 11 m. (after Woschitz 2003)

A Zeiss/Trimble DiNi11 was also investigated by Woschitz (2003). Periodic errors similar to those in Fig. 3.9d were found, but with much smaller amplitudes. Periodic patterns were found at 5 m, 9, 11 m, 19 m and 30 m. The maximum peak-to-peak variation of 0.1 mm was recorded at a sighting distance of 19 m. These errors are sufficiently small to be ignored in levelling practice.

• *Influences on the Setting Behaviour of the Compensator* (wind, traffic)

Remedy: Increase the number of staff readings: observe at least two backsight readings (BS) and two foresight readings (FS) so that the possible influences become evident in the two height difference (BS-FS) values. In precise levelling, one would measure, for example, BB FFFF BB or even B FF BB FF B.

• *Influence of Magnetic Fields* caused by direct or alternating currents

The magnetic field of the Earth has to be considered at all times. Additional fields are present near electrical installations (e.g. transformer stations). The effect of the Earth's magnetic field on compensators of levelling instruments was first reported in 1981. Laboratory tests at a field strength of 23000 nT (nanoTesla) established the following systematic errors of particular instruments for N-S levelling runs due to the Earth's magnetic field: Zeiss Ni2 - 0.2 mm/km; Wild NAK2 –> 0.5 mm/km; Zeiss Ni002–> 1.5 mm/km; Zeiss Ni1 –> 2.2 mm/km. Since 1982, all manufacturers have reduced the susceptibility of their instruments to magnetic fields by better shielding and/or the use of non-magnetic materials for the compensators. Post-1982 automatic levels (such as all digital levels) are likely to be much less affected by the Earth's magnetic field. Recent tests with a Wild NA3000 found a residual magnetic effect of 'only' 0.15 mm/km on N-S lines.

Remedy: Test in a laboratory if magnetic fields have an effect on the collimation error.

• *Temperature Effects on the Compensator and/or the Photo Detector/CCD Array* (e.g. due to lack of temperature acclimatisation or sun exposure during transport from set-up to set-up). Temperature may change the electronic collimation error and/or generate a vertical shift of the line of sight.

Remedy:

–> Shade the instrument at each set-up (and also during transport) with an umbrella.

–> Increase the number of measurements to the staffs so that jumps in the compensator's rest position can be detected in multiple BS-FS values.

–> Measure strictly from the middle between the forward and backward staff positions and use time-symmetric measurements for the BS and the FS, such as the 'red trousers' method or the modified 'Wild-Zeiss' method (see above).

• *Sinking of the Tripod*

Remedy: Employ a measurement sequence which features time-symmetric BS and FS measurements and do not set up instruments on warm bitumen surfaces.

3.1.5.2 Errors of Invar Bar Code Staffs

• *Graduation Errors in Invar Bar Code*

Remedy: As modern invar staffs are manufactured under laser interferometer control, only small random errors are to be expected. Because of the averaging over a large number of individual code elements, this small effect is reduced even further. In consequence, line-by-line calibration is not required.

• *Difference of the Zero Errors of the two Staffs* (in precise levelling)

Remedy: Use an even number of instrument set-ups between the bench marks (BMs) and always use the same staff for the connection to BMs. Do not change the staffs for the backwards run.

• *Change of the Length of the Bar Code due to Temperature*

(leads to variable height errors which depend on the staff reading)

Remedy:

– Calibrate the composite coefficient of expansion of the bar code scale (as the sum of the expansions of the invar ribbon and the aluminium case and changes in spring tension) with the staff in a vertical position. Alternatively, the data of a factory calibration may be used or an average value of +0.75ppm/°C (after Maurer & Schnädelbach 1995).

– Measure the temperature of the invar ribbon (e.g. at three heights above ground) of each staff and at each staff set-up and correct (post-mission) all staff readings accordingly using the appropriate coefficient of expansion.

• *Sinking of the Staff during the Observations from one Instrument Set-Up*

Remedy: Ensure a stable marking of the change points. Employ an observation schedule with time–symmetric BS-FS measurements.

• *Sinking of the Staff during the Move of the Instrument to the next Set-Up*

Remedy: Ensure a stable marking of the change points. This effect becomes evident in a comparison of the total height differences obtained in the forward and the backward runs. It cannot be eliminated by any other mean than a double run (–>,<–) levelling.

• *Skewness and Non-Flatness of the Foot Plate of the Staff ('Shoe')*

Remedy: Test the flatness of the foot plate of the staff. If large variations are detected, get foot plate changed. Minimise this effect (and the possible eccentricity between the optimal set-up point and the middle of the foot plate) by setting up of the staff at the point where the centre line of the invar ribbon intersects the foot plate. The manufacturer may provide a ring to achieve a correct set-up. (Not possible for BMs in walls.)

• *Maladjusted Spot Bubble of the Staff*

Remedy: Test the state of the adjustment prior to the measurements and adjust the spot bubble of the staff, if required. With invar levelling staffs, insure that the staff is set up so that the axis of the invar ribbon is in the centre of the benchmark or change plate. Refer also to Fig. 3.17 in the exercise section at the end of this chapter.

• *Movement of the Staff* (due to Wind or Traffic)

Remedy: It is essential to support of staff in two perpendicular directions. Buy optional struts or use two ranging rods (at right angle) for the purpose.

3.1.5.3 External Influences on Line of Sight

• *Grazing Rays (–> Levelling Refraction)*

Digital levels are likely to be more susceptible to refraction than other levels because they use graduations below the line of sight for the measurements. Apart of this, the digital levels suffer from the same refraction effects as all other levels. These effects may be summarised as follows (Angus-Leppan 1984):

– Levelling on a Plain: The refraction effect can amount to 1 mm over 50 m but is cancelled if the sighting distances to the foresight and the backsight staffs are strictly the same.

– Levelling on E–W Slopes: When going uphill, the foresight is more affected by refraction than the backsight. The effect is worst on gentle slopes where the slope still permits to maintain the tolerated maximum sighting distance. Errors in of 20 to 30 mm per 100 m height difference may occur. The signs of the errors in the rise and the descend over a hill are likely to be opposite so that the error may cancel in the height difference between points on both sides of the hill.

– Levelling on N-S Slopes: The refraction effects in ascend and descend no longer cancel because the sun is predominantly north or south, depending on the hemisphere. The accumulated errors vary depending on slope, season, climate and latitude; they can reach 50 mm to 1000 mm per 1000 km N-S levelling.

Recommendation: The horizontal line of sight should be more than 1 m above ground with the Wild NA2000/3000, as is uses ±0.18 m per 10 m above and below the horizontal line of sight. Reduce the sighting distance, if this condition is not fulfilled. This procedure ensures that the refraction effect with the Wild NA2000/NA3000 is not larger than with conventional levels. The refraction errors listed above may be reduced, but not cancelled, by this procedure.

• *Terrain below the Line of Sight*

Remedy: Rough surfaces (like grass) are preferred. Avoid measuring across bitumen and concrete surfaces.

• *Obstruction of Bar Code Section in Use*

Remedy: Ensure free observation sector. With the Wild NA2000/NA3000 no obstructions are tolerated at sighting distances of less than 5 m.

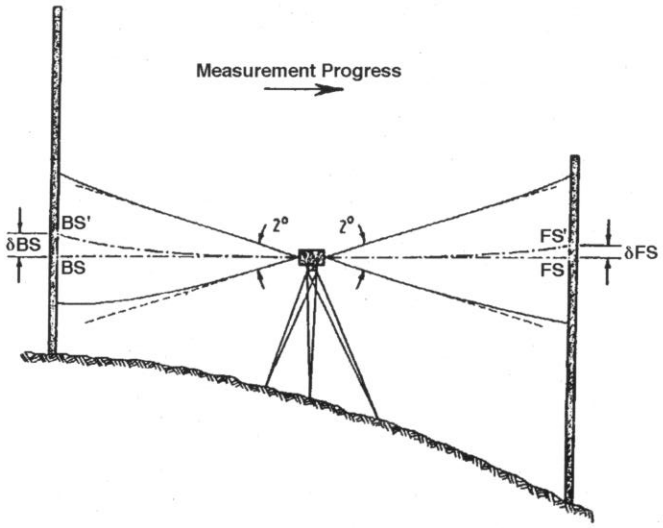

Figure 3.9f: Refraction effect on levelling on a slope. The errors caused by refraction are denoted by dBS and dFS. BS and FS are the true backsight and true foresight readings, respectively. BS' and FS' are the erroneous actual readings. The 2° angles indicate the viewing angle of the Wild NA2000/NA3000 digital levels. (after Schauerte 1993)

• *Sun Exposure* (–> heat shimmer)

Remedy: Select the optimal time of the day, the best season and the most appropriate weather conditions for any precise levelling.

• *Insufficient Illumination of the Staff*

Remedy: In poor light outdoors or under artificial lighting indoors (in tunnels, halls, buildings) the staffs must be illuminated with a lamp with 'daylight' spectrum.

3.1.5.4 Errors of the Observer

• *Inaccurate Focussing*

Remedy: The tolerance range for the focussing increases with distance. At sighting distances of less than 5 m, focussing errors can lead to 0.1 mm errors in height in Wild (Leica) NA200x/NA300x instruments. Woschitz (2003) noted that poor focussing with Zeiss (Trimble) levels increases the periodic error in these instruments. For example, a peak-to-peak variation of 0.21 mm is mentioned for a pointing of 0.5 m in front or behind the staff over 10.2 m.

• *Recording of Erroneous Observations* or omission of the recording of additional information

Remedy: Book such occurrences in handwritten notes or through the storage of additional information in the measurement file.

3.2 Laser Levels

Laser levels in general and rotating laser levels in particular have become an important surveying tool in building, construction and agriculture. In fact, rotating laser levels have almost replaced the classical levels on building and construction sites. This is reflected by the fact that most manufacturers of surveying equipment now produce rotating and other laser levels in great numbers. Although they are more expensive than the normal levelling instruments, they are much more efficient as they provide effectively a one-person levelling system. The rotating laser level consist of a tripod mounted instrument which, after levelling, rotates (about a vertical axis) a visible or infrared beam in a horizontal plane. It typically rotates at a rate of a few hundred revolutions per minute (rpm). Some models have adjustable rotation rates (e.g. between 0 and 500 rpm). In the case of visible (red) beams, the red dot can be seen on any surfaces 'hit' by the beam. For laser levels, that transmit an infrared beam, a special detector has to be used to detect the beam. A similar (or sometimes the same) detector can be used to increase the range and the precision of the visible beam instruments.

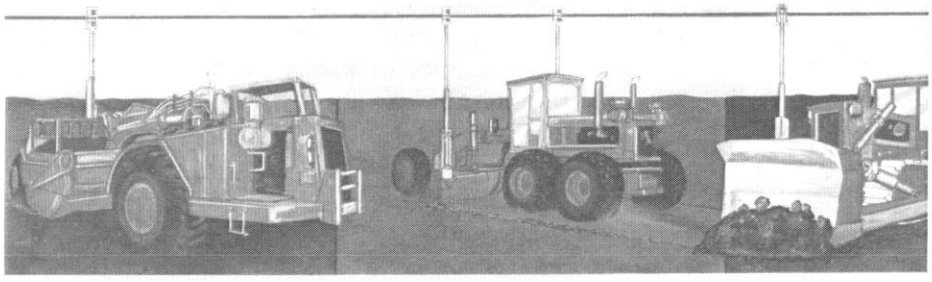

Figure 3.10: Use of laser levels in construction and agriculture (after Laser Alignment Inc 1986)

This detector is usually moved up and down a wall or a levelling staff until the detector is centred on the horizontal laser plane. Most detectors provide up-down guidance in visual and acoustic form to assist the centring and to provide better precision. For example, the detector may generate a fast beeping noise, if it has to be moved down to the laser plane, a slow beeping noise, if it has to be moved up, and a continuous tone if it is centred on the horizontal plane. Some detectors may provide different sensitivity settings. A high sensitivity provides higher accuracy under good measuring conditions (e.g. short range, indoor). For their LPD2 detector, Leica quotes a setting precision of ±0.8 mm for the high sensitivity setting and ±2.4 mm

for the low sensitivity setting (long range, outdoors). The overall accuracy of a well adjusted rotating laser level is quoted by Leica as ±2 mm at 50 m and ±4 mm at 100 m. Some building site rotating laser levels can be mounted horizontally to provide a vertical reference plane.

Outside building sites, laser levels can be used to guide or control precision grading machines in construction work (excavators, graders, bulldozers, scrapers) with horizontal, single or dual grade surfaces. These laser levels typically operate over longer ranges than those on building sites and can be set to mark non-horizontal planes. The detectors are mounted on the cutting tools and the results displayed in the drivers cabin. Another use of these devices is for land forming in agriculture, again with horizontal, single or dual grade surfaces.

The range of laser levels depends on the output power of the lasers or laser diodes used, on the atmospheric conditions and on the sensitivity of the laser detector used; it can be as much as 450 m. All systems have a much larger range at night. At longer distances, the effects of earth curvature and, in particular, refraction must be considered. This aspect will be discussed later.

Laser levels come in many forms and are not restricted to rotating laser levels. Linear laser levels are used for pipe laying, for example. They fit into pipes and project a laser beam at a selectable gradient. Pipe laying lasers provide not only the levelling but also the alignment of the pipes.

The simplest form of laser levels are hand-held and project a laser beam parallel to the principle axis of an attached tubular level. If the bubble of the tubular level is centred, the beam is horizontal. Mounting the pocket laser level on a (horizontal) swivel base permits to project a horizontal plane. Attachment of a right angle beam splitter even allows the setting out of right angles. The figure below shows one of these simple devices.

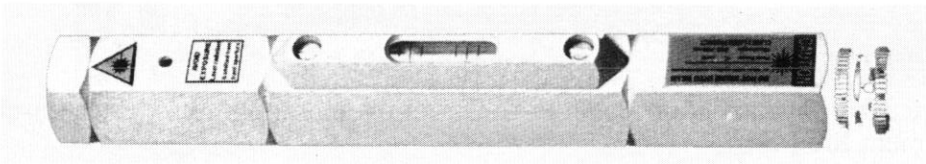

Figure 3.11: Pocket Laser Level with a visible laser diode emitting at 635 nm, 150 mm long, daytime range 30 m (after Leica Instruments Australia)

3.2.1 Construction of a Rotating Laser Level

Figure 3.12 shows the cross-section through a typical rotating laser level (Telamat by the German company Theis). The infrared beam is produced by a GaAlAs diode (nominal wavelength 780 nm, output power 0.3 mW) at the

bottom of the housing. This diode is in the focal point of the two-lens objective directly above it. The figure shows also one of the two adjustment screws for the diode. (If the instrument is out of adjustment, these adjustment screws can be used to make the laser beam horizontal in two perpendicular planes.) The laser beam travels straight up, through the lens system and to the pentagonal prism. This prism deviates the beam by 90° and rotates at a few revolutions per second. A belt connects the rotating part to the drive motor. The horizontal beam leaves through the glass plates on all sides. These glass plates protect the rotating part form the elements.

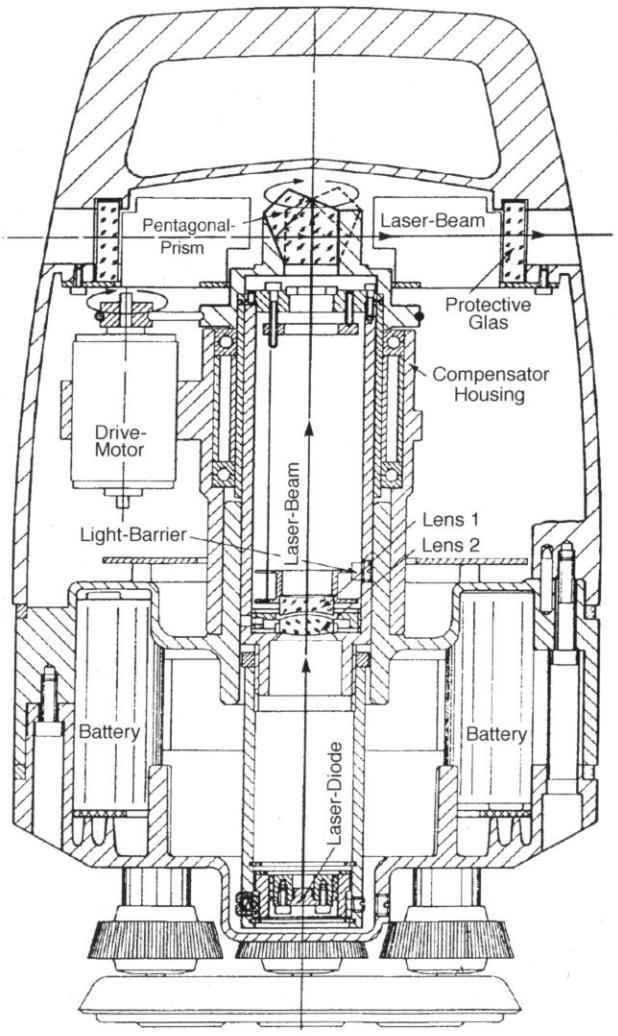

Figure 3.12: Cross-Section through a rotating laser level Theis Telamat (after Wüller 1988)

Figure 3.12 also shows that the upper (concave) lens is suspended on wires, which are attached below the rotating prism. The hanging lens acts like a two-dimensional pendulum and is used as a so-called compensator. Like in

the traditional automatic levelling instruments and the newer bar code levels, the compensator compensates the laser beam for any small non-verticality of the case of the instrument, which is typically levelled by a spot bubble (circular level) only. Light barriers check if the pendulum is freely hanging. Most instruments will not operate until the instrument is levelled accurately with the aid of the spot bubble.

The instrument shown has rechargeable batteries on-board, which can be charged with the appropriate charger and cables. Most manufacturers also provide cable connections and, sometimes, DC/DC converters for running the laser levels of 12 V car batteries. The range of the level is quoted as at least 120 m.

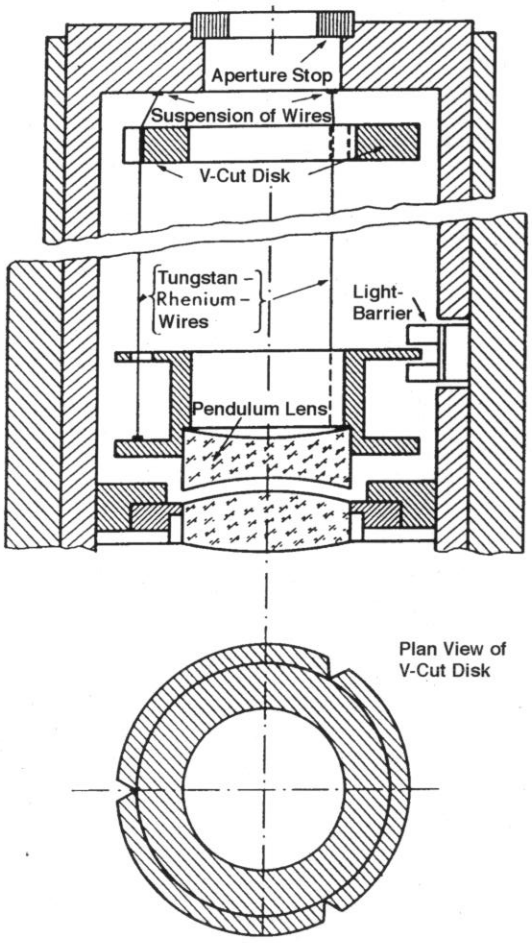

Figure 3.13: Cross-Section through the compensator of the Theis laser level Telamat (after Wüller 1988)

3.2.2 Design of a Two-Axis Compensator of a Rotating Laser Level

A more detailed diagram of the compensator of the Theis laser level 'Telamat' is given in Fig. 3.13. Figure 3.13 shows that three wires support the pendulum lens. The correct spacing and orientation of the wires is provided by the disk with the three V-cuts. The pendulum features magnetic damping and has a working range of 0.5 degrees of arc.

Figure 3.14 explains the working principle of the two-axis compensator. The beam axis of the laser diode is not coincident with the plumbline through the diode because of the small residual dislevelment α of the instrument after levelling with the spot bubble. In consequence, the laser beam travels at an angle of α to the plumbline towards the suspension point P of the concave pendulum lens. (In a perfectly levelled instrument, the point P would be strictly above the diode.) The laser beam is then refracted in the pendulum lens. Because of the type of suspension used, the plane of the pendulum lens is at right angle to the line between the diode and the suspension point P. The centre of the lens is directly below the suspension point P. Knowing this, the focal point of the lens can be plotted at the focal distance f from the centre of the lens. Because the incident beam from the diode is parallel to the optical axis of the lens (see 'f' in figure), the laser beam exits in a direction defined by the focal point and the point of intersection between the plane of the lens and the incident laser beam. It follows from the figure that the laser beam is 'bent' by an angle β (rather than the dislevelment angle α) at the lens.

3.2.3 Major Errors of Rotating Laser Levels

3.2.3.1 Compensation Error

The compensator of the laser level corrects most of the dislevelment. Some small residual error $(\alpha - \beta)$ remains. This *compensation error* $(\alpha - \beta)$ causes the laser beam rotate in an oblique plane at an angle of $(\alpha - \beta)$ against the horizon. This is sometimes referred to as *obliquity of horizon*. The relationship between the α and β follows from Figure 3.14 as (Wüller 1988):

$$x = PL \sin\alpha = f \tan\beta \tag{3.3}$$

$$\beta = \arctan\{(PL/f) \sin\alpha \tag{3.4}$$

$$\alpha - \beta = \alpha - \arctan\{(PL/f) \sin\alpha\} \tag{3.5}$$

Equation 3.5 shows that β becomes zero for zero dislevelment α. Considering the close agreement between tan and sin values for small

angles, the angle β would always be close to α and the compensation error very small. Further, the designer can select the fraction (PL/f) in such a way that the compensation error is reduced further. However, as Fig. 3.14 and Eq. (3.5) show, the distance PL has to be close to the focal distance f. In the case of the WILD LNA2, the obliquity of horizon is adjusted if (α − β) exceeds 1.25 mm over 30 m (8.6 seconds of arc).

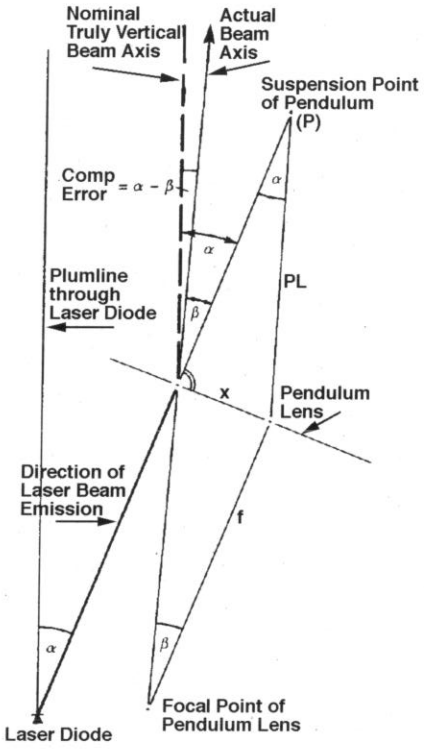

Figure 3.14: Two-axis compensator principle in Theis rotating laser level Telamat (after Wüller 1988)

3.2.3.2 Adjustment Conditions of Rotating Laser Level

Before the adjustment conditions of a rotation laser level can be introduced, three axes need to be defined. The *centre of the beam* is the centre of gravity of the beam intensity in the plane perpendicular to ray. The laser *beam axis* is the line between the centre of the beam at the target and the centre of the beam in the (rotating) pentagonal prism (or mirror). (This laser beam axis corresponds to the 'line of sight' of ordinary levelling instruments.) The *rotation axis* is the axis of rotation of the pentagonal prism or mirror assembly and corresponds to the 'vertical axis' of theodolites.

An rotating laser level is in perfect adjustment when:

- the axis of the pentagonal prism coincides with the rotation axis,
- the radiation axis of the (infrared or visible) laser diode coincides with the rotation axis,

- the optical axis of the biconvex lens coincides with the rotation axis.

The first two adjustment conditions are illustrated below in Figs. 3.15 and 3.16. The non-coincidence of the two respective axes is described by an linear eccentricity error and an angular misalignment. It is evident from Fig. 3.15 that, both, the eccentricity and the angular misalignment of prism and laser beam axes have no effect on the definition of a horizontal plane.

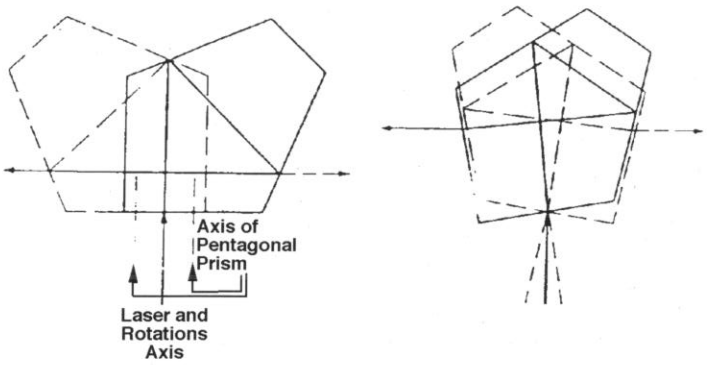

Figure 3.15: Effects of the non-coincidence of the axis of the pentagonal prism and the rotation axis. Left: Effect of the eccentricity of the axis of the pentagonal prism relative to the rotation and the laser axes; Right: Effect of the angular misalignment between the axis of the pentagonal prism and the laser and rotation axes. (after Noack 1989)

The non-coincidence of the laser beam and the rotation axes in Fig. 3.16 are more significant. The eccentricity e of the laser beam relative to the rotation axis of the prism causes the horizontal plane projected by the laser beam to change its height by 2e over a 360° rotation of the prism. In the Theis Telamat, this *height error* is minimised by an aperture stop below the rotating prism. The angular misalignment ε of the laser beam relative to the rotation axis of the prism causes a tilt of the projected laser plane of the same angle ε and a height shift of the beam of 2k over a 360° rotation of the prism. The beam shift of 2k can be computed from the dimensions of the pentagonal prism and the incident angle ε. Considering the principle of the compensator shown in Fig. 3.14, is evident that ε corresponds to the angle β and is very close to the angle α (the dislevelment of the laser level). After accurate levelling of the laser level with a spot bubble, ε should not exceed a few minutes of arc and would cause a minimal height error k.

3.2.3.3 Misalignment of a Rotating Mirror

If the rotating laser level is equipped with a rotating mirror (at 45° to the rotating axis) rather than a rotating pentagonal prism, then any error in the 45° angle will generate an error which is analogous to a collimation error in a ordinary level. The laser beam will travel on a conical rather than plane surface. The Spectra Physics EL-1 Electronic Level System is such an instrument.

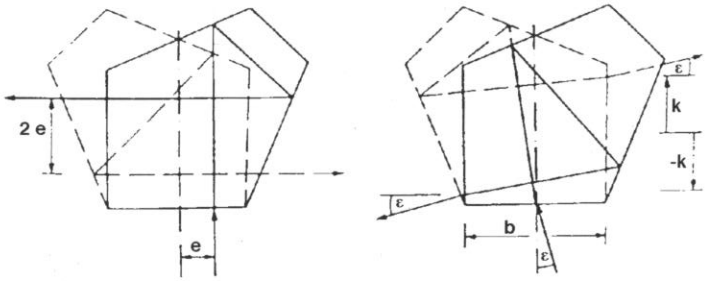

Figure 3.16: Effect of the non-coincidence of the laser beam and the rotation axis. Left: Effect of eccentricity e of laser beam relative to the rotation axis. The resulting height error amounts to ±e. Right: Effect of the angular misalignment ε of the laser beam relative to the rotation axis. The magnitude of the resulting height error is ±k. (after Noack 1989)

3.2.3.4 Secondary Height Error

Because the intensity distribution across the originally vertical laser beam is not uniform, different parts of the beam will be used by the laser detectors depending on azimuth to derive the up-down information. For the Theis Telamat the peak-to-peak variation due to this error is stated as less than 0.5 mm.

3.2.4 Calibration of Rotating Laser Levels

As the main part of rotating laser levels cannot be rotated about a vertical axis and as two components (x-y) of the compensator must be checked, the tests known from the traditional levels (e.g. Two-Peg-Test) cannot be used. The procedure outlined here only gives the principle for the testing and adjustment of the horizontal laser plane. The manufacturers of particular instruments will prescribe the exact procedures to be used.

- Set up the tripod 30 m from a house wall and make the tripod's top surface truly horizontal (in two vertical planes) by using a carpenters level. To check the latter, all readings with the carpenters level should be taken in 'two faces' (and the mean readings used). Extend and retract the adjustable tripod legs to get the tripod top truly horizontal.

- Define two vertical planes through the laser level which are at right angles to each other. Use features of the laser level to distinguish between the x and the y planes.

- Point the positive x-axis to the wall, level the instrument and switch it on. Move the detector up and down until it is centred on the beam. Mark this

position, say with X1. Rotate the laser level by 180° (till the negative x axis points to the wall). Do not touch the footscrews in this process. Mark the position of the beam on the wall with X2. For the laser level Wild LNA2, the manufacturer suggests that the x-component of the instrument be adjusted if the distance between X1 and X2 exceeds 2.5 mm (at 30 m). To do so, mark the half-way point between X1 and X2, centre the detector on it and adjust the x-component of the compensator as specified by the manufacturer until the beam is centred on the detector.

• Turn the laser level by 90° and level it by centring the spot bubble. Proceed with the adjustment of the y-component of the compensator as discussed above for the x-component.

3.2.5 Computation of Heights, Earth Curvature and Refraction

It is known from the theory of trigonometric heighting (see Rüeger 1990, pp. 108 to 114, for example) that the (ground) elevation H_T of a target station can be obtained from the (ground) elevation H_{LL} of the laser level station for a line of sight which is strictly horizontal at the laser level station as follows:

$$H_T = H_{LL} + h_{LL} - h_T + \frac{1}{2R} d^2 - \frac{k}{2R} d^2 \qquad (3.6)$$

It is important to realise that the above formula gives 'heights above sea level' or 'levelled heights'. This means that water between points of the same elevation would not flow. As in traditional levelling, the laser level is usually not set up over a mark of known height. Instead, the elevation of the laser beam plane (traditionally referred to as 'collimation height') is determined backward, by setting up the laser detector on a mark of known height. In the absence of earth curvature and refraction effects, the collimation height is obtained as

Collimation Height = Elevation of reference mark + height of detector over reference mark (3.7)

Therefore, the formula for the (ground) elevation H_T at the target point can be simplified to

$$H_T = \text{Collimation Height} - h_T + \frac{1}{2R} d^2 - \frac{k}{2R} d^2 \qquad (3.8)$$

where h_T is the height of the detector above the mark (ground) at the target station, R is the earth's radius (e.g. 6370100 m for New South Wales) and k is the coefficient of refraction. The third term on the right hand side is the

correction for *earth curvature.* This correction is positive because the spherical earth curves away from the horizontal laser beam. The laser plane is a parallel to a tangential plane to the spherical earth at the laser level station. The forth term on the right hand side corrects for the effects of *vertical refraction.* On clear sunny days close to the ground, the coefficient of refraction k is strongly negative (down to k = –3). This means that the laser plane is no longer a plane but a paraboloid pointing upwards. The offset from the horizontal plane increases with the square of the distance from the laser level. On clear nights, the coefficient of refraction is strongly positive (up to k = +3) , which means that the laser plane is bent downwards, towards the ground. The table below gives an indication of the magnitude of the effects of earth curvature and refraction.

Distance	50 m	100 m	200 m	300 m	400 m	500 m
	mm	mm	mm	mm	mm	mm
Earth Curv Corr	+0.2	+0.8	+3.1	+7.1	+12.6	+19.6
Refr Corr k=–3	+0.6	+2.4	+9.4	+21.2	+37.7	+58.9
Refr Corr k=–2	+0.4	+1.6	+6.3	+14.1	+25.1	+39.2
Refr Corr k=–1	+0.2	+0.8	+3.1	+7.1	+12.6	+19.6
Refr Corr k=0	0.0	0.0	0.0	0.0	0.0	0.0
Refr Corr k=+1	–0.2	–0.8	–3.1	–7.1	–12.6	–19.6
Refr Corr k=+2	–0.4	–1.6	–6.3	–14.1	–25.1	–39.2
Refr Corr k=+3	–0.6	–2.4	–9.4	–21.2	–37.7	–58.9

Table 3.1: Sample corrections of the elevation H_T of the target point for earth curvature and refraction in function of the distance from the rotating laser level. The coefficient of refraction is denoted by k.

Equation (3.8) can be written in a form where the corrections for refraction and earth curvature are applied directly to the height h_T of the laser detector at the target station

$$H_T = \text{Collimation Height} - \{h_T - \frac{1}{2R} d^2 + \frac{k}{2R} d^2\} \qquad (3.9)$$

This form shows that earth curvature causes the h_T readings always to be too large. Vertical refraction causes the h_T readings to be too small when the coefficient of refraction is positive (typically at night) and too large if the coefficient of refraction k is negative (typically during daytime).

On building sites, where the operating radius of laser levels if often below 50 m, the effects of refraction and earth curvature can be ignored. At a radius of 100 m, the corrections are still below the typical system accuracy of laser levels (±4 - 6 mm). At 400 m radius, the corrections do reach and exceed the laser level system accuracy (about ±16 to 24 mm).

For practical reasons, the above corrections are usually ignored even for the large radii used in land forming operations, for example. The effect of omitting these corrections are best explained with the aid of an example. Let us assume that a grader is used to prepared a horizontal surface of 800 by 800 m. In this case, the cutting blade of the grader would be set so that $h_T = h_{LL}$, assuming that the laser level is set up in the middle of the surface. In the absence of refraction, the graded surface would be strictly parallel to the laser plane. This means, in terms of sea level elevations, that the ground at 400 m from the level would be 12.6 mm 'higher' than the ground at the laser level. Water would therefore flow towards the laser level.

If we assume that this earth work was carried out during the night with the laser level set up very close to the ground (k = +3.0), then the ground at 400 m from the laser level could be 25 mm 'lower' than the ground near the laser level. If one were to check the night-time grading later on a clear sunny day, with the laser level again close to the ground (k = -3.0), then one might note that the ground at 400 m is 75.4 mm (2x37.7 mm) 'lower' than expected, that is 75.4 mm lower than the ground would have been if graded on a sunny day. (If the grading were carried out on a sunny day with h_T set equal to h_{LL}, then the ground at 400 m from the laser level would be 50 mm too high.)

The fact that the laser beam may wander 100 mm up and down between day and night over 500 m due to refraction must be considered if some work is carried out during the day and some during the night. *Refraction effects can be reduced by setting the rotating laser level as high as possible above ground and by measuring during windy, overcast days or around sunrise and sunset, when the coefficient of refraction is close to zero.*

3.3 Exercises

3.1 Name and discuss three key differences between digital (bar code) and conventional automatic levelling instruments.

3.2 Like conventional automatic levels, digital levels use compensators to make the line of sight horizontal even though the vertical axis might be out of plumb by a small amount.
Name three errors caused by the compensator and how they may be 'eliminated' in precise levelling.

3.3 The figure below highlights the effect of the contact point between invar staff and bench mark not being exactly in the axis of the invar ribbon. The actual staff reading L' does not correspond to the vertical separation L between the line of sight and the top of the bench mark.

(a) Derive an equation for the staff reading error δh as a function of L, e and the staff tilt α noting that $L' = L + \delta h$.

(b) What is the error δh if L = 2.600 m, α = 10' and e = 32 mm?

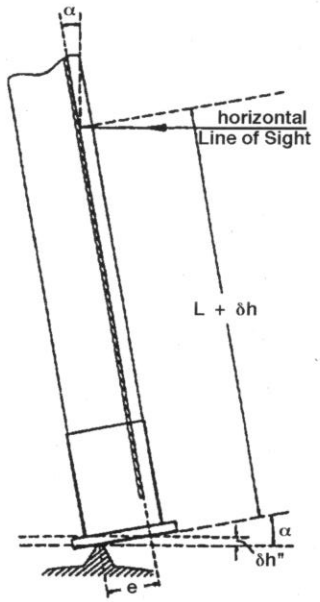

Figure 3.17: Error δh in a reading ($L' = L + \delta h$) on an invar staff due to the tilt of the staff (α) and the eccentricity (e) between the contact point (on the bench mark) and the axis of the invar ribbon. (after Schauerte 1995)

3.4 You have been asked to determine the heights of three bench marks (BMs), namely BM A at the foot of a hill on the eastern side, BM B on top of the hill and BM C at the foot of the hill on the western side. On a clear summer day, you then level from A to B, from B to C and from C back to A around the base of the hill. The misclosure in the level loop is consistent with the accuracy of the equipment and the techniques used. However, you are concerned about possible refraction effect.

(a) Explain why refraction can affect the height of BM B even though the loop misclosure was found to be effectively zero.

(b) By how much could the height of BM B be in error if BM B is 500 m higher than the BMs A and C?

3.5 You instruct a survey party to level a bench mark at the bottom of an open cut mine relative to a bench mark (of given height) on the rim of the mine. The field party uses a digital level with an aluminium bar code staff on a day with an ambient temperature of +40°C. The height difference of

about 500 m is measured forward and backwards. The height of the BM at the bottom of the pit is obtained as H = 23.148 m.

(a) Six months later, the level run is repeated with the same equipment, but at an ambient temperature of +10°C. Assuming that both bench marks were not subjected to ground movements or settlements, what elevation would you expect to find for the bench mark at the bottom of the pit?

(b) Assuming that the staffs are at nominal length at +20°C, what would the most likely height of the bench mark at the bottom of the pit be?

(c) The mine management wants you to determine all BM heights to ±10 mm or better. What type of staff will you use in future:

(i) on the (natural) plain around the mine pit?

(ii) to level down into the pit?

Explain your selection.

3.6 In the context of the levelling of the Australian continent in the 1960s, the line from Brisbane to Cairns (about 2000 km) was levelled. Large differences were found when connecting to tide gauges along the coast. Figure 3.18 shows the mean sea level heights as determined from a free continental adjustment (solid line) and from unadjusted orthometrically corrected observed heights (non-adjusted).

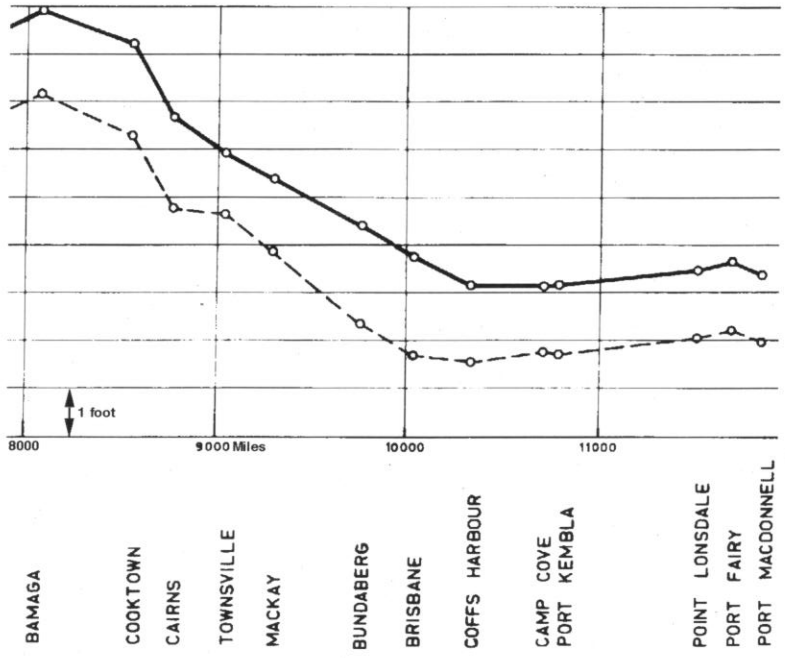

Figure 3.18: Mean sea level heights as determined from a free continental adjustment (solid line) and from unadjusted orthometrically corrected observed heights (non-adjusted) (after Roelse et al. 1975, Annex C)

Explain the likely magnitude of refraction and magnetic field errors, assuming that first generation automatic levels (e.g. Zeiss Ni2) and long sighting distances (90 m) were used.

3.7 Any levelling of importance is done in double runs, that is forward and backward. This provides the only rigorous check in levelling where the over-determination (redundancy) of measurements is, by default, quite poor. Apart from improving the precision and quality assurance, double runs also eliminate some systematic levelling errors.
Explain why the 'sinking of the staff during the move of the instrument to the next set-up' is cancelled (on average) in the mean of the forward and backward height difference.
(Hint: Draw two consecutive instrument set-ups (and three consecutive staff set-ups) on sloping ground and assume some staff readings. Analyse the height differences in the forward and return direction, noting that height differences are computed as backsight BS minus foresight FS and that the staff common to both instrument set-ups sinks by a certain amount during the move on the instrument.)

3.8 Describe a few possible surveying tasks that could be carried out on a building site with a rotating laser level.

3.9 On a building site, you have been asked to check the level of the form work of a reinforced concrete plate. To do so, you set up the rotating laser level on the form work and you adjust the laser detector to the laser plane at Bench Mark A (Reduced Level = 67.045 m), getting a staff reading of 4.613 m. Similarly, at Bench Mark B (Reduced Level = 68.919 m) a staff reading of 2.738 m is obtained.
(a) What is the collimation height of your laser level?
(b) What staff reading do you expect to get for points on the formwork if the bottom edge of the concrete plate is at a reduced level of 70.100 m?

3.10 On the basis of Fig. 3.14, explain why the laser beam travels in an oblique plane in the presence of a compensation error.

3.11 Draw a cross-section through a rotating laser level in the middle of a field of 500 m radius. Using a horizontal scale of 1:10000 and a vertical scale of 1:2, plot:
(a) how the spherical earth deviates from a tangential plane through the laser level,
(b) the curve described by the laser beam in case of a coefficient of refraction of $k = +3.0$,
(c) the curve described by the laser beam in case of a coefficient of refraction of $k = -3.0$.

3.12 Figure 3.19 shows two orientations of a rotating laser level, before and after rotation by 180° about a plumbline on a strictly horizontal tripod top.

(a) in both diagrams, draw the ray path through the laser level from the erroneous positions of the laser diode (see empty diode symbols).

(b) Explain how the tilts of the laser beams exiting to the right from the rotating prism differ in the two diagrams.

(c) Discuss how this difference can be used to calibrate the rotating laser

(d) Elaborate on why it is essential that the tripod head is perfectly horizontal (= level) during such a calibration.

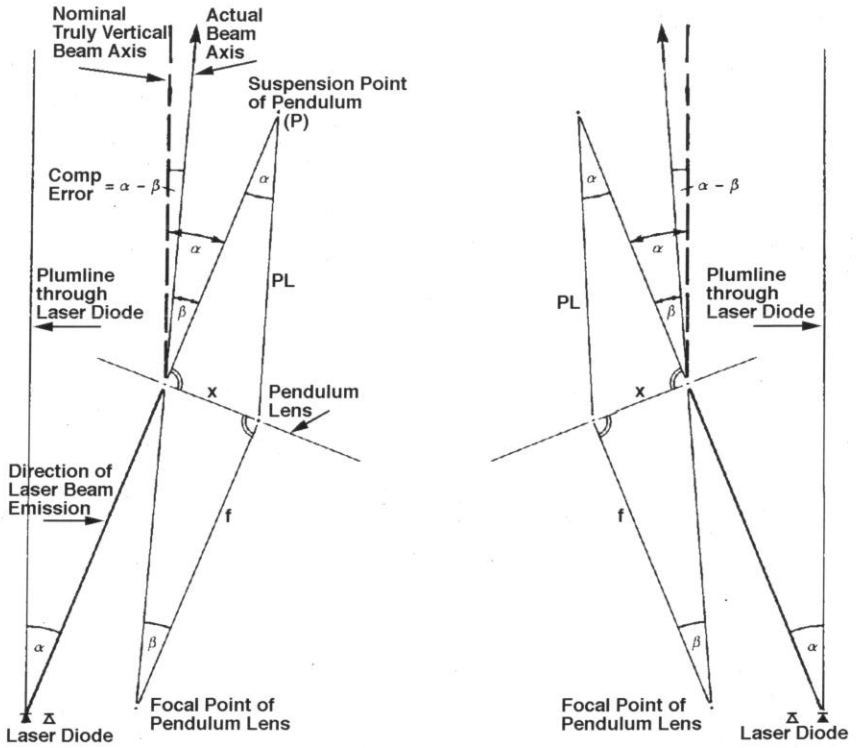

Figure 3.19: Two orientations of a rotating laser level, before and after rotation by 180° about the plumbline, on a strictly horizontal tripod top

3.13 You instructed a crew with earth moving equipment to level a field of 400 m radius around a laser level set up. The work was then carried out at night.

Later you check the work by geodetic levelling (with 50 m sighting distances) from the laser set-up to the edge of the field 400 m away.

What height difference, obtained in your levelling run, between the centre and the edge of the (nominally horizontal) field would you tolerate?

Give reasons!

4. Electronic Theodolites and Tacheometers

4.1 Types of Electronic Theodolites and Tacheometers

In the discussion below, the term 'theodolite' is used in a very broad sense. The term is applied to all devices which measure horizontal directions and zenith angles by electronic means.

This chapter deals only with the angular measurement section of electronic theodolites and tacheometers. For a complete discussion of the electronic distance measurement (EDM) aspects of electronic tacheometers, the reader is referred to the EDM textbook by Rüeger (1990 1996). The special aspects of 'reflectorless' EDM are, however, discussed in Sections 4.1.8 and 5.1.

4.1.1 Electronic Theodolites

The electronic theodolites are replacing the optical theodolites which do require a visual reading of the glass circles and do not permit real-time electronic data recording. Electronic theodolites are easier to use as the circles are read electronically and the angles displayed on a read-out screen. All electronic and optical theodolites can measure horizontal directions and zenith angles as well as distances by stadia (fixed-hair vertical staff tacheometry with the aid of the stadia hairs on the reticle).

4.1.2 Electronic Tacheometers

The electronic tacheometers (sometimes referred to as 'total stations') are replacing the older optical tacheometers (optical theodolites specialised for optical distance measurement). The latter permitted optical distance measurement with an accuracy of between ±10 mm (horizontal staff tacheometry) and ±100 mm (vertical staff tacheometry), depending on the principle used. Horizontal staff tacheometry was never widely used in Australia. Electronic tacheometers are electronic theodolites with a built-in electronic distance meter. They measure horizontal directions, zenith angles and slope distances. Using the on-board computer, height differences and horizontal distances can be computed and displayed. The electronic tacheometers can measure distances more easily and more accurately than optical tacheometers. Also, much longer distances can be measured, typically 1 to 2 km to a single prism reflector. Because of the on-board distance meter, most electronic tacheometers do not have stadia hairs on the reticle.

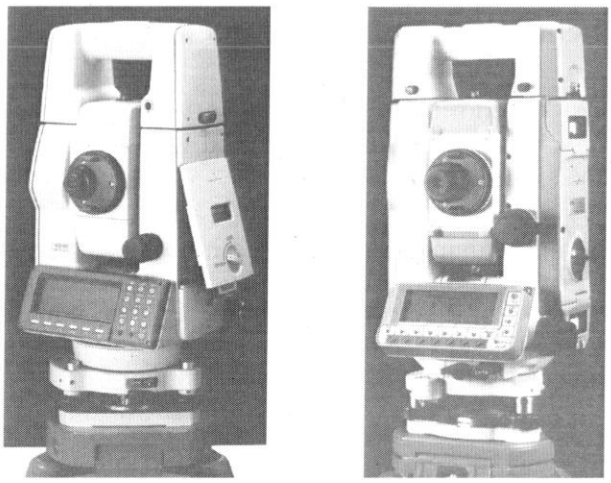

Figure 4.1: Two electronic tacheometers; Topcon GTS-701 on the left and Nikon DTM-720 on the right. Both instruments store data on PC-cards which slide into the side panels.

The first electronic tacheometers (or 'total stations') were the Zeiss Reg ELTA 14 (released in 1970) and the AGA Geodimeter 700 (released in 1971). These instruments were quite large and heavy. At that time, data recording was on paper tape (like in telex machines) with the Reg ELTA 14 and on (audio) cassette tapes with the Geodimeter 700. A second generation of instruments was released around 1978 by Hewlett-Packard, Wild and Zeiss, with the Zeiss Elta 2 being the first instrument with slide-in memory modules (RAM) for data recording. Today, all manufacturers of surveying instruments are producing electronic tacheometers and electronic theodolites. Most instruments sold are, however, electronic tacheometers

because they allow the three-dimensional coordination of points from a single instrument set-up. (Naturally, all professionals will survey important points from two different stations, for quality assurance purposes and to improve the precision by taking the mean of the two solutions.)

Electronic tacheometers have become the workhorses of surveyors and geomatic engineers for detail and contour surveys, for control surveys and for setting-out work. EDM-Height Traversing with electronic tacheometers can replace the traditional line levelling with levelling instruments (see Rüeger 1995 and Rüeger & Brunner 1981). On slopes, EDM-Height Traversing is much less affected by refraction than line levelling. Some survey work presently carried out with electronic tacheometers will eventually be replaced by GPS survey techniques, at least where GPS signals can be received. This change is likely to happen as soon as GPS techniques can compete in terms of ease of operation, efficiency, quality assurance and cost.

4.1.3 Gyro-Theodolites

The integral gyrotheodolites and the gyroscope attachments are replacing the earlier (magnetic) compass theodolites and theodolite attachments. Compass theodolites were capable of measuring magnetic bearings to ±1 minute of arc at best. Tubular compass attachments are still available for some instruments to give magnetic bearings and, in fact, may be used for the provisional orientation of gyrotheodolites to true north. The magnetic declination must be considered when using a magnetic compass for this purpose.

After approximate orientation to geographic ('true') north, the north-seeking gyroscope determines the direction to geographic north. Once the horizontal direction to north is established, other points can be sighted to. The clockwise angle between the direction to north and the direction to another point is called azimuth. The azimuth is obtained simply by taking the difference of the directions to the point and to north.

Two types of gyrotheodolites are available. The most precise gyrotheodolites are integrated instruments, such as the Sokkia AGP1 Auto Gyro Station and the DMT Gyromat *2000* by the Deutsche Montan Technologie. Both gyrotheodolites are based on the Gyromat design and give true north to ±6 seconds of arc in about 6 minutes of time. These precision gyrotheodolites are semi-automatic and are used widely underground in tunnels or mines. In long tunnels, the measurement of the azimuths of well distributed lines in traverses greatly improves the lateral precision (across-track) of such underground traverses. For example, the Gyromat 2000 gyrotheodolites were successfully used in the 42 km long tunnel between England and France.

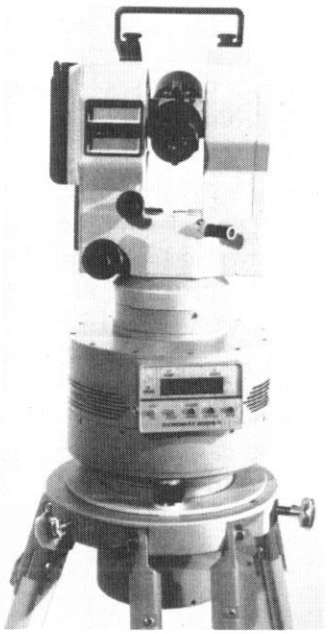

Figure 4.2: Gyromat 2000 with attached Zeiss electronic theodolite. Please note that this particular gyrotheodolite does not fit standard tribrachs or tripods.

Gyro attachments were available for a number of optical and, later, electronic theodolites. These were typically mounted on a bridge between the two standards of the host theodolites. The Wild GAK1 gyro attachment gives true north to ±20 seconds of arc in 20 minutes. A similar accuracy is quoted for the Sokkia GP1-2 Gyro Station (Electronic tacheometer SET 3 with GP1 Gyroscope attachment). The measurements with the gyro attachments are manual and require some skills of the observer.

4.1.4 Motorised Electronic Tacheometers

Motorised (servo-driven) electronic tacheometers and theodolites can be configured and used in many ways. Figure 4.3 gives an indication of the various implementations of servo-technology using the example of the Geodimeter Model 600. This servo-instrument offers different operating modes. 'Conventional Surveying' with a servo-instrument means that the use of the horizontal and vertical motion clamps is a thing of the past; the instrument is turned by the motors under control of the observer through the pointing knobs. Repeated measurements to targets can be programmed so that the instruments turns itself from one target to the next. Only the fine pointing is done by the observer. 'Surveying with autolock' with the Geodimeter 600 requires a tracker unit for the instrument and a special reflector, which assists the tracking. Once the instrument is pointed

approximately to the reflector unit, pointing is automatic; no focussing is required and the reflector is followed automatically. Geodimeter claims that the automatic pointing is more accurate than the visual pointing by an observer.

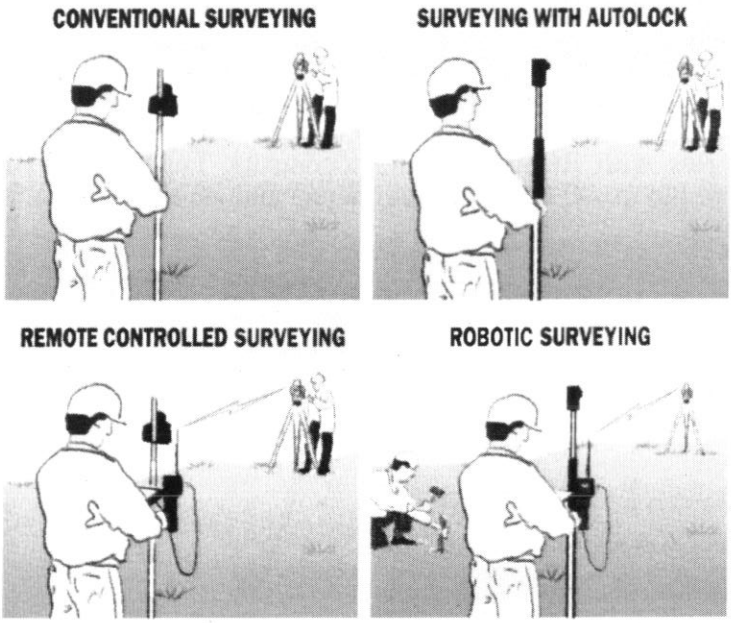

Figure 4.3: Different options of automation with a motorised electronic tacheometer (after Geotronics 1994)

'Remote controlled surveying' means that the instrument is controlled from the reflector and that point coding, recording and calculations are carried out at the reflector. All the instrument operator has to do is to point to the reflector. A radio-link connects the instrument and the reflector in this case. 'Robotic surveying' requires a tracking unit and a communication unit for the instrument and a special reflector, a radio unit and a keyboard for the reflector. The unmanned instrument will automatically locate and follow the reflector. Pointing is automatic. A search routing will pick-up the reflector again should it be lost during tracking. Surveys can be carried out at night, as the instrument operation is fully automatic. (Light is naturally required for the operator at the reflector.)

In 2003, motorised electronic tacheometers are supplied by Geotronics, Leica, Sokkia, Topcon and Trimble (now incorporating Geodimeter and Zeiss) for some or all of the modes of operation discussed above. Two important applications of motorised theodolites and tacheometers are discussed below.

4.1.4.1 One-Person-Survey-Systems

In this case, the operator carries the reflector around and inputs point information; the instrument maintains pointing to the moving prism and executes measurements when instructed through a radio or optical communication link. The one-person-survey-systems can be used for detail and contour surveys as well as for setting out work. The great advantage of these systems is that the expertise of the operator is used at the reflector, that is at the point surveyed or set out. The routine work at the instrument is taken up by the robotic instrument. In 2001, such systems are available from Leica (TPS1100 series with RCS1100 remote control), Topcon (AP-L1A and AP-L1) and Trimble (5600 Series (Geodimeter) and Zeiss Elta S10/S20 'Space').

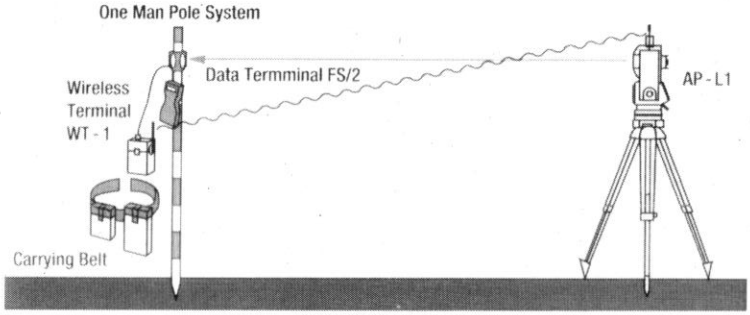

Figure 4.4: Implementation of the Topcon one-person-survey-system (after Topcon 1994)

The basic components of the Topcon one-person-survey-system are depicted in Figure 4.4. The figure shows the instrument, the 360° multiple prism assembly, the reflector pole, the radio communication units at both ends, the data terminal and the carrying belt for the battery packs at the reflector. The Topcon AP-L1 has a horizontal and vertical search facility, which can locate and point to a standard prism around 360°. The prism is found faster if additional information (approximate bearing) is communicated from the reflector operator via the radio link. The AP-L1 telescope axis is shared (coaxially) by the visual telescope, the EDM beam and the tracker. The fine pointing is carried out in steps of 2.5". Moving prisms can be tracked up to angular speeds of 10°/s (63.5 km/h at 100 m). The data terminal allows the remote operation of the instrument and stores the measured data, which are transmitted through the radio link. The usual field computations can also be carried out.

Investigations (Höglund 1994) have shown that one-person-survey systems allow a 30% increase in the number of points surveyed per hour and the survey of 200 points per person hour (against 77 points per person hour for a conventional electronic tacheometers with a two-person field party). When setting out with a two-person field party, the time spent per set-out point is half of that of conventional systems. The higher cost of a one-person-

survey-system can be recovered in less than one year because of the saving in staff costs.

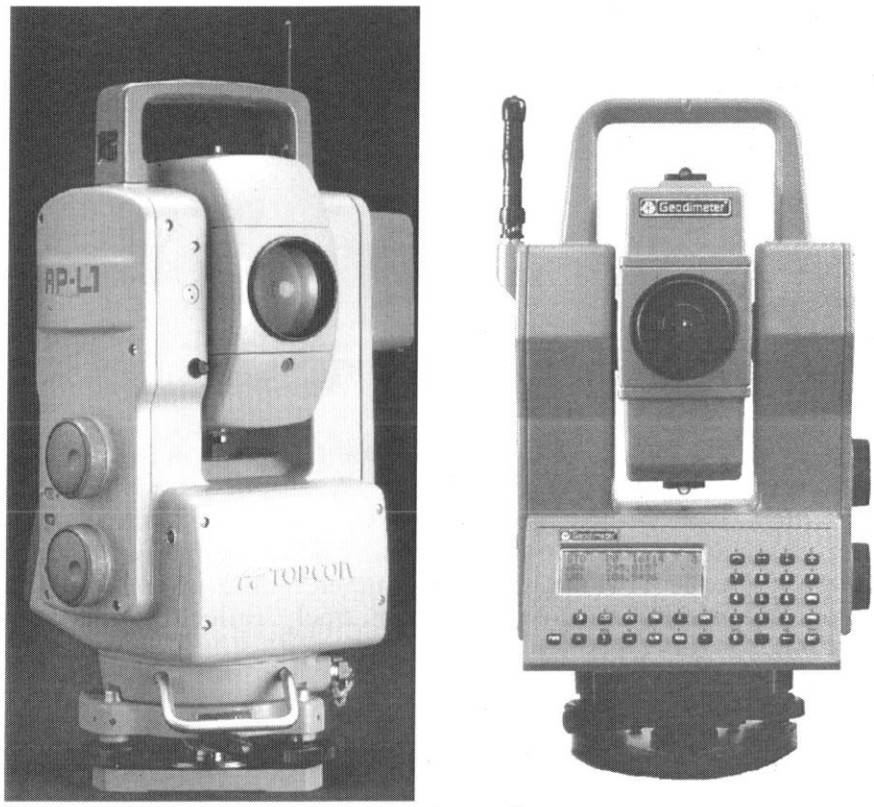

Figure 4.5: Two instrument stations of one-person-survey systems: Topcon AP-L1 on left and Geodimeter 600 on the right.

4.1.4.2 Automatic Monitoring Systems

Fully automatic systems (surveying robots) are being used for the periodic or semi-continuous monitoring of structures (buildings, bridges, walls, tunnels, railway lines), natural slopes, rock faces and mine pit walls. These systems are usually running under the control of an external computer. The latter is also used for data recording and data processing. Typically, the systems are trained by manually pointing to all targets in the desired sequence. This information is then later used to find the points again during the routine measurements. A fine pointing might be executed during the measurements in each epoch, either with the use of a separate tracker, of the EDM beam or with an on-board CCD-camera with associated image processing and pattern recognition software. A search might be launched if a point is not in the field of view after the approximate pointing.

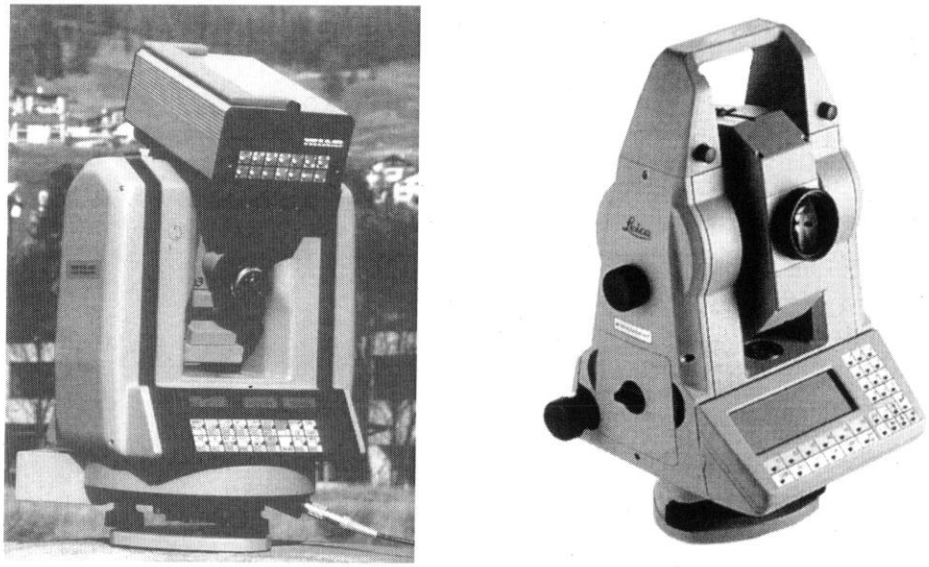

Figure 4.6: Wild TM3000D with mounted Wild DI3000 pulse distance meter on left and Leica TCA1800 on the right. A system as shown on the left was operating at UNSW using Leica's APS software. The TM3000 does not have any slow motion screws and clamps. The telescope and alidade movements are controlled by the external computer or a joy stick. The instrument on the right is motorised, can track reflectors and can automatically point to reflectors.

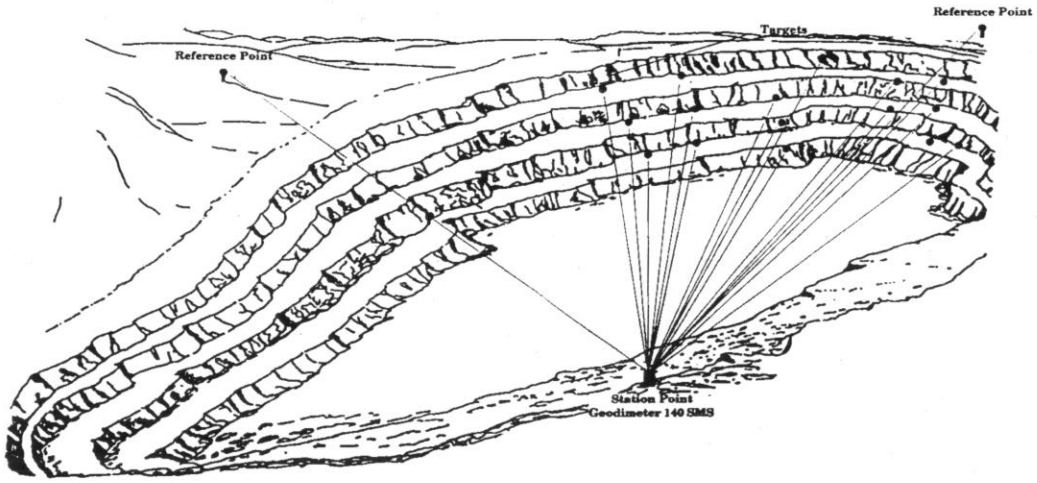

Figure 4.7: Principle of the measurement lay-out in slope monitoring (after Geotronics 1989)

With the Wild TM3000D, distances are measured to mm accuracy and the directions and zenith angles (using EDM pointing) to 2–5" accuracy. The inherent angular accuracy of the TM3000 can only be realised with the use

of an on-board video camera. Leica offers a software suite (APS Win) for the different configurations of its **A**utomatic **P**olar measuring **S**ystem (APS). This software supports deformation measurements, machine guidance, surface scanning and general purpose monitoring and can be adapted to other repetitive measuring tasks. The accuracy of the point determination depends on the accuracy of the hardware as well as on the sophistication of the processing software, in particular in the area of refraction corrections and corrections for instrument errors.

All motorised electronic tacheometers that feature automatic pointing and, possibly, automatic target searching, can be used for automatic monitoring tasks, provided that the control software for the field operation is available. In 2003, instruments such as the Sokkia SET4110M, the Topcon GMT-100/100L, the Trimble 5600 (ex Geodimeter?) / 3600 (ex Zeiss?) series of instruments and the Leica TCRA1100 series are available and have been (or could be) programmed for monitoring tasks.

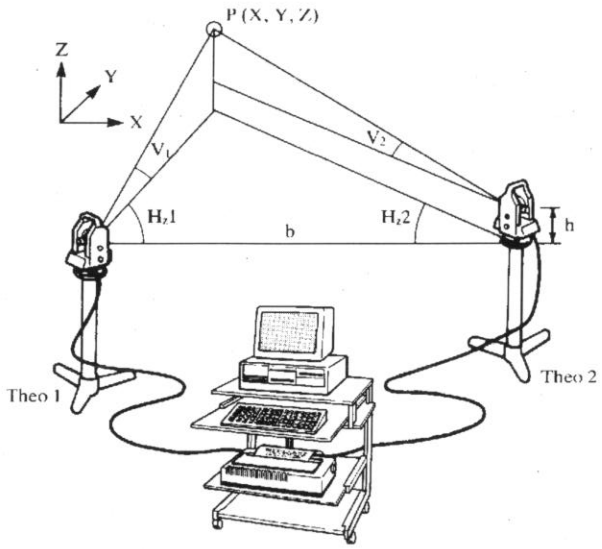

Figure 4.8: Principle of 3D-coordination with a two-theodolite measuring system (after Leica 1992). The horizontal distance between the two instruments ('baseline') is denoted by b and the height difference by h. The horizontal angles are shown as 'Hz' and the vertical angles (90° minus zenith angle) as 'V'.

4.1.5 Motorised Electronic Video Theodolites

In video theodolites, the objective projects the image of the target not only onto the reticle but also onto the image plane of an internal CCD camera. The two ray paths are split by a beam splitter in the telescope. For search

purposes, an alternative wide angle image can be switched through to the CCD camera. The CCD array of the Wild TM3000V is 8.8 mm by 6.6 mm with 500 x 582 pixels. The pixel size is 17 μm by 11 μm. The video signal is taken from a special port on the video theodolite and input into a frame grabber on a personal computer for further digital image processing. Object recognition software has to be used to locate a target on the image. Once a target has been identified on the image, the coordinates of the centre of the target can be computed. Knowing (from calibration measurements) the angular offsets of the CCD array's pixels from the centre of the cross hairs, the angular offset of the target from the crosshairs can be found and added to the instrument's readings of the horizontal direction and the zenith angle to give the angular measurements to the target.

This process can be very accurate (e.g. ±1"), so that the full resolution of the instrument is effective. In the 1990s, motorised electronic video theodolites were released by Kern and Wild (now Leica in both cases), namely the Kern E2SE and the Wild TM3000V. With video theodolites, the size, shape and illumination of the targets is very important. Sometimes, reflective targets are used and illuminated with a light on-board of the video theodolite. The Wild TM3000V could be equipped with a light which projects an infrared beam along the telescope axis. On other occasions, a strong laser beam was projected by a laser theodolite on to the object to me measured. The laser dot could then be used as a target by other (video) theodolites. Focussing was not automatic. Once a target was pointed to manually (i.e. in a 'training' session), the focus position was recorded by the computer and then reset (by a servo motor) during subsequent production runs.

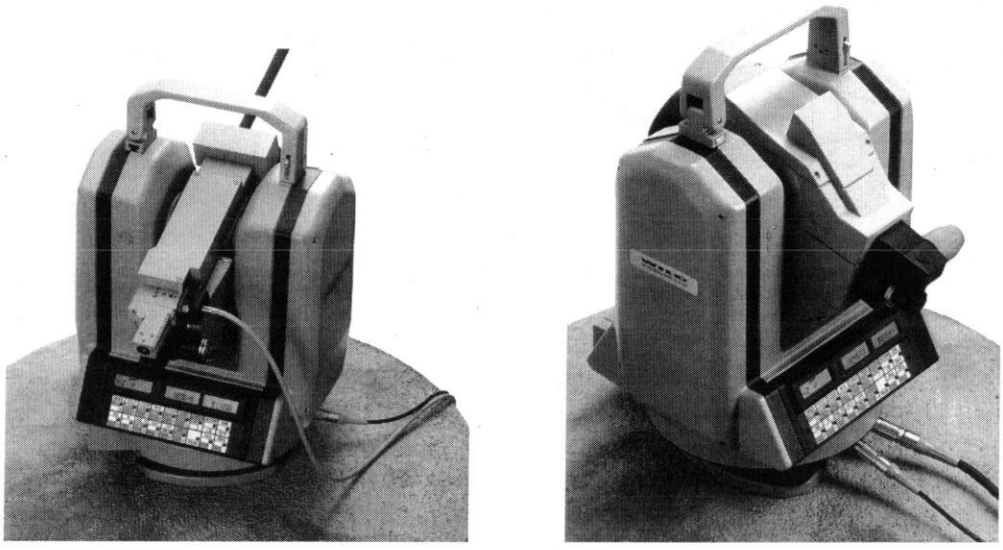

Figure 4.9: Motorised laser precision theodolite Wild TM3000L (on left) and Wild TM3000V motorised precision video theodolite (on right). A special version of the video theodolite (TM3000V/D) permits the attachment of a distance meter.

Figure 4.8 shows a typical application of motorised video theodolites. After initial training, the two (or preferable more) motorised electronic video-theodolites can take repeated measurements to the points of interest on an object. The three-dimensional coordinates are obtained by intersection. The length of the baseline is not directly measured. The positions of the two (or more) theodolites are derived from measurements to marks of given coordinates or from the measurements to the object and to a scale bar of known length. The precision of the resulting object coordinates depends on the distance from the instruments, the intersection angle, the quality of the targets and the stability of the instrument set-up. Angular measurements to one second of arc can give positions to 0.01 mm over 2 m, for example.

In 2003, the video theodolites are no longer available. Depending on application, the video theodolites are now replaced by motorised electronic tacheometers (reflective targets required), by scanning reflectorless motorised electronic tacheometers or by dedicated laser scanners. The laser scanners may be able to detect traditional (non-reflecting) survey targets on objects and structures if their reflectance is sufficiently different from the surface around them.

4.1.6 Laser Theodolites

Laser theodolites have been available before the time of electronic theodolites, either as integrated systems or as a laser eyepiece attachment to standard optical theodolites. The same laser attachments can naturally be fitted to electronic theodolites and tacheometers. Laser theodolites project a visible laser beam along its line of sight (He-Ne gas laser or visible laser diode). They can be used for machine guidance, alignment or as a targeting device for non-contact measurements of structures and objects. If a motorised laser theodolite is combined with a motorised video theodolite, the system can be programmed to scan the surface of an object or structure, with the video theodolite tracking the laser dot after an initial pointing to the laser dot.

Motorised laser precision theodolites may use an on-board semiconductor laser diode for industrial applications (close range) or a helium-neon gas laser for the monitoring or measurement of larger structures (for example in civil engineering). The latter is usually attached to the motorised instrument through a glass fibre connection. The instrument shown in Fig. 4.9 is linked to such an external HeNe laser. The laser theodolites may adjust the laser output power to mach the intensity of the laser dot to the brightness of the object surface. In order to generate a laser dot of uniform intensity, the laser beam is sometimes rotated inside specialised instruments. For example, the TM3000L rotates the laser beam at 30 rpm to give a circle of 0.68 mm diameter at 5 m.

At the turn of the century, lasers are being used less and less for machine guidance. In part, they are being replaced by motorised electronic tacheometers that can measure to reflectors mounted in critical positions on machines. This allows guidance along curves as well as straight lines. If more than one reflector is mounted on the machine, the motorised electronic tacheometer can provide information on the heading (azimuth), pitch (along-track tilt) and roll (across-track tilt) of the machine, besides horizontal and vertical position. In open air, lasers are also replaced by guidance systems based on the Global Positioning System (GPS).

4.1.7 Tracking Electronic Tacheometers

Before the appearance of the one-person-survey-systems, a number of manufacturers did develop specialised tracking electronic tacheometers ('Autotrackers'). These instruments can follow a moving reflector once an initial manual pointing has been carried out. They measure horizontal directions, zenith angles and slope distance continuously and can transmit these data to the reflector, if required. These instruments are typically used in near-shore hydrographic surveys. In this case, the instrument is set up on a shore station of known coordinates and orientated to give a bearing read-out. Bearing and (horizontal) distance are transmitted to the vessel with the reflector, where the vessel position is computed and merged with the data from the echo sounder or other hydrographic instruments.

Typical instruments were the Geodimeter 140T and the Krupp Atlas 'Polarfix'. A number of other manufacturers offered similar systems. The latter had a range of 10 km, an angular precision of ±(50 mm + 50 ppm) and a distance precision of ±(150 mm + 50 ppm). These systems were also used for the position fixing of other vessels, tracking of buoys, tracking of land vehicles, tracking of helicopters, position fixing of construction vehicles and the dynamic measurement of roads and other linear features of terrain. By the turn of the century, these tracking tasks were taken over by GPS systems or appropriately configured main-stream motorised electronic tacheometers.

4.1.8 Reflectorless Electronic Tacheometers

This section gives an introduction into the historical development of electronic distance measurement (EDM) to non-cooperative targets. The particular aspects of reflectorless EDM with current surveying instrumentation are discussed later in Section 5.1. 'Reflectorless' electronic distance measurement (EDM) to passive ('non-cooperative') targets has been used in surveying for quite some time. The first geodetic pulse distance meter became available in 1982: The Fennel 2000 was a stand-alone

distance meter, able to measure to non-cooperative targets. Military rangefinders with 1 - 10 m resolution have been around even longer. Zeiss released the first 'reflectorless' electronic tacheometer ('total station') in 1993. Broad acceptance by the surveying profession followed once Leica, Topcon and Trimble released their reflectorless instruments in 1998, followed by Nikon in 1999. The range of reflectorless EDM depends heavily on the type of surface that is measured to and its orientation to the measuring beam. At the time of writing, 50 - 100 m seem to be typical maximum distances to 'natural' targets although Zeiss (now Trimble) quoted a reflectorless range of their RecElta RL electronic tacheometer of 400 m.

The 'reflectorless' instruments can also be used to measure, in 'reflectorless' mode, to the traditional EDM glass prism reflectors. This allows the measurement of distances of a few kilometres, a range that was once reserved for the earlier class of medium range distance meters. Please refer to Section 5.1 for further information on reflectorless EDM.

4.1.9 Scanning Electronic Tacheometers

It has been mentioned before that motorised 'reflectorless' electronic tacheometers can be programmed to measure distances at predetermined values of horizontal directions and zenith angles. This would permit to create a three-dimensional model *of the visible surfaces* surrounding the instrument. As electronic tacheometers are optimised for accuracy rather than speed, special devices have been developed for pure scanning applications. These devices are sometimes advertised as *Laser Radar*, *Ladar* and *Lidar* with reference to the well-known *radar* (RAdio Detection And Ranging). Some of these scanners resemble motorised electronic tacheometers, others resemble the laser scanners used for laser shows in the entertainment industry. In the latter case, the (pulse) distance meter is usually installed with the beam axis straight up. The beam is then reflected by a scanning mirror with two degrees of freedom, with one vertical and one horizontal axis. Angular encoders on the two axes measure the equivalent of horizontal directions and zenith angles.

Three-dimensional scanners can be used for architectural surveys, volumetric measurements, object recognition, process control and collision protection. An early three-dimensional laser scanner (3D-Ladar) by Ibeo had a distance precision of ±20 mm and an angular resolution of 2^{14} in a full circle (80 seconds of arc). The range was up to 500 m and the rate of distance measurements 4600 per second (4600 Hz; Ibeo 1991). Special devices have also been developed for the monitoring of the wear of the lining of converters and ladles in steel making. In this case, distances are measured to the red-hot (1400°C) refractory linings inside the converters and ladles. The system manufactured by VTT Electronics (Oulu, Finland) gives

an accuracy of 2 mm over 20 m with a measuring rate of one point per second (Ailisto et al 1996).

By the turn of the century, laser scanners had developed as a special class of instruments for the reflectorless measurement of indoor and outdoor spaces, objects and structures. These instruments can scan a three-dimensional space at high speed and provide 3D coordinates of all objects and surfaces in view. Powerful postprocessing software is then able to convert the data into plans, 3D-representations and computer aided design (CAD) files. This class of specialised instruments is discussed in Section 5.2.

It is mentioned again that any robotic electronic tacheometer, that is motorised and permits reflectorless EDM, can be programmed to scan a three-dimensional space like a dedicated laser scanner. However, the main-stream robotic electronic tacheometers will take much longer for the measurements. Also, it is likely that the range of main-stream robotic electronic tacheometers is smaller and that no powerful postprocessing software is available (to convert the data files to CAD files, for example) for this application of electronic tacheometers.

4.2 Features of Electronic Theodolites and Tacheometers

As far as the telescope and the mechanical construction are concerned, the electronic theodolites differ very little from second order optical theodolites. In consequence, most instrumental errors are the same and most operational procedures remain unchanged. In some respects, however, the electronic theodolites and tacheometers differ significantly from the instruments with optical circles. Some important differences and similarities are now discussed to provide a better understanding of the newer technology and its use.

4.2.1 Circle Types

The horizontal and vertical circles are read electro-optically and the readings are displayed electronically. This means that power is absolutely necessary because the circles cannot be read manually. It is preferable that the essential measurements are displayed simultaneously, for example the horizontal direction, the zenith angle and the slope distance (H, V, SD). The circle graduations used in electronic theodolites are etched onto glass disks using photolithographic techniques. They have approximately the same diameter as in optical theodolites. The Topcon ET-1 features a circle diameter of 80 mm, for example. In other disciplines, electro-optical angle measuring devices are referred to as optical encoders. Three basic types of electronic circles ('angle encoders') can be distinguished.

4.2.1.1 Incremental Circles

Pure incremental circles feature only a uniform radial line pattern. An electro-optical incremental circle is shown in Figure 4.11 (on the right). The pattern is a series of equidistant light and dark fields. The individual graduations cannot be identified as they have no 'labels'. The changes in the horizontal direction and the zenith angle are obtained by counting the number of light and dark fields passing through an electro-optical read-out during the rotation of the theodolite and telescope, respectively, and by multiplying the number of cycles with the angular equivalent of one graduation. The instrument resets the count to zero after switch-on. So, in principle, the zero of the circle (circle orientation) is lost at turn-off or in the case of a loss of power. (Some modern instruments store the last horizontal circle reading into non-volatile RAM in the on-board computer and reset this value after switch-off. If the instrument is rotated in any way whilst turned off, the horizontal circle will have a wrong orientation after re-powering the instrument.) It should be noted that most modern instruments do not have pure incremental circles. The reading of the electro-optical incremental circles is discussed in more detail later, in another section.

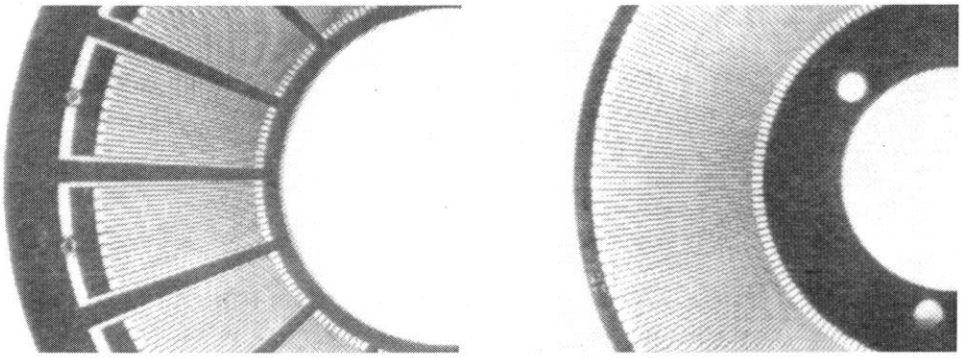

Figure 4.10: Part of a rotor and a stator of a circular Inductosyn (after Inductosyn Corp. and Walcher 1985)

Incremental circles do not have to be of the electro-optical type. Some Geodimeter (now Trimble) instruments are equipped with an inductive circle reading system that operates on the Inductosyn principle. Two parallel disks (rotor and stator) carry equivalent conducting square wave patterns. (Refer to Fig. 4.10.) The square wave patterns are applied to glass disks using the same principles as in the manufacture of printed circuits. One of the disks is fixed. The other one moves with the alidade (horizontal circle) or the telescope (vertical circle). When turning one disk against its opposite, the phase of the measuring signal changes. This phase change is averaged over the entire square wave pattern around the circle and is, thus, free of any circle eccentricity errors and circle graduation errors. Inductive circles reading systems can be as accurate as 2" and are less susceptible to contamination by dust than optical circles. On the other hand, they are more susceptible to electro-magnetic interference. The manufacturing tolerances

are quite tight. Measuring the phase to one part in one thousand gives a resolution of 1.3 seconds of arc. Inductosyn systems are widely used for radar antennas, in engineering-works, machine-tools and coordinate measuring machines.

4.2.1.2 Quasi-Absolute Circles

In this context, quasi-absolute circles are defined as incremental circles with one additional reference mark. The reference mark (see Figure 4.11, at top, on the right) allows to start the cycle count at an absolute reference. This means that the circle readings before a power loss can be recovered after recommencement of the measurements (unless the instrument was instructed to set a specific circle reading in a particular direction before the power loss). To initialise the vertical circle, the telescope is typically tilted through the horizon (zenith angle of 90°); to initialise the horizontal circle, the user has to rotate the alidade through (a maximum of) 360°. It should be noted that all vertical circles must be at least quasi-absolute as the zenith angles could not be referenced to the zenith otherwise.

Figure 4.11: Basic layout of an absolute circle (on the left) and an incremental circle (on the right), after BEI (1987). The incremental circle also carries a reference mark (at the top). The innermost graduation of the absolute circle is equidistant, like the graduation of the incremental circle. Each graduation on the absolute circle can be identified by the unique binary code on the seven outer tracks.

4.2.1.3 Absolute Circles

On absolute circles, each circle graduation can be uniquely identified. Figure 4.11 (left) shows an absolute circle, with the incremental (equidistant) graduation on the innermost track. The outer tracks carry a binary pattern, which fully identifies each of the basic graduations. In Figure 4.11, seven code tracks are visible. This code has a resolution of 128 and, thus, fully identifies the 64 graduations on the innermost track. It is obvious that absolute circles with binary patterns must have a readout system for each track. This is expensive in manufacturing.

Not all electronic theodolites and tacheometers with absolute circles have a binary pattern for the identification of the incremental high resolution graduation. The Wild T2000/T3000 theodolites from Leica use a rotating quasi-absolute circle, which is read against the fixed part and the rotating part of the instrument. This gives the (absolute) angle between the fixed readout and the moving readout. Since the Wild TC1600 family of instruments, Leica uses a bar code pattern on the circle which uniquely identifies each position. (See Figure 4.12.) The processing (image matching) is similar to that of the Leica bar code levels.

Instruments with absolute circles do not 'lose' the circle readings in case of a power loss, be it due to a change of battery, the automatic power-off facility of modern instruments or an accidental switch off.

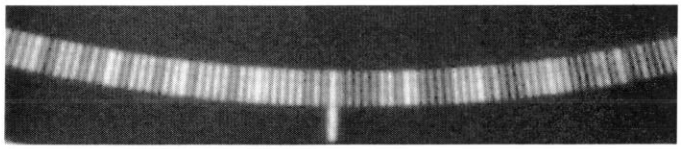

Figure 4.12: Part of the bar code circle of a Wild TC1600.

4.2.2 Diametrical Circle Reading

Circle eccentricities are a very important source of error in angular measurements. In the case of horizontal direction measurement, they can be eliminated by measuring in two faces. In zenith angle measurement, observation in FL and FR do not eliminate the circle eccentricity completely. A number of techniques can be used to eliminate the circle eccentricities in single face measurements with more accurate theodolites and tacheometers. (The coincidence reading micrometer was used in optical (one-second) theodolites to read the circle simultaneously at two points 180° apart and, thus, to eliminate the circle eccentricity by reading the mean). The elimination of circle eccentricities through appropriate instrument design is more important for zenith angle measurement, because the user cannot eliminate the effect by measurement in two faces.

For more accurate work (like the surveys previously done by optical 'one-second theodolites'), most surveyors and geomatic engineers use only instruments which eliminate the circle eccentricity one way or another. Several techniques are presently employed to 'eliminate' the effects of circle eccentricity on angular measurements:

- Some instruments average the circle reading all around the circle. This effectively eliminates the eccentricity error, as the sum of the error around the circle is zero. This averaging approach is used by Geodimeter with the Inductosyn circle reading and by Leica with the rotating circles in the T2000/T3000 instruments.

- Most accurate electronic theodolites and tacheometers employ the traditional diametrical circle reading, where the circles are read separately and simultaneously on opposite sides of the circle. The two readings are then merged electronically.
- Some other instruments read the circles only on one side, but use a factory calibration of the circle eccentricity to correct all measurements on-line before the readings are displayed and stored. Such instruments were the Wild TC1010/1610/1600 electronic tacheometers, for example. The accuracy of the on-line correction depends on the accuracy of the original calibration as well as the stability of the circle mounting over the life of the instrument.

4.2.3 Electronic Level Sensors versus Vertical Circle Compensators

4.2.3.1 Definition of an Electronic Level Sensor

A tilt sensor measures the dislevelment of the vertical axis in digital form and the associated computer corrects at least the zenith angles accordingly. Instruments with single-axis level sensors (parallel to the telescope) can only correct the zenith angles. Instruments with dual-axis level sensors are better for precise measurements or steep sights because they can correct the zenith angles and the horizontal directions for the two components of the measured dislevelment of the vertical axis. Most electronic theodolites and tacheometers use level sensors. Precise instruments feature dual-axis level sensors. With a dual-axis level sensor, the inclination of the vertical axis can, sometimes, be displayed and used for the levelling of the instrument.

4.2.3.2 Definition of a Vertical Circle Compensator

The optical reading of the vertical circle is deviated physically to compensate for the dislevelment (parallel to the plane of the vertical circle) of the vertical axis. This ensures that the zenith angle readings are truly referenced to the zenith. Some electronic theodolites and tacheometers may use vertical circle compensators. The Wild (Leica) TC1600 was such an instrument.

As defined above, the difference between a compensator and a level sensor is that the mechanism of a compensator optically deviates the vertical circle reading whereas a level sensor measures the dislevelment of the vertical axis and corrects the vertical circle reading in real-time by the on-board computer. Both approaches ensure that the correct zenith angle is obtained even when the vertical axis is not truly vertical. Before the introduction of vertical circle compensators, altitude bubbles were used to set the vertical circle reading index to horizontal. As this had to be done before every single zenith angle reading, it was less convenient, less accurate and quite time consuming.

Two types of compensators were used in optical instruments. One used a mechanical pendulum to define the vertical direction and the other the surface of a suitable liquid to define a horizontal plane. Vertical circle compensators are different from those in levels in the sense that they deviate only the ray path of the vertical circle readings and not the entire telescope image. The vertical circle compensators were (almost) always uni-directional. The Kern (now Leica) DKM-2AM did have a dual-axis compensator, but the trunnion axis component of the inclination of the vertical axis had to be read-out with an additional device (trunnion axis micrometer) and the corrections to the direction measurements applied by hand calculation.

As compensators are being phased out in electronic theodolites and tacheometers (and replaced by independent level sensors) they are not discussed any further in this context. Level sensors are discussed later in more detail. Instruments without level sensors (or compensators) are not up to the standard required by geomatic engineers and surveyors as they do not relate the zenith angles directly to the plumbline. In this case, the zenith angles refer to the mechanical vertical axis, the verticality of which depends entirely on the accuracy of the levelling of the instrument.

4.2.4 Data Recording

Electronic data recording saves a lot of time by replacing the manual booking (and the 'booker' assisting the observer). Data recording also avoids the well known gross errors experienced in manual booking, at least as far as the actual electronic measurements (horizontal direction, slope distance, zenith angle) are concerned. Additional input (e.g. height of instrument, height of reflector, point number, point description) through the keyboard is still subject to the well known problems.

Most electronic theodolites and tacheometers can electronically store data on one or more of the following media:

- on-board RAM
- (computer) industry standard memory (PCMCIA) cards (**P**ersonal **C**omputer **M**emory **C**ard **I**ndustry **A**ssociation), now known as PC-cards
- make specific memory cards and modules
- make specific external data recorders ('electronic field books')
- external notebook or laptop computers

The data stored in one of the four first devices need to be down-loaded to a computer for further processing. Additional cables and/or devices and software are required for this purpose. PC cards may be inserted into laptop and desktop computers, that feature a PC card port, for the transfer of data. Data can also be up-loaded, for example coordinates for setting-out work. It should be noted that some instruments, that accept PC cards, cannot record

data on-line onto the cards. In these cases, the data are recorded onto RAM and have to be transferred to the PC card later, for example before moving the instrument or at the end of a day.

Unfortunately, all makes of instruments (or even different types of the same make) have different recording formats. There are also some differences between makes and types on how a full data set can be recorded (e.g. one or more key strokes). The sophistication of entering point numbers and other attributes of surveyed points varies greatly. Alpha-numeric entry is sometimes restricted or not possible.

4.2.5 On-Board Computing

Some on-board computing is available on all modern instruments. Sometimes, software modules are offered as optional items by manufacturers. A number of instruments support the personal computer industry's operating systems (initially DOS, now Windows) and programs written by the user. Some examples of what pre-stored programs can do are:

- working out the mean of FL and FR observations, and executing the error analysis in direction measurement with multiple arcs. To be useful, such programs must be able to cope with the standard procedure of direction measurement, namely the sequence FL_1–FL_2–FL_3– ... –FL_n–FR_n– ... –FR_3–FR_2–FR_1.
- computation of the co-ordinates and the elevation of the instrument station using resection (free stationing). The horizontal positioning should work with directions only as well as with directions and distances and should allow and use redundant data. The precision of the determined coordinates should be displayed. The determination of the elevation should be possible with zenith angles only or with zenith angles and slope distances and should allow and use redundant data. The precision of the determined elevation should be displayed.
- computation of bearings, for example for the purpose of orientating the instrument to 'north'.

The many on-board programs, which use the electronic distance measurement (EDM) part of the instruments, are not listed here. Some additional computations are usually available for the guided instrument calibration routines. More on these below.

4.2.6 Power Supply

All electronic theodolites and tacheometers need power to operate. Depending on the make and the type of instrument, direct current is supplied by one or more of the following sources:

• internal rechargeable (nickel-cadmium, NiCd, or nickel-metal-hydride, NiMH) batteries. These are make and type specific. The voltage varies between makes and, sometimes, different types of the same make. Common voltages are: 6 V, 7.8 V, 8.4 V, 12 V. Some surveying instrument manufacturers are now using widely available video camera ('camcorder') batteries as standard power sources for their instruments.

• external rechargeable NiCd batteries. These are also make and, sometimes, type specific.

• lead-acid 12 V car or motor bike batteries. These can be attached to electronic tacheometers and theodolites with the conversion cables supplied by the manufacturers. These make and, sometimes, type specific 12V DC battery cables may include a dc-dc converter to reduce the voltage to the level required by the instrument. As it is easy to connect the 12 V batteries the 'wrong-way-round', the 12 V battery cables should always include reverse polarity protection.

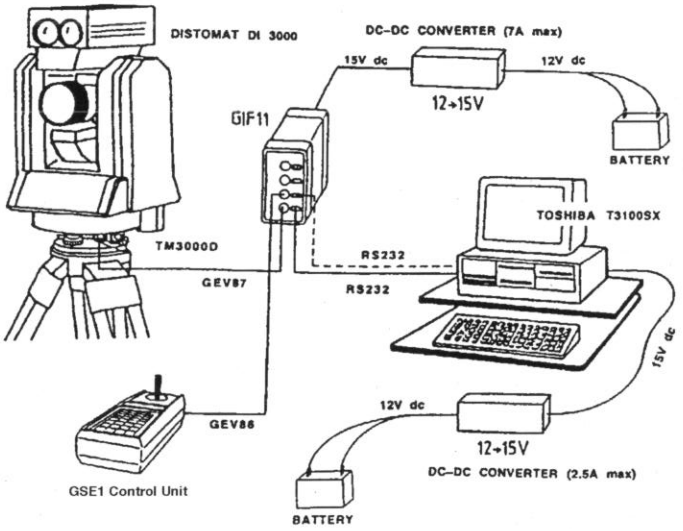

Figure 4.13: Configuration of the Wild (Leica) Automatic Polar System (APS) once used at UNSW. The Wild (Leica) T3000D/DI3000 system did operate entirely under the control of software running on the computer. The 12 V to 15 V dc-dc converter supplying the interface unit (Wild GIF11) was custom built. The dc-dc converter for the computer was supplied by Toshiba.

4.2.7 Communication with Personal Computers

A two-way communication between an instrument and a computer is often possible via a RS-232C interface. Some newer instruments support DOS commands, at least for the import and the export of files. If the instrument's

command language is known, the instrument can be instructed to carry out functions which are usually triggered by buttons on the keyboard.

An example for the implementation of a communication link between an electronic tacheometer and a computer is shown in Figure 4.13. The figure shows the connections between a motorised theodolite (Wild TM3000D) with mounted pulse distance meter (Wild DI3000), a computer and a joystick unit (Wild GSE1). In this case, an interface unit (Wild GIF11) is placed between the instrument and the computer. The cable between the interface and the instrument carries not only the supply current but also the two-way communication. As the figure shows, the instrument can be run either from the computer or from the control unit (GSE1). The selection between the two modes is by either a switch on the interface (GIF11) or by software selection. (The latter requires the second RS232 link between the interface and the computer.) A 'joystick', or the arrow keys on the computer keyboard, are required for any manual pointing since the instrument does not feature slow motion screws. All data are recorded on the hard disk of the laptop computer.

4.2.8 Automatic Focussing, Searching and Pointing

4.2.8.1 Automatic Focussing

The first instruments with an automatic focus were the video theodolites. These instruments could 'remember' the position of the focussing lens only after training. Today, auto-focus as in still and video cameras is available in a few electronic theodolites and tacheometers, such as the Topcon 600AF Series and the Pentax R-100 and R-300 Series. The first Auto Focus Levels (Pentax AFL240/280/320) were released earlier in 1996. According to Pentax, the phase contrast method is used by their autofocus system.

4.2.8.2 Automatic Searching

Before an automatic pointing in the narrow sense (see the following section) can be executed by a robotic electronic tacheometer, the glass prism reflector has to be 'found' first and, typically, brought into the field of view of the telescope. Robotic electronic tacheometers, that can find a prism in a 360° sector around the instrument, are available from a number of manufacturers, such as Geodimeter (ATS, 600 Series, now Trimble), Leica (TPS1100 Series with Powersearch, Topcon (GPT8000A, GTS-800A, APL1A), Trimble (5600), Zeiss (Elta S10 'Space', now Trimble). Most instruments transmit a special beam for the fast acquisition of a (reflecting) target and rotate with a maximum speed of, typically, 45°/s. Typical acquisition times are less that 15 s over a 360° sector. Most systems allow to define smaller search sectors to speed up the search, where possible. Naturally, the search times can also be minimised by continuously following (tracking) of a (usually 360°) reflector.

Some systems require an 'active' reflector assembly, that emits a structured infrared light. Others do not absolutely need an 'active' reflector assembly, but achieve the target acquisition faster with one. The use of an active reflector assembly has the advantage that the robotic instrument does not accidentally lock onto the wrong reflector nor, for that matter, onto another 'foreign' reflecting surface in the landscape. The drawback is that batteries are required at the reflector end.

4.2.8.3 Automatic Pointing

Various forms of automatic pointing were implemented in earlier motorised electronic tacheometers, such as:

- pointing under computer control (either on-board or external) to previously established (and 'trained') points,
- recognition of the image of a target on an internal CCD camera,
- tracking (with a video theodolite) the laser dot projected by a laser theodolite onto a surface, and
- tracking the infrared beam of the EDM instrument which is returned by a reflector.

With time, manufacturers started to implement pointing systems that operate separately from the distance meter and tracking systems but use the same reflector to return the transmitted beam. Typically, these systems allow to determine the angular offset between the line of sight of a roughly pointed telescope and the reflecting target, and then use the servo motors to 'move' the cross hairs onto the (centre of the) reflector. The coarse pointing may be done manually (through the gun sight) or with an automatic search or tracking system.

Since only Leica has explained the principle of it's 'Automatic Target Recognition' (ATR) system in any detail (Haag et al. 1997), this system is discussed further. The Leica ATR uses a separate (coaxial) infrared beam and a built-in two-dimensional CCD sensor. Since this beam is of fixed focus, no focussing is required. On return from the prism, the ATR beam is split from the EDM beam and the visual image and projected onto the CCD sensor. To speed up the processing, the pixel values are summed along columns and rows. Histograms of the column-by-column values and the row-by-row values will show peaks at the centre coordinates of the returned ATR beam. Checks for multiple prisms in the ATR beam are made and the beam power and the exposure times of the CCD array are optimised for background brightness and distance. Once the coordinates of the return beam on the sensor are known, the offsets from the 'centre' of the CCD sensor can be computed. Using the servo motors, the telescope is then automatically pointed very close to the centre of the prism. This is necessary to allow electronic distance measurements and to permit a visual check by the observer.

Figure 4.14a shows the configuration during a typical measurement. The field of view of the telescope is indicated by the letter 'A', the EDM beam diameter by 'D' and the diameter of the initial ATR beam by 'C'. The ATR beam diameter is about one third of the visual field of view. If no return beam is received on the initial coarse pointing ('C' in Fig. 4.14a), the servo motors are used to drive the ATR beam around the initial pointing. This is indicated by the letter 'E' in Fig. 4.14a. The letter 'B' shows the total field of view covered by ATR, after initial pointing and fine search.

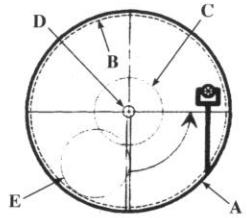

Figure 4.14a: Principle of Leica's Automatic Target Recognition (ATR) of a Leica TCA1800 for measurements to a reflector. The letters are explained in the text. (after Haag et al. 1997)

For a measurement to a reflector, the telescope is pointed with the gun sight. No focussing is required. The observer then starts the measuring routine. The instrument checks if the reflector is within the ATR field of view ('C' in Fig. 4.14a). If not, the ATR beam is driven in a spiral pattern around 'C', as indicated by 'D' and 'E' in Fig. 4.14a. After that, the automatic pointing occurs and the distance is measured. This is followed by the measurement of the direction and the zenith angle, which are then corrected for the offsets of the ATR return beam from the centre of the CCD array and 'frozen' in a buffer memory. Finally, the distance and the 'frozen' angles are recorded. The buffer memory is then cleared.

The accuracy of Leica's automatic pointing (ATR) varies between instruments. The measuring principle discussed above applies to the most accurate Leica instruments. For the Leica TCA2003 and TDA5005 precision instruments, the ATR pointing precision is quoted as 1 mm for distances less than 200 m and 2-3 mm for distances between 200 and 500 m. For the Leica TCA1800, the ATR pointing precision is given as 2 mm to 400 m. The Leica TPS700 and TPS1100 Series of instruments are likely to feature a less sophisticated ATR procedure, since the ATR precision is given as 3 mm below 300 m and 'equivalent to angular accuracy' at longer distances.

All Leica instruments with ATR provide an on-board routing to calibrate the CCD sensor's origin (or 'zero' in Fig. 4.14b) in relation to the centre of the normal crosshairs. This requires careful manual measurements in two faces to a reflector at a specified distance. Figure 4.14b shows the two calibration

values that have to be determined. Once determined, the calibration values are applied to all subsequent ATR measurements. Haag et al. (1997) make a few suggestions for precision ATR measurements: Let the instrument acclimatise to ambient temperature, use only reflectors with clean glass surfaces, do a very careful ATR calibration when mixing ATR and manual pointing to targets in the same arc of directions. The latter is best done on site before critical direction measurements and, possibly, between arcs.

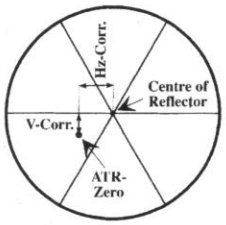

Figure 4.14b: Calibration of CCD array for the offset of its 'centre' or 'zero' from the centre of the (normal) crosshairs. (after Haag et al. 1997)

4.2.9 Computer Assisted Instrument Calibration

Most instruments feature built-in computerised measuring routines for the calibration of some instrumental errors. Such routines may determine and store the following instrument errors or constants (for later real-time correction): horizontal collimation error, index error of vertical circle, additive constant(s) of single-axis (or dual-axis) level sensors, trunnion axis tilt, calibration values of automatic pointing systems (e.g. V-Corr and Hz-Corr in Fig. 4.14b).

These computer assisted instrument calibrations allow some 'mechanical adjustments' to be replaced by 'electronic adjustments'. Rather than physically adjust components into their nominal positions, as in the past, the errors are now determined, then stored on-board (in non-volatile RAM) and corrected in real-time during the measurements.

Similar to the physical adjustments of the older optical instruments never being perfect, the corrections determined by the pre-programmed routines are only as good as the measurements taken. The stored corrections are thus not error free. Users are reminded that some instrument errors do change with time, temperature and shocks. In consequence, instrumental errors must still be removed by appropriate field procedures (e.g. measurement in two faces) if the specified accuracy of an instrument is to be realised, even if the instrument applies the stored corrections in real-time. Also, the users are well advised to check the stored corrections before starting single face measurements. An inexperienced observer may have stored calibration values that are totally wrong!

4.2.10 Modern Vertical Axis Systems

The construction of the vertical axes of theodolites has changed considerably over the last 50 years. The left side of Figure 4.14c shows the modern bearing used for the vertical axes of the Zeiss (Oberkochen) theodolites. The weight of the upper part is carried by the load bearing (No. 3 in Fig. 4.14c). The stability of the vertical axis is, however, provided by the second and cylindrical bearing (No. 1 in Fig. 4.14c), which extends over the full height of the bearing. This gives a better stability (less wobble) of the vertical axis than two single ball bearings (one at the top, and one at the bottom) could provide. Figure 4.14c also shows a second cylindrical bearing (No. 2 in the figure) for the rotation of the horizontal circle about the vertical axis.

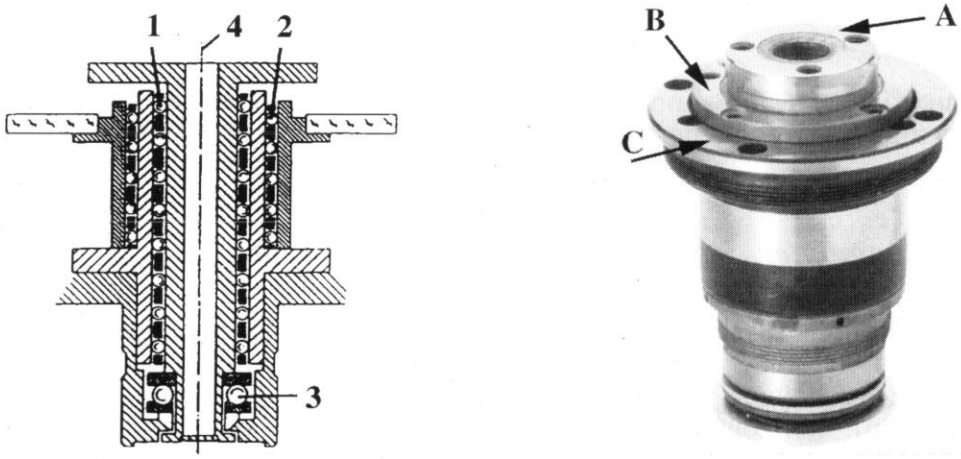

Figure 4.14c: Modern vertical axis systems: Zeiss (Oberkochen) on the left and Topcon ETL-1 on the right. The parts shown on the left are: 1 = ball cage for the cylindrical vertical axis bearing, 2 = ball cage of the bearing of the horizontal circle, 3 = ball bearing carrying the full load of the alidade, 4 = vertical axis. The parts shown on the right are: A = upper plate (on which the rotating upper structure of the theodolite is mounted), B = lower plate (with carries the horizontal circle), C = non-rotating part (attached to the base of the theodolite).

The vertical axis assembly of a Topcon ETL-1 electronic theodolite, shown on the right hand side of Fig. 4.14c, gives a visual impression of a modern design. This instrument was still designed as a 'double-centre', 'double-plate' or 'repetition' theodolite, with two clamps and two slow motion drives for the horizontal motion about the vertical axis. The three layers of holes for mounting screws are testimony to that. The top most level (see 'A' in Fig. 4.14c) carries the upper part of the theodolite, the middle one (see 'B' in Fig. 4.14c) the horizontal circle and the lowest ('C' in Fig. 4.14c) is attached to the (non-rotating) base of the instrument. The upper set of clamp and slow motion drive acts between 'A' and 'B', the lower between 'B' and 'C', allowing the circle to move with the upper part of the theodolite.

Most modern electronic theodolites do no longer have a second bearing, that allows the rotation of the horizontal circle against the base of the theodolite (as explained for the axis systems shown in Fig 4.14c). This means that the horizontal circle cannot be physically turned any more (other than by turning the instrument 120° inside its tribrach) and cannot be set to a given reading (other than by electronic means).

4.3 Circle Reading System of the Electronic Tacheometer Nikon DTM-1

The Nikon DTM-1 uses an electro-optical circle reading. The light and dark increments are produced by the equidistant bars and equidistant gaps. The horizontal circle of the DTM-1 is a fully incremental circle. The vertical circle, by default, is a quasi - absolute circle. The basic principle of the horizontal circle reading is shown in Fig. 4.15. The figure shows that diametrical circle readings are used to eliminate the residual circle eccentricities. The circle of the DTM-1 has a diameter of about 92 mm and carries 10000 graduations. The radius of the circle is 46 mm and the circumference 289.0 mm. Considering the number of graduations over the circumference, the width of the gaps and the bars can be calculated as 14 μm. The radius of an atom is 0.0001 μm and may be used for comparison.

Figure 4.16 outlines the components of the circle reading system of the Nikon DTM-1. Many other instruments operate on very similar principles. On the left of the figure, the two electro-optical systems that read the circle are shown. A light emitting diode (usually infrared) is mounted in the focal point of a lens. The circle is, therefore, illuminated by parallel rays that continue through the glass circle, through the index patterns (masks on glass) onto the photodiodes. According to the mask shown in Fig. 4.15, six separate photodiodes are required to convert the light received in the six windows into electrical currents.

Whenever the readout optics move against the fixed circle (as it happens with the horizontal circle) or whenever the circle rotates through the fixed readout optics (as in the case of the vertical circle), the intensity of the light received by the photodiodes A and B varies. When an opaque field of the mask fully covers a transparent field of the circle, no light is received (= minimum of the sine curve). When a transparent field of the mask fully covers a transparent field of the circle, the maximum of light is received (= maximum of the sine curve). Between the two states, the signal will change, approximately, as a sine curve.

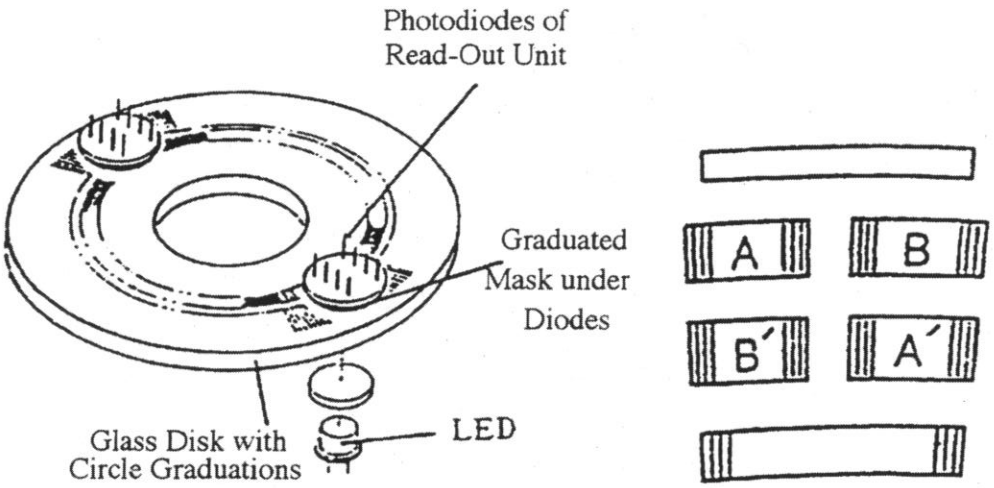

Figure 4.15: On left: View of the circle reading system of the Nikon DTM-1. A light emitting diode and a collimating lens are below the circle. The graduated masks and the photodiodes are above the circle. On right: graduations on the index masks. The top window is blank. This transparent part is used to monitor (and regulate) the light output of the LEDs. A and B refer to the SIN and COS masks, respectively. 'A' and B' duplicate the masks A and B, most likely to reduce systematic errors by a symmetrical lay-out. The bottom window is used on the (quasi-absolute) vertical circle for the detection of the 'zero'- (reference) mark.

The processing of the two signals is shown in Fig. 4.16, namely those of the A (sine) and the B (cosine) masks from both sides. The cosine signal has a 90° delay against the sine signal. The two signals from the other side of the circle feature phase shifts of 180° (-sin) and 270° (-cos). The output signals of the photodiodes are first amplified and then fed into a differential amplifier. The two differential amplifiers take the differences of the two input signals and amplify the result:

$$\sin \phi - \sin (\phi + 180°) = \sin \phi - (-\sin \phi) = 2 \sin \phi \qquad (4.1)$$

$$\sin (\phi + 90°) - \sin (\phi + 270°) = \cos \phi - (-\cos \phi) = 2 \cos \phi \qquad (4.2)$$

The above equations show that taking the difference of the two input signals already doubles the amplitude. The resulting sine and cosine signals are split for the execution of the coarse and the fine measurement.

4.3.1 Coarse Measurement

The sine and the cosine signals are converted to square waves for the coarse measurement. The coarse measurement is obtained by counting the number

of periods (full cycles) which occur between the start and the end of the rotation to be measured. The basic resolution of the coarse measurement is the angular equivalent of the period of the sine and cosine signals, namely 400 grads/10000 = 0.04 grads = 0.04 gon. The coarse measurement of any instrument or telescope rotation is obtained simply by multiplication of the number of counts with 0.0400 grads. The question on how to find out the sense of the rotation (clockwise: positive coarse measurement; anticlockwise: negative coarse measurement) will be addressed later.

The resolution of the coarse measurement (about 130 seconds of arc) is not accurate enough. To get a better resolution, it is necessary to determine the fraction ϕ of a graduation interval between a circle graduation and a graduation on the mask. This process is called interpolation or fine measurement.

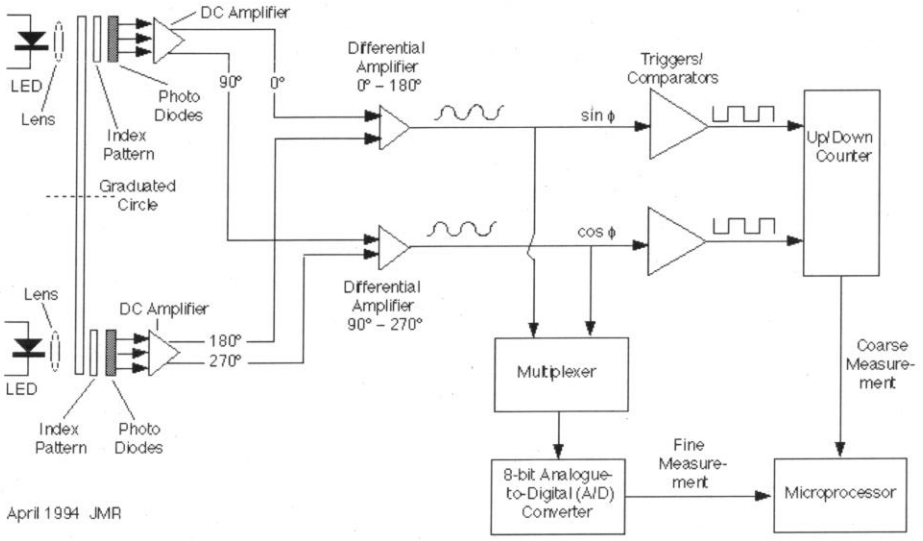

Figure 4.16: Block diagram of the circle reading system of the Nikon DTM-1.

4.3.2 Fine Measurement

The sine and cosine signals are multiplexed for the fine measurement. This means that the sine and the cosine signals are processed one after the other in a time sharing mode. The two signals are available in analogue form as voltage levels, which change for any introduced rotation. For digital processing, the voltage has to be converted to a number. This is achieved with an analogue-to-digital converter. In the DTM-1, the maximum voltage

is converted in 256 increments (2^8). The 8–bit analogue-to-digital (A/D) converter changes the amplitudes of the sine and cosine signals to numbers (e_0, e_{90}) between 0 and 256. Assuming that the maximum signal voltage is very close to the maximum input voltage of the converter, the least count of the fine measurement is 1.6^{cc} or 0.00016 grads or 0.00016 gon or 0.16 mgon or 0.52". At each circle position, the phase angle ϕ between the circle and mask graduations must be evaluated. The following relationship is used:

$$\tan \phi = \sin \phi / \cos \phi \qquad (4.3)$$

Using e_0 (the digitised amplitude of the sin ϕ signal) and e_{90} (the digitised amplitude of the cos ϕ signal) and solution for ϕ leads to

$$\phi = \text{arc tan} (e_0/e_{90}) \qquad (4.4)$$

The unit of ϕ depends on how the trigonometric function is computed. The circle interpolation ϕ must be converted to grads to be consistent with the previous derivations. Because of the incremental nature of the circles of the Nikon DTM-1, the display of the angular values has to be referenced to the horizontal circle position at switch-on and to the vertical circle reading at the time of the pick up of the reference mark (quasi-absolute circle).

The *displayed direction* value at an alidade position (x) may be derived as Direction (x) = 0.0000 grads (= direction at switch-on) + {number of pulses counted (positive or negative) x 0.04 grad} + ϕ(x) – ϕ(at switch on), where ϕ(x) and ϕ(at switch-on) are the fine measurements (interpolation values) at the arbitrary (x) and 'switch on' alidade positions, respectively. Before the horizontal direction is displayed, it is converted into the unit requested by the user (degrees-minutes-seconds, decimal degrees, mils).

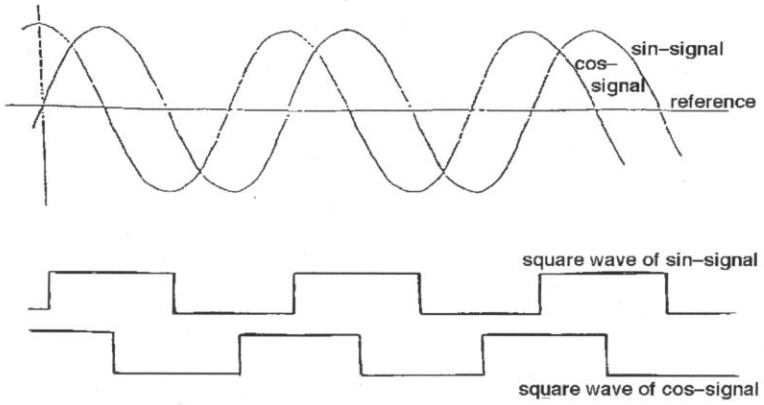

Figure 4.17: Direction Sensing (Up-Down) logic of the Nikon DTM-1. The horizontal axis represents the angle of rotation, positive to the right.

The zenith angle is initialised by tilting the telescope through the horizon. When doing so, the instrument picks up a reference mark on the quasi-absolute circle and 'zeros' the circle reading (setting z = 100.0000 grads). The *displayed zenith angle* value at a telescope position (y) can then be derived as z(y) = z(ref) (= 100.0000 grads) + ϕ(y) – ϕ(ref) + {number of pulses (+ or –) from reference mark x 0.04 grad} where ϕ(y) and ϕ(ref) are the fine measurements (interpolation values) at the arbitrary (y) and 'reference' telescope positions, respectively. Before the zenith angle is displayed, it is converted into the unit requested by the user (degrees-minutes-seconds, decimal degrees, mils).

4.3.3 Sensing of the Direction of Rotation

The only problem left is find out whether the coarse measurement pulses need to be counted positive or negative by the up/down counter. A logic is required for the detection of the clockwise (+) and the counter clockwise (–) rotation. The basic principle of the direction sensing is shown in Fig. 4.17. As discussed before, the sinusoidal signals are converted to square signals by the two triggers. The rotation sensing logic uses the square signals only. Based on the 'high' and 'low' states of the two waves, it determines if the sine-signal leads the cosine signal or vice versa. Two possible implementations are discussed below. In reality, the sense of the direction can be derived four times over the period of the square signal, namely for each rise and fall of the two signals. This provides redundant data.

In Fig. 4.17, moving to the right on the time axis corresponds to a clockwise rotation of the alidade. The logic makes use of the fact that a zero crossing (rise) of the sine signal is followed by a negative zero crossing (fall) of the cosine signal. In other words, if the sine is high and a fall of the cosine is recorded, we know that the alidade rotates clockwise. The counted pulses are thus positive and must be added by the counter.

On the other hand, a movement to the left in Fig. 4.17 refers to an anticlockwise rotation of the alidade. A positive zero crossing (rise) of the sine signal is followed by a positive zero crossing (rise) of the cosine signal. In other words, if the sine is high and a rise of the cosine signal occurs, the logic concludes that the alidade is turned anticlockwise and that the counted interval must be subtracted.

4.4 Electro-Optical Level Sensors

Level sensors are commonly used in modern theodolites and tacheometers. They provide the actual value of the dislevelment and simplify the circle reading optics. Typically, a level sensor uses a liquid surface to provide a

horizontal plane and measures the tilt of the vertical axis opto-electronically. A controlling microprocessor is used to compute the tilt corrections automatically. When enabled, the displayed zenith angle readings (and, for dual-axis level sensors, the horizontal directions) are largely free of the effects of a small residual dislevelment of the vertical axis.

There are two types of level sensors, namely single-axis and dual-axis devices. To permit the real-time correction of the horizontal directions for a small dislevelment of the vertical axis, the instrument must be equipped with a dual-axis level sensor. Instruments with dual-axis level sensors are becoming more common because they are very useful whenever highly accurate directions are required to points with steep lines of sight. It is well known that, at zenith angles of 45°, a 10" levelling error (in trunnion axis direction) causes a 10" error in the horizontal direction. (For even steeper sights, the errors in the directions exceed those in the levelling.) This cannot be eliminated by measuring in two faces but can be removed by an instrument with a dual-axis level sensor and associated software.

Early instruments to use dual-axis level sensors were the Hewlett-Packard HP3820A (1978), Kern E2 (1983), Zeiss Elta 3 (1986), Geodimeter 420/440 (1986) and the Wild T2002/T3000. As dual-axis level sensors are useful whenever steep sights are involved in direction measurements (for example in engineering surveying), most modern electronic tacheometers and theodolites feature such devices.

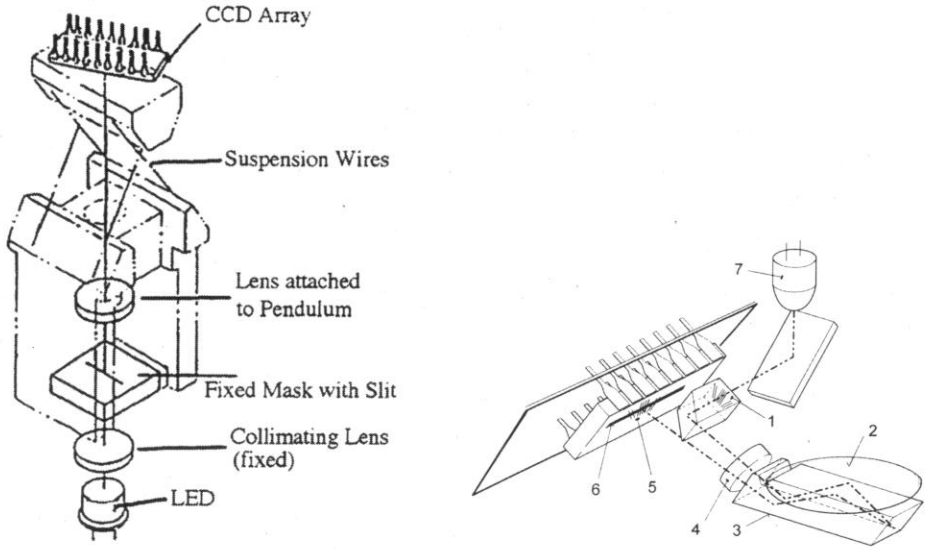

Figure 4.18: Single-axis pendulum level sensor of the Nikon DTM-1 electronic tacheometer on the left and dual-axis liquid level sensor of Leica TPS1100 series on the right. The numbered items are defined in the text. (Figure on the right after Zeiske 1999.)

4.4.1 Nikon DTM-1 Single-Axis Level Sensor

The Nikon DTM-1 electronic tacheometer uses a pendulum–type level sensor. Like most other pendulum sensors, it is a single-axis device. It uses a light emitting diode (LED) to illuminate a transparent slit on a fixed mask. The light bar is projected through a lens onto a CCD array. The lens is attached to a conventional mechanical pendulum system that hangs vertically under the effect of gravity. The position of the light bar on the CCD array is converted into a reading of the tilt of the vertical axis parallel to vertical circle. This value is then used to correct the zenith angle reading into the true zenith. (Refer to Eqs. (4.15) and (4.17).)

4.4.2 Leica TPS1100 Series Dual-Axis Level Sensor

The Leica TPS1100 series of instruments incorporates liquid level dual-axis level sensors. The layout of this level sensor is shown on the right of Fig. 4.18. This particular design was developed to allow to install the liquid horizon in the centre of the instrument, that is in the vertical axis. This has the advantage that the rotations of the upper part of the theodolite exert minimal centrifugal forces on the liquid. In consequence, this level sensor requires less time to settle after a rotation than a level sensor mounted (as usual) in the standards of a theodolite (see Fig. 4.19 for example of the latter design). Also, centrally mounted level sensors are not affected by temperature induced deformations in the standards (Zeiske 1999).

On the right of Fig. 4.18, the ray path through the Leica TPS1100 level sensor is depicted. The prism ('1' in Fig. 4.18) carries a line pattern that is illuminated by a light emitting diode (LED, see '7' in figure). The line pattern is projected through a lens ('4') and a deviation prism ('3') onto the liquid horizon, where it is reflected twice at the surface of the liquid. The image ('5') of the line pattern falls on the linear CCD-array ('6'). Because of the use of V-type lines at both ends of the line pattern (besides the parallel lines in the centre), it is possible to measure both components of the tilt of the vertical axis with one linear ('single-axis') CCD sensor. A longitudinal tilt of the vertical axis (i.e. parallel to the vertical plane defined by the rotating telescope) changes the distance between the V-type lines of the pattern. A traverse tilt (in the vertical plane parallel to the trunnion axis) moves the centre of gravity of the line pattern on the CCD sensor.

Leica quotes the 'setting accuracy' of the level sensors of the TPS1101 and TPS1102 instruments as 0.5". Since no distinction is being made between the two components of the dual-axis level sensor, one may assume that they are equally accurate. For comparison, the angular accuracy of the TPS1001 instruments is quoted as ±1.5" (after ISO 17123-3). It is appropriate that the

accuracy specification of the level sensor is only a third of the angular accuracy rating.

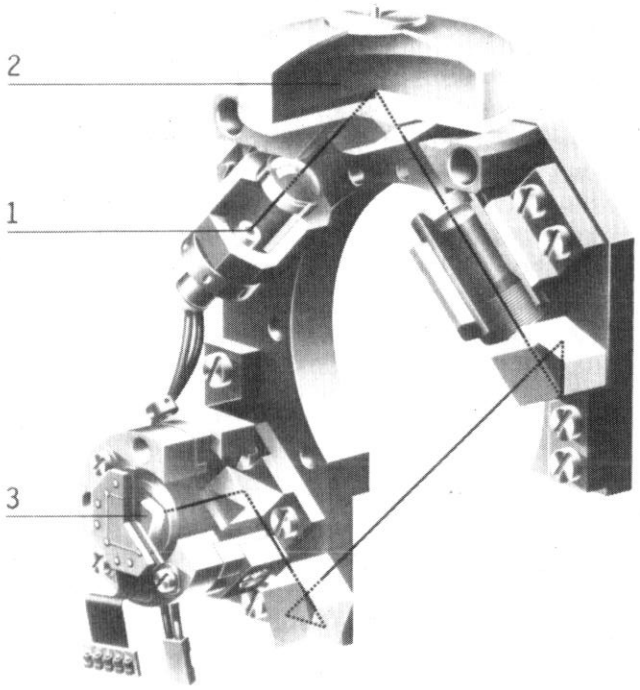

Figure 4.19: Cross section through the dual-axis level sensor of the Kern E2 electronic theodolite (after Lardelli 1988). A light emitting diode (1) emits a light beam that is focussed to infinity by a lens with a short focal length. The parallel rays are reflected downwards at the top surface of the liquid horizon (2). The reflected beam is then focussed onto a position sensitive quadrant photodiode (3) by a second lens with much longer focal length. To save space, the read-out ray path is bent three times.

4.4.3 Kern E2 Dual-Axis Level Sensor

The dual-axis level sensor of the electronic theodolite Kern E2 is similar to the proven liquid compensator of the Kern DKM-2A one-second theodolite. (Some Zeiss electronic theodolites use the same device in a slightly modified form.) Figure 4.19 shows a three-dimensional view of the device and explains the basic principle. Because the liquid horizon is intrinsically two-dimensional, the light beam is reflected in two dimensions, one component being parallel to the plane of the light path (parallel to the vertical circle) and the other perpendicular to it (parallel to the trunnion axis).

The quadrant photodiode measures the x-y coordinates of the light spot created by the reflected rays on the diode relative to the centre of the diode.

The two components of the diode readout are a measure of the two components of the vertical axis tilt, namely the tilt parallel to the vertical plane described by the telescope axis rotating about the trunnion axis and the tilt parallel to the vertical plane through the trunnion axis. The output currents (i_1, i_2, i_3, i_4) of the diode are used to derive the x and y coordinates of the light dot.

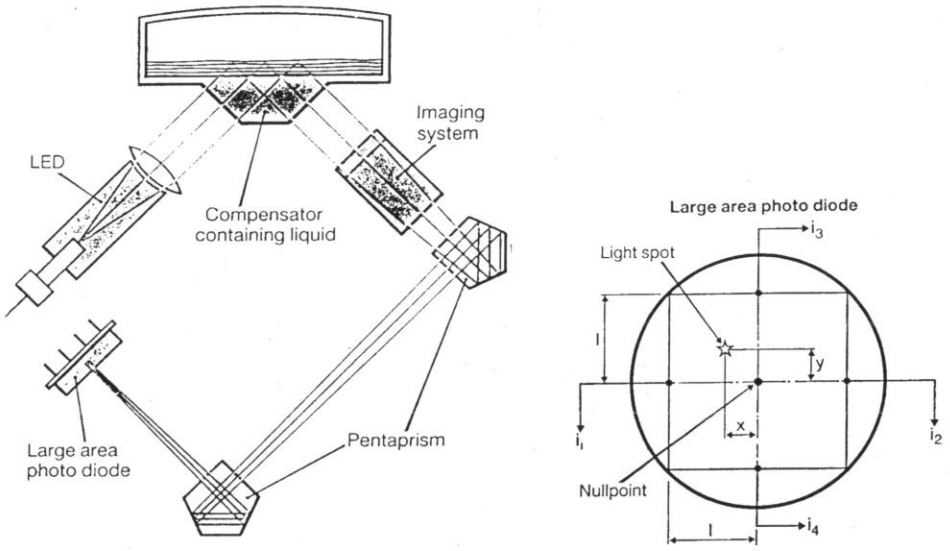

Figure 4.20: Side view (parallel to the plane of the vertical circle) of the Kern E2 dual-axis level sensor (on the left) and the principle of the two-component read-out on the position sensitive quadrant photodiode (on the right). The photodiode has five electrical connections, one in the centre and one each (i_1, i_2, i_3, i_4) for the four quadrants. (after George 1984)

In simple terms, the derivation can be given as follows:

$$i_1 \, k \, (l - x) = i_2 \, k \, (l + x) \qquad \text{and} \qquad i_3 \, k \, (l - y) = i_4 \, k \, (l + y) \tag{4.5}$$

where l is one half of the side length of the photosensitive area of the diode and k a constant. Solving for x and y leads to

$$x = l \left(\frac{i_1 - i_2}{i_1 + i_2} \right) \qquad \text{and} \qquad y = l \left(\frac{i_3 - i_4}{i_3 + i_4} \right) \tag{4.6}$$

The units of x and y are the same as that of l, namely a length unit. Angular units are obtained by dividing x and y by the focal length of the lens system between the liquid horizon and the photodiode. Any errors in the length of the focal distance used for this purpose will cause *scale errors* in the angular values and, eventually, in the displayed vertical axis tilts. In Fig. 4.20 it is assumed that the optical axis of the lens system intersects the centre of the

photodiode. In practice, this is not exactly the case. Small corrections *(the additive constants of the level sensor)* need to be applied to the measured x-y values to reference them to the point where the optical axis intersects the photodiode.

Changing the inclination of the vertical axis (see Fig. 4.20) causes a movement of the light dot on the position sensitive photodiode. This information is used to compute the two-components of the vertical axis tilt. The next section discusses this principle in more detail for a simplified ray path.

4.4.4 Principle of the Determination of the Theodolite's Dislevelment

The unfolded ray path of a liquid level sensor is shown in Figure 4.21 for three different cases. The sensor design is a simplified version of the type shown in Section 4.4.3. In all three figures it is assumed that the optical axis of the lens on the photodiode side intersects the photodiode in the centre. Figure 4.21a depicts the ideal case where the plumbline is coincident with the vertical axis and the symmetry axis of the level sensor. In consequence, the light travels along the optical axes and is projected into the centre of the position sensitive photodiode. The angle between the symmetry axis and the optical axes of both lens systems is denoted by ϕ.

Figure 4.21b gives the same view as Fig. 4.21a, but for a dislevelled theodolite or tacheometer. The instrument is out of plumb by an angle α. The angles between the optical axes of the two lens systems and the symmetry axis of the level sensor (and the inclined vertical axis) are still the same (ϕ). Because of the tilt, the liquid horizon is no longer perpendicular to the vertical axis. This affects the reflection of the rays. The incident angle at the liquid horizon is ($\phi - \alpha$) as is the emerging angle. The figure shows that the optical axis and the reflected rays are at an angle of 2α to each other. In consequence, the light dot is no longer in the centre of the photodiode but rather $2 \times \alpha \times f$ towards the vertical axis, f being the focal length of the photodiode optics.

The configuration, after a rotation of the alidade by 180° about the vertical axis, is shown in Fig. 4.21c. In the absence of a wobble error in the vertical axis bearing, the direction of the vertical axis will still be inclined at an angle α. The incident angle of the rays on the liquid horizon is now ($\phi + \alpha$), because the rays are coming from the right. The emerging angle is also ($\phi + \alpha$), whereas the angle between the optical axis on the photodiode side and the plumbline is now ($\phi - \alpha$). The figure shows that the optical axis and the reflected rays are at an angle of 2α at the photodiode. The light dot is again not in the centre of the diode but rather at a distance of $2 \times \alpha \times f$ away from the vertical axis. If the coordinates of the light dot on the photodiode are

measured in face left and in face right, then the change of the coordinates between the two faces will be equivalent to 4 times the dislevelment of the vertical axis. This rule applies to both components.

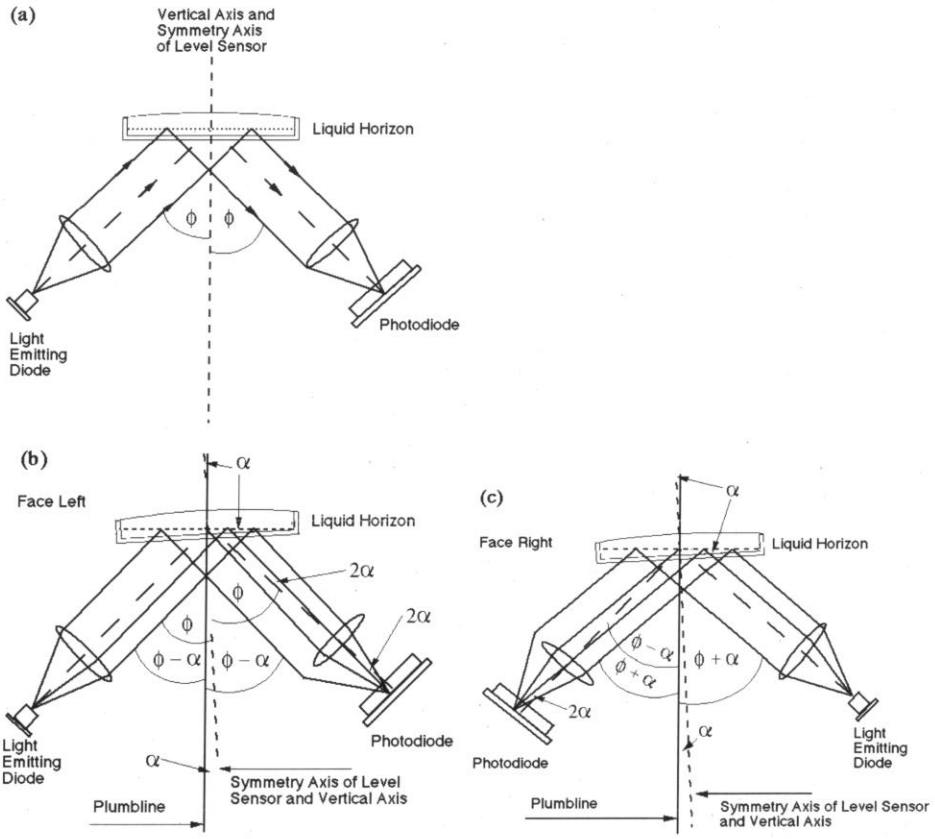

Figure 4.21: Working principle of (one component of) a liquid level sensor

As only coordinates on the photodiodes are recorded, the angle α has to be expressed in terms of these measurements. Let S_{FL} be the coordinate reading on the photo diode in face left, S_{FR} the coordinate reading on the photo diode in face right and S_{REF} the coordinate reading for the optical axis. S_{REF} should be zero if the theodolite is truly vertical and if no index error (additive constant) of the level sensor is present. In face left, the following formula applies in the right angled triangle between the centre of the lens, the centre of the photodiode and the light dot:

$$2\alpha = \arctan\left(\frac{S_{FL} - S_{REF}}{f}\right) \tag{4.7}$$

$$\alpha = (S_{FL} - S_{REF}) \times \frac{206265''}{2f} \tag{4.8a}$$

$$\alpha = S_{FL} \times C - S_{REF} \times C \tag{4.8b}$$

where ($S_{FL} - S_{REF}$) is positive, S_{FL}, S_{REF} and the focal length f are taken in mm and where C is the scale factor which converts the photodiode output into the (single) vertical axis tilt α, in seconds of arc. In face right, the following relationship holds:

$$-\alpha = (S_{FR} - S_{REF}) \times \frac{206265''}{2\,f} \tag{4.9}$$

$$-\alpha = S_{FR} \times C - S_{REF} \times C \tag{4.10}$$

Taking the difference between Eqs. (4.8) and (4.10) gives the measured component of the dislevelment α of the vertical axis

$$2\alpha = S_{FL} \times C - S_{REF} \times C - S_{FR} \times C - S_{REF} \times C \tag{4.11}$$

$$\alpha = (S_{FL} \times C - S_{FR} \times C) / 2 \tag{4.12}$$

Adding Eqs. (4.8) and (4.10) gives the additive constant ($S_{REF} \times C$) of the measured component of the level sensor

$$0 = S_{FL} \times C - S_{REF} \times C + S_{FR} \times C - S_{REF} \times C \tag{4.13}$$

$$0 = S_{FL} \times C + S_{FR} \times C - 2S_{REF} \times C$$

$$S_{REF} \times C = (S_{FL} \times C + S_{FR} \times C) / 2 \tag{4.14}$$

It follows that it is very easy to determined the additive constants of level sensors: Read the level sensor in two faces and take the mean. Also, a theodolite or tacheometer is truly vertical, if the level sensor reads the same value ($S_{REF} \times C$) in all orientations of the alidade.

Please note that each coordinate is individually multiplied with C as it is the product of S_i and C that is displayed by instruments.

4.5 Properties of Electronic Level Sensors

The error patterns of mechano-optical vertical circle compensators and compensators in automatic and digital levels are similar. In theodolites, the errors are reduced, because the theodolites can be (and should be) levelled more accurately than levelling instruments. The error patterns of electronic level sensors and vertical circle compensators are also similar because the basic sensor elements are the same, namely mechanical pendulums and liquid horizons.

4.5.1 Compensation Error ε

For the traditional vertical circle compensators, the compensation error ε is defined as the residual inclination of the vertical circle reading system caused by under- or over-compensation of the compensator. It is a function of the dislevelment α of the vertical axis. Figure 4.22 demonstrates the principle of the compensation error of mechano-optical compensators and applies equally to FL and FR observations.

The compensation error is caused by the positioning tolerances (errors) in manufacturing, the inaccuracy of the optical-mechanical design and the effects of changing gravity. The compensation error may also depend on ambient temperature. The magnitude of the compensator error ε in classical instruments with compensators is usually less than 1%-5% of the dislevelment α.

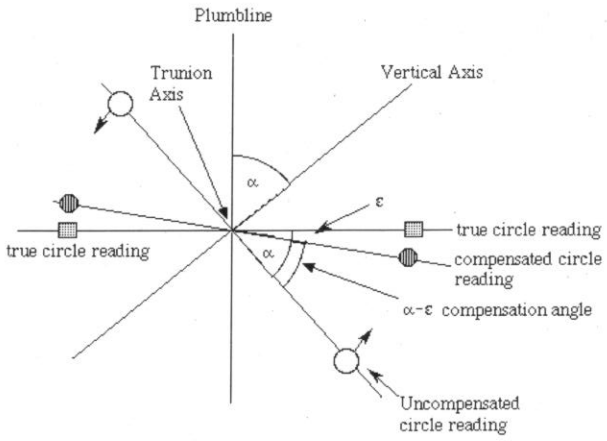

Figure 4.22: Principle of the compensation error ε in mechanical vertical circle compensators. The dislevelment of vertical axis is denoted by α.

4.5.2 Scale Factor Error ΔC

In electronic level sensors, the scale factor error causes errors that are equivalent to the compensation errors of the vertical circle compensators. As before, the errors in the measured inclination of the vertical axis, as well as in the corrections to zenith angles and directions computed from these tilts, are a function of the dislevelment α. The scale factor C of level sensors has been defined previously (Eqs. (4.8a) and (4.8b)). It is a function of the focal length f of the sensor's optics.

An error ΔC in C may be due to the manufacturing tolerances (positioning of lens, emitting diode and photo diode) or due to the conversion of the electronic read-out of the photodiode output current to length units. The magnitude of the scale factor error in electronic level sensors is typically less than 1%-2% (of α).

The scale factor errors are dangerous (as are the compensation errors), because the measured zenith angles are affected but not the vertical circle index error. This error cannot be detected in the usual way (by checking the sum of FL and FR zenith angle readings). *The scale factor error (as well as the compensation error)* ***cannot*** *be eliminated by measurement in two faces!*

4.5.3 Setting Error

4.5.3.1 Random Component

This reflects the setting accuracy of the level sensor after a disturbance (such as a rotation of the alidade or another instrument manipulation). This repeatability is typically better than 3" – 1". The setting accuracy specified by manufacturers for some instruments is given as a guide:

Sokkia SET 2C/3C	±1"	Leica TPS1100	±0.5"
Wild T2000	±0.3"	Nikon DTM-821	±1.0"
Sokkia SET 5C	±5"	Topcon GTS-603C	1.0"
Zeiss Elta 2/3	±0.6–1.0"	Zeiss Elta S10/S20	±0.3"

It is unfortunate that some manufacturers (e.g. Sokkia, Trimble) do not specify the accuracy of their level sensors. The presumption is that, in these cases, the specifications of the angular accuracy include the level sensor uncertainty.

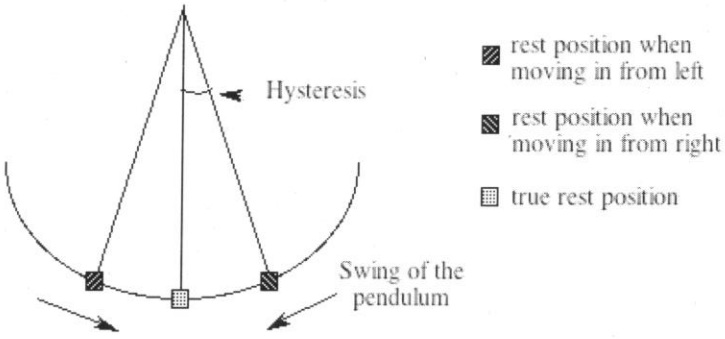

Figure 4.23: Principle of mechanical hysteresis ('compensator drag')

The setting time of the level sensors depends on their design. The mechanical devices (pendulum) need about 1 second of time to reach an equilibrium position. The liquid level devices require longer times, typically

3 to 5 seconds. Even longer times are required in cold weather, because of the change in the viscosity of the liquid. It is likely that level sensors located in the vertical axis (see right of Fig. 4.18) need less time to settle. The observer should wait long enough before reading and/or recording measurements. This is essential for all zenith angle measurements. If dual-axis level sensors are used to correct horizontal direction measurements, then the same waiting period applies for horizontal angle measurements.

4.5.3.2 Systematic Component

Mechanical hysteresis exists if the final rest position of the pendulum depends on the direction from which the pendulum moves into its rest position. See Fig. 4.23. The error caused by the mechanical hysteresis is a function of the inclination of the vertical axis (α) and of ambient temperature. In the last version of the classic Wild T2 theodolite, a push button ensured that the compensator always 'moved in' from the same side. The hysteresis effect will then be similar for all readings and, thus, become part of the vertical circle index error. Some experiments did establish the magnitude of the hysteresis effect as less than 3" - 25" for a selection of optical third order theodolites. *Liquid level compensators and level sensors are not affect by hysteresis.*

4.5.4 Vertical Circle Index Error and Correction

As optical theodolites, electronic theodolites and tacheometers have an index error of the vertical circle reading system and require a vertical circle index correction (VCIC). This error has two components, which might be explained with reference to an instrument, which reads the zenith angle in the horizon through the trunnion axis. Firstly, the line between the 90° and the 270° mark on the circle might not be exactly parallel to the line of sight. Secondly, the reading mechanism might not be exactly in a horizontal plane trough the trunnion axis. The two components cannot be separated; the sum is determined and corrected for. The previously discussed additive constant of the electronic level sensor constitutes an additional (third) component of the total VCIC. If the level sensor correction is enabled and the VCIC is determined in the usual way, the resulting value will include the additive constant of the level sensor (component parallel to telescope axis). If the level sensor is 'switched off' during the determination of the VCIC, then the resulting VCIC value will not include the additive constant of the level sensor. See Eqs. (4.15) and (4.17) for proof.

The (total) vertical circle index error may be affected by ageing (long-term changes), shocks, lateral tilts (cross-tilts), sticking of a mechanical compensator level sensor and temperature. Only the last effect is discussed further.

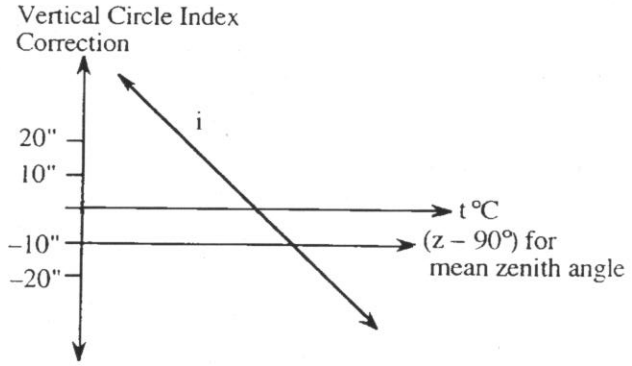

Figure 4.24: Temperature dependence of the index error and temperature independence of the mean (of two faces) zenith angle (z) for a particular theodolite

Experiments have shown that the vertical circle index correction (VCIC) and/or level sensor correction can be strongly dependent on temperature. Some examples of test results may illustrate the magnitude of the problem in electronic tacheometers and level sensors:

KERN E2	+0.30"/°C
WILD T2000	–0.88"/°C
KERN DKM 2A	+0.91"/°C

As the ambient temperature changes as a function of time, the temperature effects caused by the level sensors in the zenith angle measurements can be reduced by appropriate field procedures. The linear changes with time of the index or level sensor correction may be eliminated by measuring zenith angles in the following sequence: $z_{FL} - z_{FR} - z_{FR} - z_{FL}$.

4.6 Circle Graduation Errors

There are two types of circle graduation errors, namely random errors and systematic errors. The systematic errors are usually referred to as periodic errors. All systematic circle graduation errors are caused by imperfections in the devices that produced the master circles and those used for the transfer to the instrument's circles.

First and second order theodolites read circles at diametrically opposite points on the circles. In these cases, the actual *graduation error* is of little interest. What is of interest is the sum of the opposite errors, namely the *diameter error*. In some precision theodolites, the circles are read in four positions, 90° apart.

4.6.1 Periodic Errors

Periodic errors can be modelled with sine and cosine functions. Periods vary from 360° down to multiples of the basic circle graduation interval (from 180° downwards for instruments with diametrical circle reading). Most tests are usually restricted the fundamental wave period (360° or 180°) and some of its harmonics.

The periodic errors are traditionally determined by measuring the same angle between two (or more) collimators at different zeros of the (horizontal) circle. Other methods involve comparison against a laser interferometer or against a high precision theodolite. An example of the latter technique is shown in Fig. 4.25. Periodic circle graduation errors can be eliminated to a certain degree by appropriate observation procedures. These are discussed later.

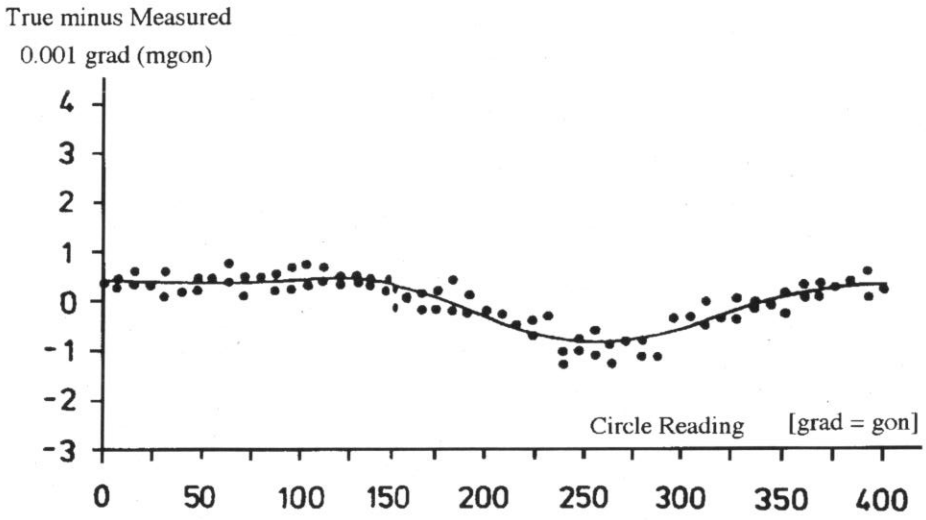

Figure 4.25: Periodic error of a specific electronic tacheometer Zeiss Elta 6. As the instrument does not feature diametrical circle reading, the fundamental period is 360° (or 400 grads; after Hennes & Witte 1991)

4.6.2 Interpolation Errors

Interpolation errors are the systematic errors of the fine measurement during the circle reading. As discussed previously, the circle interpolation is the measurement of the position of the reading index between two graduations of the circle. The interpolation errors are equivalent to the errors of the micrometer reading ('micrometer errors') in the classical instruments with visual circle reading.

The error patterns across the interpolation interval depend on the type of the interpolation system used. They may be due to errors in the index patterns on the mask, unequal illumination, a deviation of the actual signal from the (assumed) sinusoidal wave shape, and any errors in the spacing of the multiple reading indices (e.g. the spacing of the diodes that generate the 0°, 90°, 180° and 270° signals).

The interpolation errors can be determined in laboratories and modelled by sine and cosine curves (Fourier series). Figures 4.26a and 4.26b show the results of such tests and the fitted curves. If the calibration is done by the manufacturer, then there is a possibility of real-time correction (used in Zeiss ETh3, for example). However, if the calibration is done by the user, then post-correction is possible, in principle, but usually too cumbersome to be practical. Fortunately, the interpolation errors are usually very small. The table gives the results of some tests. For the horizontal direction measurement only, the interpolation errors could be reduced in the field, as the micrometer errors were with optical instruments. However, a physical change of the zero of the horizontal circle by a fraction of the interpolation interval is not practical and, in most cases, not possible.

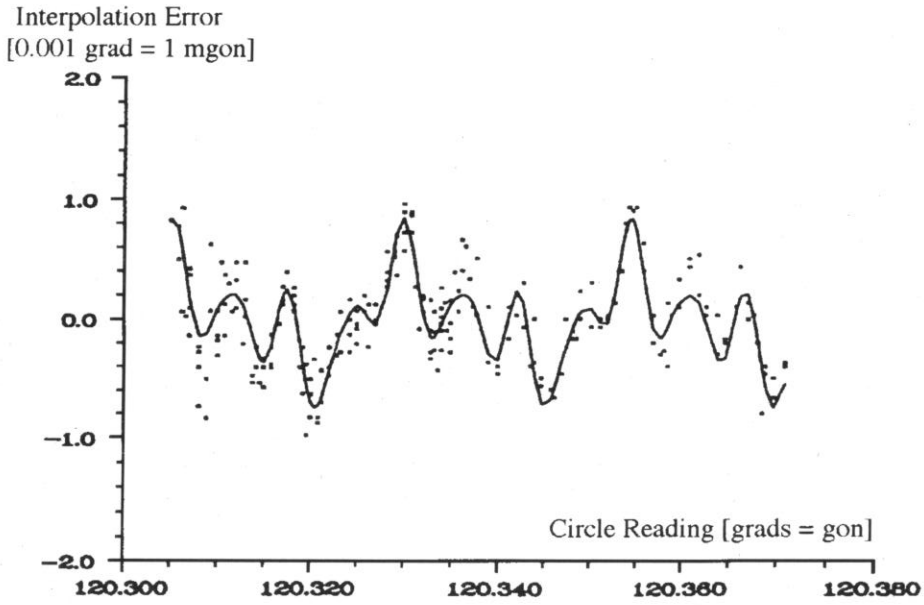

Figure 4.26a: Interpolation error of an electronic theodolite Zeiss ETh3. As the circle graduation interval is 82.3" (0.0254 grad), the interpolation error repeats a few times over the circle section shown. The peak-to-peak (p-p) variation is 5.2". (after Hennes and Witte 1991)

The interpolation error of another instrument (Nikon DTM-750) is shown in Fig. 4.26b. This electronic tacheometer features 16200 graduations over the

full circle (360°) and, thus, has an interpolation interval of 80" exactly (in Fig. 4.26b shown as 24.69 mgon or 0.0247 grads). In this case, the peak-to-peak variation of the circle reading is 3.05" (or 0.94 mgon). The angular accuracy quoted by the manufacturer is ±2" (after the German industry standard DIN 18723). The curve shown in Fig. 4.26b (Schauerte et al. 1994) is the sum of a first order (period = 80") and a second order periodic error (period = 40") fitted by least squares. The corresponding amplitudes are 0.55" and 0.96", respectively.

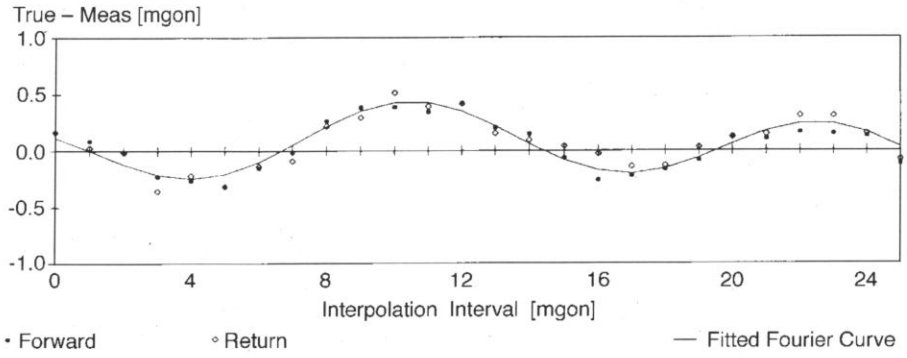

Figure 4.26b: Interpolation error of an electronic tacheometer Nikon DTM-750. Since the circle graduation interval is 80.0" (0.02469 grad, 24.69 mgon), the figure shows the interpolation error without repeats across one interpolation interval. The peak-to-peak (p-p) variation is 3.05". The dominant periodic error term has a period of 40.0" and an amplitude of 0.96". One second of arc is equivalent to 0.3 mgon or 0.0003 grads. (after Schauerte et al. 1994)

Instrument	Peak-Peak Variation	Interpolation Interval
Nikon DTM-750	3.0 "	80.0 "
Topcon GTS-6B	1.7 "	80.0 "
Topcon GTS-301	3.3 "	80.0 "
Zeiss ETh3	5.2 "	82.3 "

Table 4.1: Measured interpolation errors for a selection of individual instruments.

4.7 Some Notes on the Use of Electronic Theodolites and Tacheometers

It has been mentioned before that, in principle, the electronic theodolites and tacheometers should be used in the same way as the older optical instruments in general, and the one-second theodolites in particular. A few aspects have changed however and need to be considered. Only some

aspects are discussed here. The aspects relating to electronic distance measurement are not covered. Readers may refer to the EDM textbook by Rüeger (1990, 1996), for example.

4.7.1 Levelling of Electronic Theodolites and Tacheometers

If an electronic tacheometer or theodolite is equipped with a dual-axis level sensor, and if the level sensor and the correction function for zenith angles and directions are enabled, then and only then is the levelling less critical than in the past. Because of the scale factor error of level sensors, it is suggested that the instruments be levelled to about ±20" to ±30" (one division on most plate levels) all the same.

Some instruments with dual-axis level sensors have displays like the one shown in Fig. 4.27. For instruments with identical displays on both sides, an operator can completely level an instrument without moving around the tripod. This saves time. The operator starts by levelling the fictitious bubble on the display in the first alidade orientation. After each turn on the footscrews, one should let the values settle for about three to five seconds (to a 'constant' value). This is equivalent to getting the values for the x and y tilts to zero. (Normally, it is not possible (nor necessary) to make the x and y tilts exactly zero as the pitch of the footscrews is not fine enough and the tripod often not stable enough.) The alidade is then rotated 180° about its vertical axis. If the fictitious bubble moves out of the centre position (and the x and/or y tilt values change), the levelling is changed half-way back (to the mean values/position of both 'faces'). The theodolite or tacheometer is truly vertical, if the level sensor reads the same values of x and y in all orientations of the rotating upper part ('alidade') of the theodolite.

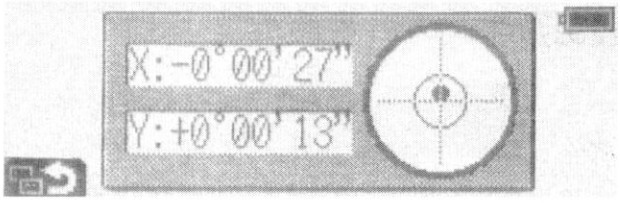

Figure 4.27: Level sensor read-out and levelling display on an electronic tacheometer Topcon GTS-6

4.7.2 Selection of Measuring Units

Since the introduction of the electronic theodolites and tacheometers, the units of the angular (and distance) measurements can be changed easily by the observer. Typically, 400 grads (gon), 360° decimal, 360° sexagesimal

(° ' ") and 6400 mils are offered. Many users don't realise that the resolution can be quite different, depending on the selected unit. For example, the Wild TC1610 has the following resolutions: 1^{cc} (0.33"), 1", 0.0001° (0.36"), 0.001 mil (0.20"). Note that 1^{cc} = 0.1 mgon = 0.0001 gon = 0.0001 grad. Clearly, the best resolution is achieved in the military mil setting.

When recording data, users of electronic instruments should ascertain that the post-processing software can use the selected units. Unfortunately, this may greatly limit the choice available in the field. *When booking by hand* and doing the post-processing by hand, it is suggested to use a decimal unit, like decimal degrees (or grads(gon) for that matter). This simplifies the field reductions and avoids the cumbersome conversions from degrees, minutes and seconds to decimal degrees on calculators.

4.7.3 Use of Umbrella

There are many good reasons why an umbrella should be employed to provide shade for the observer, the instrument and the tripod. Some of these are given below.

4.7.3.1 Electronic Theodolites

- Australia has the highest incidence of skin cancer in the world. (One in 45 Australians is affected by melanoma!) Similarly, extensive exposure to sun can cause permanent eye damage. To provide shade for field parties is, thus, essential and an occupational health and safety (OHS) requirement.
- The operating temperatures of instruments are specified as ambient, shadow temperatures. In full sunlight, the inside of the instrument can be 20°C higher. Some instruments cut-out automatically when the upper limit of the specified operating temperature is reached. A shaded instrument may work whilst an unshaded may not!
- The pointing to targets, either manually or automatically, can be very difficult, if not impossible, when the sun is shining into the optics. This increases the time required for the pointing and may reduce the accuracy of the measurements.
- A change of the temperature of the instrument leads to temperature gradients through the mechanical and optical components. Temporary misalignments and changes of instrument errors occur. Typically, about 5 minutes per °C temperature change are required for an instrument to reach a dimensional equilibrium at a new temperature. This waiting time after temperature changes (e.g. after moving the instrument from an air-conditioned car into 40°C heat) should be observed before beginning high precision measurements. Proper acclimatisation of instruments is particularly important when using automatic pointing systems. In consequence, it is advisable not to leave instruments in a hot, stationary car;

rather, they should be unloaded and stored in a shadowed area in the open air (e.g. under an umbrella).

- The level sensors are usually mounted in one of the two standards and thus fully exposed to heating by the sun in the absence of an umbrella. Changing face alternates the level sensor between the sun and the shadow side, with all the negative effects on it temperature equilibrium.

4.7.3.2 Electronic Tacheometers

- Do not aim the telescope at the sun: You may burn out the transmitting and receiving diodes in doing so and, thus, permanently damage the instrument. Do not carry out sun azimuth observations with an electronic tacheometers unless a *sun filter* (approved by the manufacturer) is *always attached* to the objective. (Not on the eyepiece, as in the past!)

4.7.4 Automatic Power-Off

To extend the charge of batteries in the field, some instruments switch themselves off after being idle for a specified time. For *measurements of highest precision*, the instrument should **not** be turned off during measurements. This ensures that the temperature inside the instrument remains as constant as possible.

4.7.5 Two-Way Radios and Cellular (Mobile) Phones

It is advisable not to transmit from walkie-talkies and cellular phones during actual measurements. Since mobile phones respond to incoming calls without user input, they should be totally switched off when operating an electronic theodolite or tacheometer. Transmitting devices may interfere with measurements, leading to an erroneous result or to a total failure of the measurements. Instances of the latter were reported at UNSW with respect to distance measurements.

4.7.6 Real-Time Corrections to Measured Data

The vertical axis tilt(s) is(are) computed by electronic tacheometers and theodolites and used to correct the zenith angles (single-axis level sensors) or the zenith angles and the horizontal directions (dual-axis level sensors). These corrections are combined with other on-line corrections. For example, for face left:

$$z_{FL} = z'_{FL} + S^{TE}_{FL} \times C - S^{TE}_{REF} \times C + VCIC \qquad (4.15)$$

$$r_{FL} = r'_{FL} + \frac{c}{\sin(z_{FL})} + (S^{HA}_{FL} \times C - S^{HA}_{REF} \times C + TAI) \times \cot(z_{FL}) \quad (4.16)$$

where z is the corrected and z' the raw zenith angle measurement, r is the corrected and r' the raw horizontal direction measurement, VCIC is the vertical circle index error correction, c is the collimation error correction, TAI is the correction for the trunnion axis inclination and where the 'exponents' TE and HA denote the **te**lescope and the **h**orizontal **a**xis components of the level sensor measurements. In face right, the formulae are a function of the face right zenith angle:

$$z_{FR} = z'_{FR} + S^{TE}_{FR} \times C - S^{TE}_{REF} \times C + VCIC \quad (4.17)$$

$$r_{FR} = r'_{FR} + \frac{c}{\sin(z_{FR})} + (S^{HA}_{FR} \times C - S^{HA}_{REF} \times C + TAI) \times \cot(z_{FR}) \quad (4.18)$$

The Equations (4.15) and (4.17) highlight that the electronic theodolites and tacheometers have two 'index errors', one for the vertical circle reading mechanism (VCIC) and one for the level sensor (S_{REF}). Please note that any errors in S_{REF} will be cancelled if the mean of face left and face right is taken in zenith angle and horizontal direction measurements. Any errors in C will **not** be cancelled by this procedure.

The correct sign of the level sensor readings will depend on the construction of the level sensor and the position inside the instrument. When using a liquid level sensor for the measurement of the vertical axis tilt, it should be noted that it takes longer to settle down than a mechanical pendulum device, due to the viscosity of the liquid. It takes about 3-4 seconds to settle in normal conditions, longer in cold conditions. This waiting time must be observed (for zenith angles **and** direction measurements) if the above on-line corrections are enabled.

The Eqs. (4.16) and (4.18) are not defined when pointing to the zenith because of the division through zero. If Eqs. (4.15) and (4.17) are not applied, the displayed and recorded zenith angles will not refer to the plumbline but rather to the (inclined) vertical axis. The real-time corrections after Eqs. (4.15) and (4.17) may have to be disabled in cases, where the instrument is set-up on a moving or vibrating platform. Measurements are then taken in a coordinate system defined by the instrument's vertical axis and the zero direction of the horizontal circle.

4.7.7 Direction Measurements

The electronic theodolites and tacheometers are, as far as the mechanical design and the telescope are concerned, not very different from classical theodolites with visual reading of circles. In consequence, most of the

existing rules of measurements with classical theodolites still apply. These accepted procedures are part of good professional practice and have been established over decades if not centuries.

The new technology used in electronic theodolites may require a revision of some of the accepted procedures, a drop of others and an introduction of new procedures. Only the observation rules that relate to the circle reading (resolution), the circle zero and the level sensors (replacing compensators and altitude bubbles) need to be reassessed. All other rules are still valid and should be adhered to.

4.7.7.1 Single-Face versus Dual-Face Measurements

The decision between single-face (FL only) and dual-face (FL & FR) measurements is the same as in the past. *Single-face observations* are acceptable whenever:

- the combined effects of all residual instrument errors are smaller than the required angular accuracy,
- the validity of the values of the corrections for instrumental errors stored on-board for real-time correction are confirmed in the field,
- the required angular accuracy is less than the resolution of the instrument and
- the gross errors can be detected by means other than a second measurement.

The fact that some instrument errors are corrected by computations in real-time, does not change much. In fact, the errors in the corrections for the physical errors can be quite large if the calibration measurements were not carried out properly. (In other words, the correction for an error might be a bigger problem than the error as such.) The stored corrections (like the mechanical adjustments in the past) may also change with temperature and time.

Single-face measurements are typically used in tacheometry, detail surveys and setting-out. When measuring in FL only, the speed of surveys increases considerably. However, the accuracy and reliability of single face measurements must be assured always. Quality assurance requires that all data are checked one way or another.

Dual-face measurements are executed whenever:

- the accuracy of the measurements is to approach the resolution of the instrument,
- as many as possible instrument errors are to be truly eliminated on the spot, and
- any gross errors are to be avoided or detected immediately by a second set of data.

Dual-face measurements are used for control surveys (traversing, trilateration) and for high precision surveys, usually in engineering applications. Dual-face measurements improve the reliability of the data

considerably, as all points are pointed to at least twice. The errors of identification are reduced.

4.7.7.2 Sequence of Direction Measurements

If an arc of direction is to be measured to targets 1,2,3,4 .. ,t, then the accepted sequence of the direction observations is:

- {rotate alidade clockwise by 360°}
- in clockwise (cw) direction: FL(1)–>FL(2)–>FL(3)–>....–>FL(t)
- change face {and rotate alidade counterclockwise by 540°}
- in ccw direction (read from right): FR(1)<–FR(2)<–FR(3)<–....<–FR(t)

Actions listed in { } brackets are suggested for high precision measurements for the lubrication of the bearings. The sequence of the points is selected in such a way that the smallest sector is covered (FL(t) – FL(1) = minimum). This minimises the walking around the tripod or the pillar. The accepted sequence does also eliminate most of the effect of the tripod or pillar rotations (the so-called 'tripod twist'). The assumption for this is that the time spent on measuring to each point is about the same.

A *horizontal angle* is an arc of direction with two rays and is measured the same way. In traverses, the clockwise angle from the backsight to the foresight station is measured, irrespective of it being the smaller of the two possible angles or not.

4.7.7.3 Elimination of Periodic Errors

For high precision direction measurements, the periodic graduation errors and diameter errors should be eliminated by a physical change of the circle's orientation between multiple arcs. (A real *change of the zero* of the circle is required. Changing the circle reading through the keyboard *does not help*!) When measuring n arcs, the circle orientation should be changed physically by 180°/n for electronic theodolites with diametrical circle reading and 360°/n for electronic theodolites with a single index.

Unfortunately, most electronic theodolites and tacheometers do no longer feature a horizontal circle setting screw. The rotation (by 120°) of the whole instrument inside its tribrach between arcs is then the only feasible approach. This should be done for high precision direction measurements.

4.7.7.4 Circle Setting

With optical theodolites and manual booking, it was appropriate and beneficial to set the circle to a little bit more than zero to the left most target, in face left, in the first arc. For subsequent arcs, the 180°/n or 360°/n rule (see previous paragraph) was employed. If manual booking is used with electronic theodolites and tacheometers, this procedure is still appropriate, even if the (virtual) change of the circle reading is achieved through keyboard entry of the desired value.

When using *electronic instruments with electronic data recording*, however, setting of the circle to zero (or any other value) is a waste of time. It is

suggested to start at whatever orientation the circle is after the set-up. When measuring multiple arcs of directions in precision work, the procedure outlined in the previous section on the *Elimination of Periodic Errors* should be used. If the circle cannot be rotated physically one way or another, multiple arcs might as well be measured with the same circle orientation and readings when using data recording. Entering a new starting value for each arc through the keyboard does not change any errors and is, thus, a waste of time.

4.7.8 Zenith Angle Measurements

Good levelling of the theodolite is required, despite (and because of) the fact that an electronic level sensor or a compensator is being used. For more precise work, all zenith angle readings should be done in a certain sequence, e.g. FL-FR-FR-FL, to offset time varying changes of the vertical circle index correction (VCIC) and the additive constant of the level sensor. In this routine, the corresponding FL and FR readings follow each other immediately. It can be assumed that any errors in the additive constant of the level sensor are the same and, thus, cancelled. Also, the vertical refraction is unlikely to change significantly in the few seconds that elapse between the FL and FR readings. The FL and FR readings are, thus, subject to the same refraction error.

Large magnetic fields can affect mechanical pendulum level sensors. A liquid level sensor is recommended for measurements in electro-magnetic fields. The liquid level sensors take longer to settle down due to the viscosity of the liquid. On average they take 3-4 seconds in normal conditions to settle, longer in cold conditions.

As the zero of the zenith angle is traditionally fixed, the only way to eliminate the periodic graduation or diameter errors is to determine them and to correct the measurements later in the office or on-line, through a linked personal computer. As the circle graduation errors of vertical circles are not easily determined, the calibration and the post-correction are usually not carried out. This is another reason why zenith angles, typically, are less precise than horizontal directions.

4.7.9 Simultaneous Direction, Zenith Angle and Distance Measurements

With electronic tacheometers, the cross hairs **must** be pointed to the centre of the reflector for a distance measurement. On longer distances, where the apex of the glass prism cannot be seen, the pointing occurs to a target plate symmetric to the reflector. It is convenient (also for recording purposes), to use the same pointing for the directions and the zenith angles. The errors

caused in angular measurements by an erroneous pointing of the apex of the reflector are not discussed here. Please refer to Rüeger (1978, 1990, 1996), for example.

If the standard measuring routine for arcs of directions is followed (see above), the quality of the zenith angles will depend on the elapsed time (and any changes in the ambient temperature) between the corresponding FL and FR readings. The vertical refraction and the additive constant of the level sensor do change with time. This is because the ambient temperature and the vertical temperature gradient also change with time. Simultaneous direction, zenith angle and distance measurements might be possible for precise measurements, if the temperature and the refraction conditions remain the same. One such case arises in close range three-dimensional (3D) industrial measurements indoors. Otherwise, simultaneous direction, zenith angle and distance measurements are not recommended for precision work.

4.7.10 Plumbing of Structures

Theodolites can be used for the plumbing of structures in two major ways. The first technique establishes a point directly above the instrument, for example in a vertical shaft or well. The second is used to establish the verticality of the corners of a building.

4.7.10.1 Plumbing Shafts and Wells

Plumbing from the bottom to the top of a shaft or well is possible, if a diagonal ('broken') eyepiece is attached to the electronic theodolite or tacheometer. These attachments are offered as accessories for most instruments. To establish a point directly above the intersection of the vertical and trunnion axes of an instrument, level the instrument in the normal way, switch the level sensor and the tilt corrections on, turn the alidade to read 0° on the horizontal circle, tilt the telescope until a zenith angle of 0° 00' 00" is read. Mark the intersection of the line of sight on a suitable target at the top of the shaft or well. Then turn the alidade to read 90° on the horizontal circle, reset the telescope to a zenith angle of 0° 00' 00" and mark the intersection of the second line of sight on the target at the top. Turn the alidade to read 180° on the horizontal circle, reset the telescope to a zenith angle of 0° 00' 00" and mark the intersection of the third line of sight on the target at the top. Then turn the alidade to read 270° on the horizontal circle, reset the telescope to a zenith angle of 0° 00' 00" and mark the intersection of the fourth line of sight on the target at the top. These four measurements are taken in the same face. Because of instrumental errors, the line of sight travels on a cone when rotating the alidade about the vertical axis and 'draws' a circle on the target. The centre of the (imaginary) circle is the (error free) plumbing point. The accuracy of the plumbing depends on the accuracy of the level sensor, how accurately the plumbing points are marked and on how accurately the zenith angle can be set to zero (exactly). The latter also depends on the stability of the tripod.

4.7.10.2 Plumbing a Building

When checking the verticality of building corners, for example, instruments with dual-axis level sensors are preferred since they correct the direction measurements for (residual) tilts of the vertical axis. This is important for steep sights. (The diagonal eyepieces mentioned in the previous paragraph may also be useful.) To check the verticality of a corner in one direction, set up the instrument in line with one of the two facades and sufficiently offset from the corner to avoid zenith angles less than 45°. Level the instrument in the usual way, switch on the dual-axis level sensor and the tilt corrections, point (in FL) to the corner at the top, read the (corrected) direction, point (in FL) to the corner at the bottom, read the (corrected) direction, point (in FR) to the corner at the top, read the (corrected) direction, point (in FR) to the corner at the bottom and read the (corrected) direction. Calculate the mean direction to the top and the mean direction to the bottom. The building is vertical (at the corner and in the direction measured), if the two values are the same. The accuracy depends on the angular accuracy of the instrument, the pointing accuracy and the accuracy of the level sensor. The latter has to be multiplied with cot(z), since the tilts of the vertical axis, measured by the level sensor, are multiplied with cot(z) to derive the corrected directions. Refer to Eqs. (4.16) and (4.18) for details.

4.8 Exercises

4.1 List three important differences between optical and electronic tacheometers ('total stations') and briefly explain their significance.

4.2 Explain the major differences between two robotic surveying systems, namely a one-person-survey-system and an automatic monitoring system.

4.3 Describe two completely different types of incremental circles used in electronic tacheometers.

4.4 Explain how the field operations differ between instruments with electro-optical incremental and absolute horizontal circles.

4.5 Describe the key differences between vertical circle compensators and electronic level sensors in electronic tacheometers.

4.6 What are dual-axis level sensors good for? How valuable are these activities?

4.7 An electronic tacheometer, designed according to Fig. 4.15, features an incremental circle with 21600 graduations.
(a) What is the resolution of the coarse measurement on the circle?
(b) At what intervals would you expect the interpolation error to repeat itself?
(c) Assuming that the instrument employs a 6-bit analogue-to-digital converter, what would the resolution of a single circle reading be?

4.8 Based on Fig. 4.17, design two other logical tests for the determination of the sense of the rotation, one each for the clockwise and the counterclockwise movement.

4.9 Redraw the window (b) of Figure 4.20 for the case, where the vertical axis is tilted the other way (by the same amount).

4.10 Using Eqs. (4.12) and (4.14), investigate the effect of a 1% error in C on α and S_{REF}, respectively.

4.11 How significant is the systematic component of the setting error in liquid level sensors?

4.12 You have been measuring zenith angles with an electronic theodolite with a dual-axis liquid level sensor. The corrections for the dislevelment were 'switched-on'. At +20°C, you noted a total vertical circle index correction (VCIC) of –12". At +35°C, you found a VCIC of +2". What do you attribute this change to? Why?

4.13 Would you prefer to level a theodolite with the procedure outlined in Figure 4.27 or with the traditional method with the plate level? Give reasons!

4.14 (a) Considering Figs. 4.21(b) and 4.21(c), Eqs. (4.15) and (4.17) and assuming that $S^{TE}_{REF} = 0.000$, how do S^{TE}_{FR} and S^{TE}_{FL} relate to each other?
(b) Noting that the mean zenith angle is $\bar{z} = 0.5\,(z_{FL} + (360° - z_{FR}))$, how would an error of 2% in C affect $\bar{z}$ for $S^{TE}_{FL} \times C = 20"$ and for $S^{TE}_{FL} \times C = 100"$, respectively?

4.15 Considering Eq. (4.16) and Eq. (4.18), $\bar{r} = 0.5\,(r_{FL} + (r_{FR} \pm 180°))$ and $z_{FR} = 360° - z_{FL}$ and assuming $c = 0.0"$, $TAI = 0.0"$, $S^{HA}_{REF} \times C = 0.0"$,
(a) prove that the level sensor readings $S^{HA}_{FL} \times C$ and $S^{HA}_{FR} \times C$ are not cancelled in $\bar{r}$, and
(b) discuss the effect of $S^{HA}_{FL} \times C = +10"$ on $\bar{r}$ for zenith angles z_{FL} of 90°, 70°, 50°, 30° and 10°.

4.16 You have been asked to check the verticality of a hight rise building. For this purpose, you have set up an electronic theodolite with a dual-axis level sensor. You are pointing in face left (FL) to a point at ground level on the building as a reference and you set the direction reading to 0°00'00". (Here, it is assumed that the zenith angle to this point is 90° exactly.) You then check the verticality of points above the reference (in FL) by tilting the telescope to zenith angles of 70°, 50° and 30°.

(a) Assuming that your instrument employs the Eqs. (4.16) and (4.18) to correct directions in real-time and that c = +15", TAI = –8", $S_{REF}^{HA} = 0.0$ exactly, $S_{FL}^{HA} \times C = -15"$, what direction would you read after tilting the telescope (without any alidade rotation) from the reference mark to z=70°, z=50° and z=30°?

(b) What would you do next, at each zenith angle setting (z=70°, 50°, 30°) before assessing the verticality?

(c) Give reasons why you would repeat the process in face right (FR) afterwards?

5. Specialised Equipment

5.1 Reflectorless Electronic Distance Measurement

The evolution of reflectorless EDM in surveying has been discussed in Section 4.1.8. In this section, the special aspects of measuring to non-cooperative targets with modern instruments are discussed.

Since reflectorless EDM relies on the spurious reflectance of features of the landscape, the range is much reduced in comparison to measurements to normal EDM glass prism reflectors. To increase the range of reflectorless EDM instruments, manufacturers have to increase the power output of the emitting diodes, use the pulse distance meter principle, where short and powerful pulses are separated by idle times (low duty cycle), increase the sensitivity of the receiving diodes, focus the EDM beam (noting that most electronic tacheometers feature fixed focus distance meters) or any combination thereof. Reflectorless instruments measure the distance to the area ('footprint') on the target that is illuminated by the distance meter's beam. If the distance meter uses a visible beam, then the footprint may be visible trough the telescope, at least on close range If the distance meter uses an infrared beam, then the observer has to assume that the optical line of sight is properly aligned with the EDM beam. Should the EDM beam be out of alignment, then the distance is not measured to the point indicated by the crosshairs on the object. Note that some instruments transmit a visible light beam for target identification, even though the distance measurement is carried out with an infrared beam. In such cases, the same uncertainties arise as between the optical line of sight and an infrared EDM beam.

5.1.1 Basic Properties

Figure 5.1 shows some of the basic properties of reflectorless EDM. At the top left of Fig. 5.1, the ideal case for reflectorless EDM is shown where the beam hits a flat surface that is at a right angle to the central ray (i.e. angle of incidence is zero) and where the footprint of the beam is well within the surface. This is clearly the preferred configuration for reflectorless measurements. The average distance across the footprint will be measured. At the top right of Fig. 5.1, the flat surface is not at a right angle to the beam any more. The angle of incidence on the surface is no longer zero and the footprint is now an ellipse. It is likely that less light will be returned to the distance meter, when compared to the first case, and that the measuring range is reduced. Again, the average distance across the footprint is measured. Unfortunately, the centre of gravity of the illuminated area ('footprint') does not coincide with the point where the central ray intersects the surface. This error was calculated by Köhler (1994) for a Zeiss Reg Elta RL as 3 mm at 60 m for an (extreme) angle of incidence of 81°. For angles of incidence closer to zero, this error is insignificant.

The case of a rough (structured) surface is illustrated at the bottom left of Fig. 5.1. Again the average distance across the illuminated area is measured. Note that tape measurements would be to the 'highest' point of the structured surface rather than the average and, thus, will differ from reflectorless measurements. Reflectorless EDM measures to a point inside the structured surface. Shiny surfaces (bottom right of Fig. 5.1) may act as mirrors and reflect the EDM beam. Typically, the reflectorless measurement will fail to such surfaces. Should the *deflected* EDM beam hit another surface of sufficient reflectivity, then an (erroneous) distance may be measured to the other target surface, through the shiny surface. In consequence, glass and shiny surfaces should be avoided.

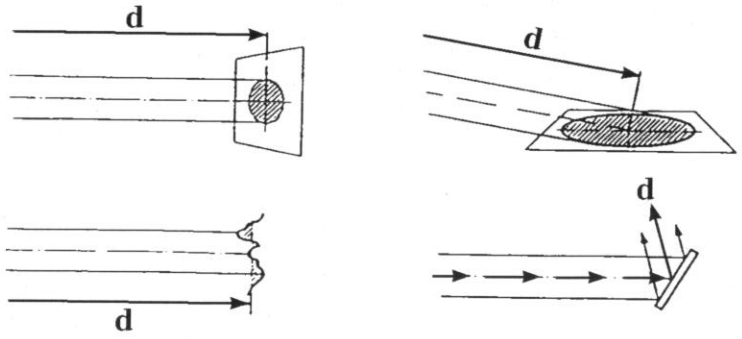

Figure 5.1: Basic properties of (reflectorless) distance measurements to natural targets (after Ibeo 1986)

Since a reflectorless EDM instrument illuminates a circular area (footprint) rather than a dimensionless point, all distance measurements to corners and

rounded surfaces will be wrong to a certain extent. Distances to convex corners (on left in Fig. 5.2) will be measured too long and distances to concave corners (in the middle of Fig. 5.2) too short. The magnitude of the error depends on the angle of incidence, the diameter of the footprint and, thus, on the instrument used and the distance to the corner. The distance to rounded surfaces, such as cylinder and spheres (see right of Fig. 5.2), are also measured too long. Typically, the errors will be less than those to corners.

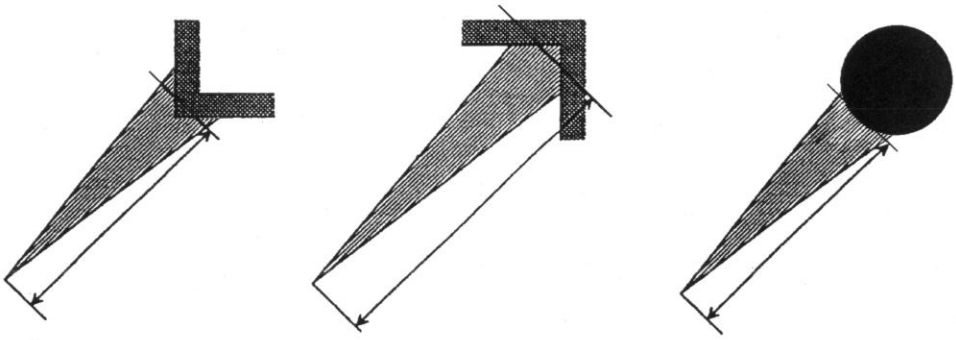

Figure 5.2: Measurement to corners and round surfaces (after Buchmann & Scherer 1994)

5.1.2 Beam Size and Shape

Because reflectorless EDM instruments do measure to the area that is illuminated by the instrument, it is important for the user to be fully aware of the dimensions and shape of the beam of the reflectorless distance meter when measuring to surfaces. Nikon, for their NPL-821 reflectorless pulse distance meter, write that the reflectorless EDM beam is circular and has the same diameter as the central circle present on the crosshairs of the instrument. The latter is 5.00 minutes of arc. The beam diameter, thus, increases linearly with distance. Nikon also states that focussing the telescope of the NPL-821 onto a target also focusses the reflectorless EDM beam. (As far as known, the other manufacturers use fixed focus EDM beams.) Leica quotes different beam cross-sections and dimensions for different distances for their instruments operating in reflectorless mode. Figure 5.3 gives the information for the reflectorless mode of the Leica 1100 Series of instruments. The reflectorless EDM beam is coaxial with the telescope when properly adjusted.

In normal EDM, the knowledge of the EDM beam dimensions is less critical, since the glass prism reflector has the same diameter as the objective lens of the instrument. As long as no strongly reflecting surfaces are located behind the prism, only that part of the EDM beam, that illuminates to prism, will be reflected back to the instrument and used for the distance

measurement. In contrast to reflectorless EDM, it is quite clear in normal EDM to what point a measurement refers to, namely the intersection of the reflector's horizontal and vertical axes.

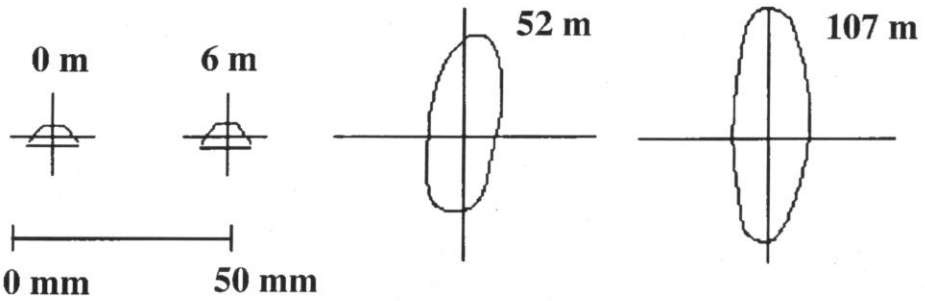

Figure 5.3: Beam shape and dimensions of Leica Series 1100 reflectorless electronic tacheometers (after Leica 2001)

The effective beam size and shape can be easily determined by the user. Since this information is essential for reflectorless measurements, tests should be carried out at a number of distances and vertically and horizontally. The principle is shown in Fig. 5.4.

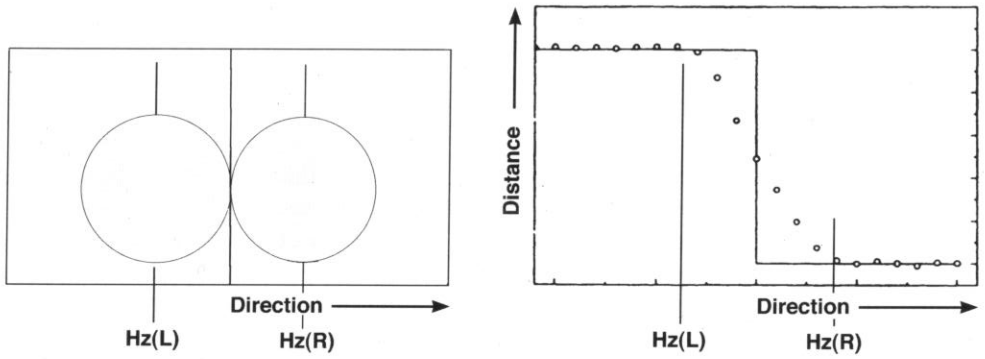

Figure 5.4: Scanning across an edge to determine the (horizontal) beam width of a reflectorless distance meter. Front view on the left, plan view on the right. On the right, the dots represent possible changes in distance measurements across the edge (after Meier-Hirmer 1996). The EDM footprints at the direction readings Hz(L) and Hz(R) are shown on the left.

To determine the horizontal width of the EDM beam, two blocks (for example, of wood) are arranged in such a way that their front faces are approximately perpendicular to the beam and separated by 0.1 m or so. On the right hand side of Fig. 5.4, the block on the right is closer than the block on the left. The view from the distance meter is shown on the left hand side of Fig. 5.4. The vertical edge that separates the left and the right block should be about vertical, as shown. To determine the horizontal beam width, one points the vertical crosshair to the edge and records the distance and the

horizontal direction. (Since half the beam hits the back target and half the front, one expects to read the average distance to the two surfaces.) Then, the scan to the left starts by measuring distance and direction at appropriate angular intervals. Once the distance readings stabilise (at the distance reading to the back block on the left), the left hand scan is terminated. Point the vertical hair again to the edge, and record direction and distance. Then, start the scan to the right, using the same angular intervals as before. Once the distance readings stabilise (at the distance reading to the front block on the right), the right hand scan is terminated. As a check, point the vertical hair again to the edge, and record direction and distance. As Fig. 5.4 shows, the positions Hz(L) and Hz(R) are the closest points to the edge, where the beam is still fully on the front or back target. The beam width (in angular units) is obtained as Hz(R) - Hz(L).

The test should then be repeated in a vertical direction, across a horizontal edge. Afterwards, the beam width should also be determined at another distance. As a minimum, the beam width should be established at the shortest and longest distance experienced in daily practice. The beam width test discussed here allows to check if the EDM beam is properly aligned to the telescope's crosshairs. For a EDM beam, that is properly aligned in the horizontal direction, the direction readings to the edge (at the beginning, middle and end of the test) should be the mean of Hz(R) and Hz(L), to use the example of Fig. 5.4.

5.1.3 Multiple Target Problem

Since reflectorless instruments are usually pointed to non-cooperative targets in the landscape, it can happen that the EDM beam exceeds the diameter of the target. It is then possible that the part of the beam, that overlaps the intended target, is returned by a surface behind the target. A similar case arises if small reflecting surfaces (such as leaves), located between the instrument and the intended target, interfere with the beam. The effect of multiple targets on the distance displayed by the instrument is different for phase measuring reflectorless instruments (e.g. Leica instruments) and pulse reflectorless distance meters (e.g. Nikon and Topcon instruments, Zeiss Rec Elta RL).

5.1.3.1 Pulse Distance Meters

The effect of multiple targets for pulse distance meters varies with the distance between the two targets as well as the relative strength of the signals returned by the two targets. Figure 5.5 shows experimental results obtained by Meier-Hirmer (1995) with a Zeiss Reg Elta RL. The closer target was 22 m (distance s_0) from the instrument. The second one was set up behind the first one so that both targets were visible from the instrument. The more distant target was then shifted in steps (distance s_1) until it was 4.000 m behind the first target. Each time, the instrument was pointed to the edge

between the two targets, focussing to the closer target in all cases. The back dots in Fig. 5.5 represent the measurements. In Fig. 5.5, the abscissa shows the distance ($s_1 - s_0$) between the two targets (in the direction of the EDM beam). The ordinate shows the difference between the EDM measurement (s) and the distance (s_0) to the first target. Since half of the footprint is on the forward target and half on the backward target, one expects to measure the average distance, that is $(s - s_0) = 0.5\ (s_1 - s_0)$. This line is shown in Fig. 5.5. The measurements follow the line up to a step interval of 0.3 m. After that, the distant target has lesser influence. As soon as the step interval exceeds 3.000 m, the distance meter readout approaches again the distance value (s_0) to the closer target.

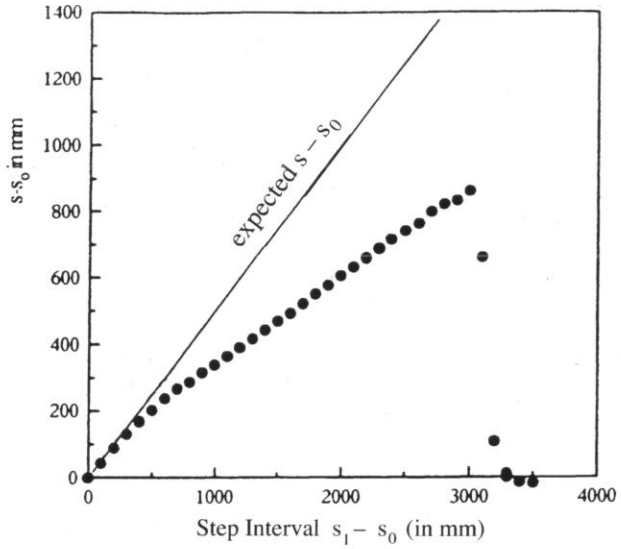

Figure 5.5: Measurements with a pulse distance meter (Zeiss Reg Elta RL) to two targets, the separation of which changes from 0 to 4 m. The closer target was steady at 22 m. See text for explanation. (adapted from Meier-Hirmer 1995)

The pattern shown in Fig. 5.5 may be caused by the pulse length of the Zeiss Reg Elta RL. Assuming a 50% return by each target, a type of average distance is measured if the double of the difference in the distances to the two targets is less than the distance equivalent of the length of the pulse transmitted by the instrument. This is because the leading edge of the return pulse from more distant target arrives at the instrument before the return pulse from the closer target has died down. Once this critical separation is exceeded, it is likely that only the distance to the closer target is measured. Experiments have established this critical separation at about 3 m for the Zeiss Rec Elta RL (Meier-Hirmer 1996 and Fig. 5.5) and at about 1.8 m for the Nikon NPL-821.

5.1.3.2 Phase Measuring Distance Meters

As with the pulse distance meters, the effect of multiple targets for reflectorless phase measuring distance meters varies with the distance between the two targets as well as the relative strength of the signals returned by the two targets. The effect was investigated by Scherer (1999) with a Leica TCRM electronic tacheometer. The experimental set up was similar to the one discussed in the previous section. The closer target was always at 4.3 m and the more distant target at distances from 4.3 to 7.3 m. At each target separation, Scherer (1999) carried out a lateral scan across the edge of the targets, like the test explained in Fig. 5.4. This means, when scanning to the right, the return from the distant target increased from 0% to 100%. Figure 5.6 depicts the results on two scans only. The left part of Fig, 5.6 shows the result of the scan with the second target at 6.6 m, the right part the scan with the second target at 5.2 m.

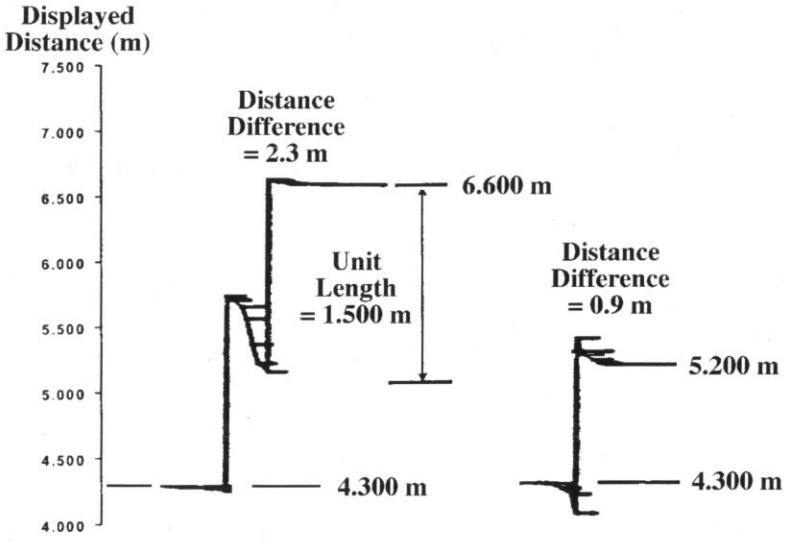

Figure 5.6: Scanning across two targets with a (phase measuring) Leica TCRM instrument. The first target is at 4.300 m. The second target is 2.300 m (on the left) and 0.900 m (on the right) behind the first. Scanning (from left to right) begins with the full beam on the closer target (on left) and continues then in equidistant lateral steps until the beam is fully on the back target. (from Scherer 1999)

It follows from Fig. 5.6 that the displayed distances are either close to the distance to the closer target or close to the distance to the more distant target, but never half way in between, if the separation does not exceed the unit length of the instrument (1.5 m in this case). The matter of concern is that the displayed distances may be shorter than the distance to the closer target, or longer than the distance to the distant target. Scherer (1999) reported magnitudes of such errors of up to 0.20 m. The behaviour of phase measuring distance meters is quite different from that of pulse distance

meters. Clearly, it is best to avoid measuring to multiple targets!

5.1.4 Influence of the Material and Colour of the Target

The material, roughness, reflectivity and colour of a target affect the maximum distance and precision that can be achieved. Also, gross errors can occur in certain conditions.

The experiments by Kogoj (2001) established the following maximum distances with a Leica TCR307 to targets at 90° to the EDM beam (zero angle of incidence): sheet metal (60 m), render (85 m), wood (100 m) and styrofoam (110 m). When measuring to coloured paper with a Leica TCRM1100, which uses a visible (red) EDM beam, white, red and yellow gave the best return signal and blue and green the worst (Möser 2000).

Kogoj's (2001) experiments with a Leica TCR307 showed that the precision gets worse with distance. However, there was no noticeable difference in precision between the measurements to sheet metal, render, wood and styrofoam.

Möser (2000) investigated the variations in distance measured with a Leica TCR1100 to number of different target materials at the same physical distance. Errors of less than 0.5 mm were recorded for paper, (smooth) PVC, (smooth and rough) steel. Wood and wallpaper were within 1 mm. At 20 m, errors of 15 mm were recorded for acrylic glass, 7 mm for styrofoam and 4 mm for sandpaper. Clearly, measurements to (and through) glass should be avoided as should measurements to styrofoam and sandpaper.

5.1.5 Target Orientation

The target orientation (or, in other words, the angle of incidence) does have an effect on the maximum distances that can be achieved to a particular material. For sheet metal and render, Kogoj (2001) recorded a 5% and 6% reduction in the maximum distance, respectively, from zero to 45° angle of incidence with a Leica TCR307.

Another problem of target inclination is shown in Fig. 5.7 (Köhler 1994). The figure shows the distances measured in two faces with a pulse distance meter Zeiss Reg Elta RL to a target with different tilts about a horizontal axis. The angle of incidence is given on the abscissa (in grads). In the Zeiss Reg Elta RL, the EDM beam is transmitted coaxially. The receiver optics is, however, below the main telescope. Even though the misalignment is corrected, some adjustment errors remain. As Fig. 5.7 demonstrates, the

mean of distance measurements in face left and face right is free of errors caused by the misalignment.

It should be noted that any reflectorless distance meter, with a misalignment between the line of sight and the EDM beam, will exhibit similar errors. Measuring in two faces to an target at an angle of incidence of say 45° can, therefore, be used to check for possible misalignments of the EDM beam. Rotations of the target about horizontal and vertical axes should be checked.

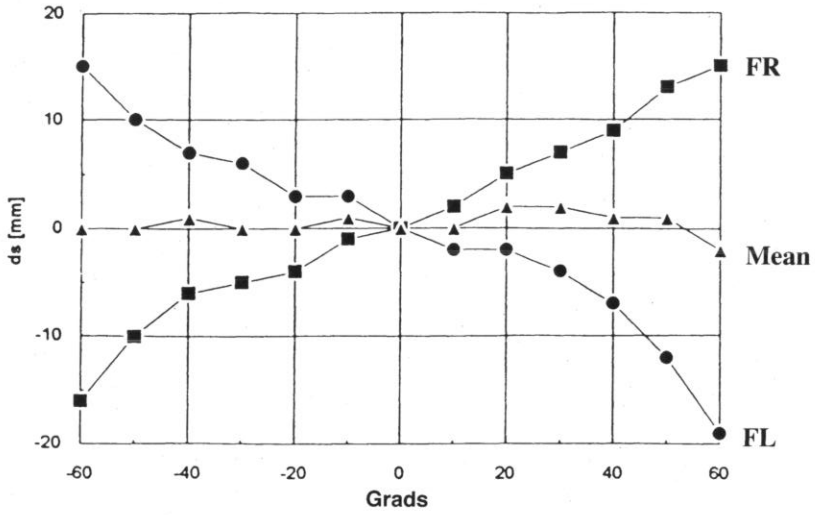

Figure 5.7: Errors in distance for reflectorless distance measurements with misaligned optics, measured for a Zeiss Reg Elta RL (after Köhler 1994)

5.1.6 Measurement to Corners

The fundamental problem of reflectorless EDM measurements to corners and similar shapes has already been outlined in Fig. 5.2. Since corners and other edges are one-dimensional features, the two-dimensional footprint of the EDM beam will (usually) not deliver the correct distance. Unfortunately, it is very often the edges and corners of structures and objects that are of interest to surveyors. Because of that, most manufacturers provide on-board software to remedy the problem. The solutions provided rely usually on the fact that corners are at the intersection of two planes or three planes. All one has to do is to measure in reflectorless mode to three (arbitrary and unmarked) points on one of the planes and then point to the corner. The on-board software will calculate the equation of the plane and, then, the slope distance (or coordinates) of the corner from the measured direction and zenith angle to the corner. No distance is measured to the actual corner.

The accuracy of the special measurements to corners depends on the flatness and size of the plane used for the corner definition and on where the three

points are selected in relation to the corner. For example, the corner between two vertical walls of a room, halfway up the wall, is best determined by measuring to two points near the (two-dimensional) corner on the wall, one close to the floor and the other close to the ceiling, and a third point at the other end of the same wall. The accuracy of a corner determination can easily be checked by doing a second measurement using the second wall. Such a check is only useful if the corner point is (temporarily) marked.

On close range, the footprint of the reflectorless beam may be sufficiently small to allow direct measurements to corners. Small errors (see Fig. 5.2) will remain but may not be worse than the assumed flatness of walls or the verticality of wall corners.

5.1.7 Some Notes on the Use of Reflectorless EDM

(1) The target must be larger than the footprint of the reflectorless EDM beam. If the instrument used features a visible reflectorless EDM beam, note that the footprint used by the actual distance measurement may be (slightly) larger than the illuminated area seen by the eye.

(2) Avoid measuring to two targets at the same time. Make sure that there are no objects (e.g. leaves) in the beam between the instrument and the target. Make sure that there are no other reflecting surfaces behind the target.

(3) Since the knowledge of the actual beam width at different distances is essential, the user should establish the beam width using the test outlined in Section 5.1.2 and illustrated in Figs. 5.4.

(4) With instruments that do not employ a visible beam for the reflectorless measurements, it is essential that the user checks that the EDM beam is colinear with the line of sight of the instrument. Use the tests outlined in Sections 5.1.2 or 5.1.5 and illustrated in Figs. 5.4 or 5.7.

(5) Flat targets at 90° to the line of sight (at 0° angle of incidence) are preferred.

(6) Measure in two faces if there is any doubt on the accuracy of the alignment of the reflectorless EDM beam onto the telescope's line of sight.

(7) Do not measure to materials that give erroneous results, such as glass, acrylic glass, styrofoam, glazed ceramic tiles. Mirror like surfaces may deflect the beam to another surface (see Fig. 5.1).

(8) The range of reflectorless EDM is reduced when the incidence angle is large, the target is wet (see Item (7) above) and the target is in full sun light. Shading helps in the latter case.

(9) The range of all reflectorless EDM instruments can be increased considerably by measuring at night and by using cooperative rather than non-cooperative targets. Self-adhesive reflective sheeting targets are available from most manufacturers, in varying sizes (e.g. 20 by 20 mm, 40 by 40 mm, 60 by 60 mm).

(10) The additive constants of the normal distance meter and the reflectorless distance meter in the same instrument may not be the same. Calibrate the instrument separately for the two modes of operation, with the respective targets or reflectors.

(11) Non-cooperative ('natural') targets have a nil reflector constant. Most glass prism reflectors used in normal EDM have a substantial reflector constant. Never forget to change the reflector constant setting when switching between normal and reflectorless EDM. Frequent switching between reflectorless and normal EDM requires great discipline on the part of the operator.

(12) Reflectorless EDM to the normal glass prism reflectors is possible. The maximum measurable distance is typically double that of normal EDM. For example, for the Leica TPS1100 series, the reflectorless range is 5000 m (with slightly reduced precision) whereas the normal EDM range is 3000 m. For the Nikon NPL-350, the range increases from 2000 m to 5000 m.

Manufacturers may specify a minimum distance that must be observed when using glass prisms with reflectorless instruments (e.g. 10 m for Nikon NPL-350). Because of the high power of reflectorless instruments, glass prisms may reflect the EDM beam at points and surfaces other than the faces of the glass cube. Nikon suggests not to use prisms with scratches, a chipped apex or with thick edges for reflectorless EDM. Since the front surface of the prism can also reflect the beam, Nikon further suggests to mispoint the prism slightly for close range reflectorless measurements to glass prism reflectors. This is good advice for all reflectorless instruments.

(13) Reflectorless EDM through traffic (pedestrians or vehicles) can cause problems. If the cars have a similar reflectance than the intended target, and are close to the target, distances may be measured to the car and not the target, or an average distance may be displayed. It is best to measure distances across roads (or footpaths) multiple times, and to start the measurements when the line if sight is (temporarily) clear.

Nikon warns of possible errors with their NPL-350 reflectorless pulse distance meter, if the car is within three metres of the intended target. Considering Fig. 5.5, it can be inferred that an average distance will result

within the three metres (length of transmitted pulse) and that the shorter distance (to the car) might be measured if the car is more than three metres in front of the target.

(14) Check the safety rating of the (lasing) diodes used in reflectorless instruments. Class I (Class 1) instruments are safe for any reasonable usage. Reflectorless instruments using visible (lasing) diodes are usually labelled as Class II (Class 2). Do not look into the transmitter (front lens) at close range.

5.2 Laser Scanners

The laser scanners are a further development of the scanning electronic tacheometers discussed in Section 4.1.9. They are optimised for speed of measurement and fast data acquisition and are supported by sophisticated software packages that allow a conversion of the data to formats readable by computer aided design packages. As discussed previously, the laser beam transmitted by the scanner is deviated vertically and horizontally to scan the surrounding space in a grid pattern. The step interval can be selected. Some instruments can scan around the full circle (360°), others only in a limited sector. The distances are measured reflectorless using the pulse method.

Company Country	Callidus Germany	Cyra(Leica) USA	Riegl Austria	Mensi France
Model	Callidus 1.1	Cyrax 2500	LMS-Z210	GS 100
Wavelength	NIR	green (532 nm)	NIR (905 nm)	???
Safety Classification	Class 1	Class 2	Class 1	Class 2
Distance Range	0.15 - 150 m	1.5 - 100 m	2 - 350 m	2 - 100 m
Accuracy/Distance	±5 mm/32 m	±4 mm/50 m	±25 mm/200 m	±1mm/3-6 mm
Angle accuracy	±61"	±25"	±130"	6.6"
Hor Field of View	360°	40°	340°	360°
Vert Field of View	±90° & –60°	40°	80°	60°
Time for Scan	4-9 min	10 min	2 min	1000 points/s
Intensity Recording	no	yes	yes	yes
Camera	CCD	video	RGB channel	video
Can be centred	yes	no	yes	yes
Can be levelled	yes	no	yes	yes
Dimensions (mm)	460x300x300	400x330x430	435x210x210	320x420x280
Weight	13 kg	28.2 kg	13 kg	13 kg

Table 5.1: Major technical data of a selection of laser scanners

Table 5.1 gives some technical data of a small selection of laser scanning systems. Three systems are depicted in Fig. 5.8. The range and accuracy specifications of these and other systems vary greatly, from ±0.5 mm at 5 m to ±50 mm at 1000 m at the time of writing. Some systems employ infrared lasers, others visible ones. The latter have more stringent safety requirements. Of the systems listed in Table 5.1, the Mensi GS100 seems to be the most precise in its 'high precision' mode. Three of the four systems described in Table 5.1 (and all systems shown in Fig. 5.8) can be centred and levelled like conventional surveying equipment.

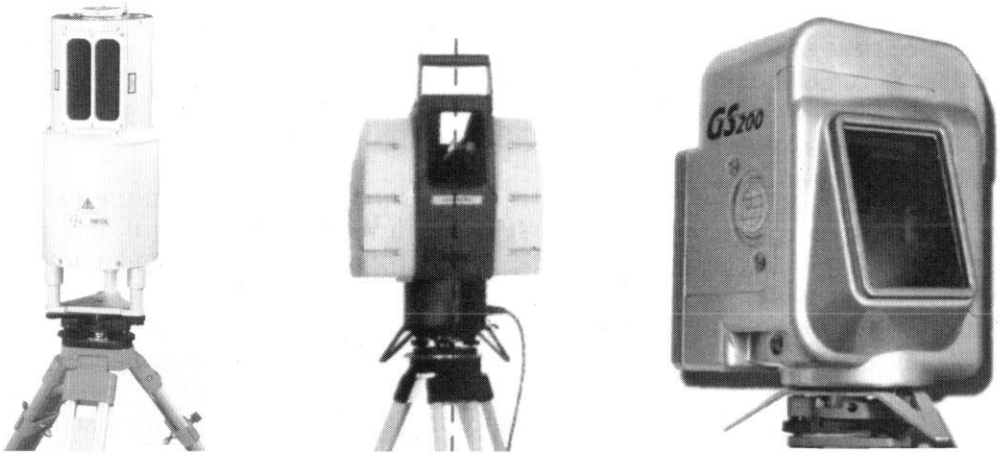

Figure 5.8: Riegl LMS-Z210 '3D-imaging-sensor' on the left, Leica HDS3000 'high definition surveying system' in the middle and Mensi GS200 'long range scanner' on the right.

The typical results of a laser scan are the x, y, z coordinates of the large number of points 'seen' by the scanner. The precision of these coordinates depends on the precision of the angular measurements (directions, zenith angles) and the precision of the distance measurements. Some laser scanners also record the intensity (signal strength) of the returned laser beam. This permits to generate something that resembles a photograph. A significant computing effort is required to convert the large number of measured coordinates ('point clouds') to useful plans and computed aided design (CAD) files. Some systems do record photographic images simultaneously. These can be used to render three-dimensional computer images, that may be derived, with realistic colours.

Since laser scanners mostly measure to non-cooperative targets, namely the natural and man-made features around the scanner, the problems associated with reflectorless EDM must be considered when interpreting laser scanner data. Refer to the discussions in Section 5.1 for details. In reflectorless EDM, an operator manually points to a passive target and, thus, can select suitable surfaces to a certain degree; in contrast, laser scanners measure in a grid pattern to whatever surface is found in the beam. Apart from being

faster and less precise, laser scanners have typically a much narrower beam than the reflectorless EDM instruments. Some potential problems are reduced because of that, some others may be created.

Liechti & Harvey (2001) have investigated a few aspects of the Cyrax 2400 laser scanner, which features a beam diameter of 5-6 mm. They found, for example, that measurements to glass prism reflectors reveal significant errors in the distances measured, wire mesh fences in the scene (3 m in front of instrument) are being picked up (even though the wire is thinner than the laser beam) and water on surfaces can change the distance reading by up to 3 mm at 53 m.

5.3 Motorised Levelling

Motorised precision levelling is not a new technique. It has been used in the 1970s to remeasure the entire first order levelling network of the then German Democratic Republic. The method was greatly assisted with the development of the Zeiss Ni002 automatic level with its swivel eyepiece; with this instrument, the foresight and the backsight can be observed without any movement of the observer. A total of three vehicles is needed. The (invar) staffs are attached to cars and the instrument is mounted on a car. This method uses the same staffs as normal and normal sighting distances. In (East) Germany, the achieved one kilometre precision was ±0.3–0.4 mm Please note that this precision is much better than the precision specified for Class A (Order 1) vertical surveys in Australia.

Figure 5.9: Motorised precise levelling in Sweden (after Becker 1979). In this case, two instrument vehicles and three staff vehicles can be seen.

The method was further developed by the National Survey of Sweden for the re-survey of 40 000 km of double run levelling lines, beginning in 1980.

The Swedish equipment is based on cars with automatic transmission, a one-ton truck for the instrument, an electronic calculator for the data recording, an instrument tripod with extra-long legs and changeable tripod shoes (like spikes and plates), a quick level tribrach, adjustable staff supports fitting a variety of vehicles as well as wind and rain protection. In Sweden, precise levelling is carried out between April and September and between 07.00 h and 17.00 h in all weather. Sighting distances do not exceed 50 m. The measurement tolerance (maximum permissible difference between the forward and the backward run height difference) is 2 mm $\sqrt{L}$, with L in km. It is only necessary to leave the vehicle when connecting to benchmarks. The Zeiss Ni002 was the preferred instrument for motorised levelling before the introduction of precise digital levels. The Swedish equipment is shown in Figs. 5.9 and 5.10 (Becker 1979).

Figure 5.10: Instrument vehicle in motorised precise levelling in Sweden with Zeiss Ni002 (after Becker 1979)

The advantages of motorised levelling can be summarised as follows:

- better progress rates (quicker)
- less dangerous
- higher line of sight reduces refraction (avoid car exhausts)
- better stability of staff
- immediate on-board check of data

- less tedious than conventional levelling on foot

	Distance Levelled (km)	s_{1km} (mm $\sqrt{L}$)
East Germany (double run)	~5000	±0.38
Sweden (double run)	>2000	±0.32–0.55
Denmark (double run)	>46	±0.44
The Netherlands (double run)	>540	±0.58
West Germany (double run)	201	±0.24

Table 5.2: Precision of motorised double-run precise levelling (s_{1km}) over 1 km with classical automatic levels, usually of the Zeiss Ni002 type. The precision values refer to the mean of double-runs. (L in kilometres)

The Swedish National Survey did investigate the progress rates with different types of precise levelling. The following progress rates were found: on foot: 3.4 km / day, by bicycle: 5.5 km / day; fully motorised: 11.5 km / day. In Sweden, the cost of motorised levelling was about 50% of the cost of foot levelling, including the costs of setting the motorised system up. Initial tests in (West) Germany, with sighting distances of 25 m - 40 m and invar staffs attached to motor bikes, showed progress rates of 7.4 km / day when using the BFFB observation routine, and 9.4 km / day when using the BBFF routine. Table 5.2 gives a summary of the precision achieved with motorised levelling in various countries.

Since 1990, the digital levelling instruments of the types Wild NA2000 and NA3000 were also tested by the National Survey of Sweden for their suitability in motorised levelling. Because of the lack of a swivel eyepiece as a standard item, the broken eyepieces known from theodolites had to be used. The resulting image rotations were not found to be suitable for a production environment. Becker et al. (1994) also noted the problems caused by

- the fact that 70% of the measurement sector must be free (particularly when connecting to bench marks),
- measurements into a low sun (a longer sun shade did reduce but not eliminate the problem),
- shadow patterns on the staff from bare trees (measurements along some roads through forests were simply not possible),
- poor light (in spring and autumn, measurements had to stop half an hour earlier than with optical instruments due to poor lighting; time was also lost on heavily overcast days),
- rain, smoke and heat (measurements take longer to make),

- the increased workload of the observer (normally, in motorised levelling, the driver of the instrument vehicle carries out the bookkeeping).

A poor temperature stability of the line of sights of the digital levels NA2000 and NA3000 were reported by Becker et al. (1994). These authors also noted the longer set-up time required per station (in comparison to the Ni002) and the increase in the number of set-ups per kilometre (5% - 20%). They suggested a standard swivel eyepiece for the NA3000 and the removal of the lowest 30 cm of graduations on the bar code staff (to reduce the effects of differential refraction). Refer to Section 3.1.5.1 for more information on the errors of bar code levels.

5.4 Laser Profiling and Laser Altimeters

5.4.1 Laser Profiling on Land

Laser profilers for aircraft and helicopter operations have been available for a number of years. At the centre of a laser profiler is a high power pulse distance meter, usually based on a Nd:YAG laser operating at an infrared wavelength of 1064 nm. Such systems are available, for example, from:

- Azimuth, 13 Park Drive, Westford MA 01886, USA
- LH Systems / Leica Geosystems GIS & Mapping LLC, 2801 Burford Highway, Atlanta Georgia 30329, USA
- Measurements Technology and Systems, Avco Everett Research Laboratory Inc., Everett Massachusetts 02149, USA
- Optech Systems, 701 Petrolia Road, Downsville Ontario, Canada M3J 2N6

The early Avco Airborne Laser Mapping System operated at 5, 10 or 20 pulses per second. This translated to one measurement per 7.5 m on the ground at a ground speed of 275 km/h and at a pulse repetition rate of 10 Hz. The typical operating altitude was 350-600 m above ground. The vertical mapping accuracy was specified as ±1.4 m on land and ±0.15 m on water. The roughness of the ground coverage has, naturally, an effect on the accuracy. Most systems are, however, able to process multiple pulse returns, such as those for the shortest and the longest distance for each pulse. Otherwise, only an average distance in the footprint area is measured. The horizontal mapping accuracy was based on a microwave distance measuring system; the specified accuracy was ±3.2 m. The Avco system required 28 V DC supply and required 1.1 kW to run. The dimensions and weight were 1470 x 910 x 790 mm and 180 kg, respectively.

Besides the pulse distance meter, an aircraft positioning system and an

attitude measurement system are required as well as powerful data recording facilities. Today, the former is typically a GPS receiver and provides the coordinates of the aircraft or helicopter. The attitude angles (roll-angle and pitch-angle) are required to transfer the coordinates of the GPS antenna to the laser system and to measure the deviation of the laser beam from the plumbline. The attitude information can be provided by an inertial navigation or reference system or, possibly, by an array of three to four GPS receivers. Rather than measure the attitude angles, the laser transmitter might be installed on a stabilised (gimballed) platform that is kept in a strictly levelled state irrespective of aircraft movements. This solution also requires inertial sensors for the platform stabilisation. Some laser profilers are able to scan the terrain (or water) sideways. In this case, a scanning mirror is required to deflect the laser beam off the vertical. The laser beam deflection introduced must be measured and recorded to be able to compute the ground position.

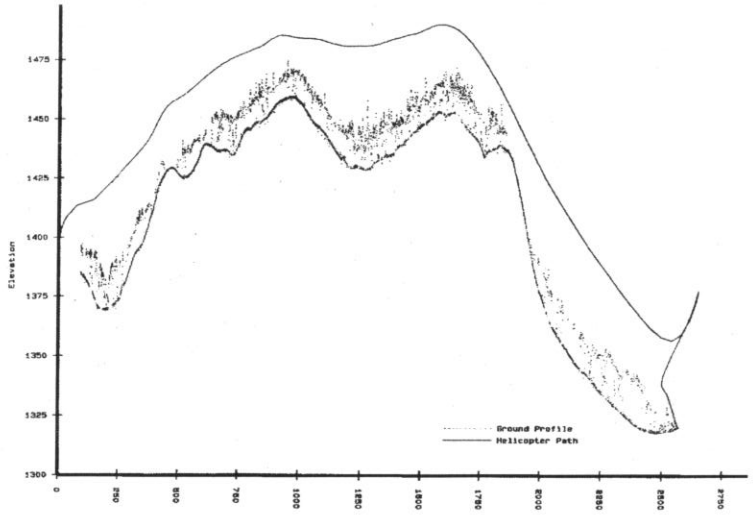

Figure 5.11: Longitudinal profile surveyed with a helicopter-borne laser profiler. The graduation intervals on the vertical and the horizontal axes are 25 m and 250 m, respectively. Flight time: 270 seconds. The continuous upper curve is the helicopter path and includes the take-off on the right hand side. The lower curve shows the ground level and the dots between ground and helicopter the upper foliage level. (from Nortech Surveys brochure)

The ALS50 Airborne Laser Scanner by LH Systems (Leica Geosystems) achieves rates of 52000 pulses per second, (lateral) scan rates of 70 Hz and a swath width of 75°. Flying altitudes above ground from 500 m to 4000 m are possible. The position of the helicopter or aircraft is determined by GPS and the roll, pitch and heading (azimuth) data by an inertial measuring system. The ALS50 can record up to three times per pulse; this permits to measure to tree tops and ground heights, for example. The system also records the signal intensity. This information can then be displayed in a photograph like form. The height accuracy is listed as 0.13 to 0.30 m and

the horizontal accuracy as 0.11 to 0.46 m, depending on flying height and scan angle.

Figure 5.11 shows a terrain profile mapped with a helicopter based laser scanner operated by Nortech Surveys (of Calgary, Canada). The figure shows that the ground level below trees can be recovered in certain circumstances, as the system records the shortest and the longest distance measured from each pulse. The laser profiler used by Nortech Surveys has a high pulse repetition rate (4000 Hz). It is ideally suited for corridor surveys along proposed pipelines, transmission lines, roads or microwave links, either in a single profile or multiple profiles, 25 m apart. Areas are surveyed by surveying parallel profiles. Nortech Surveys quote progress rates of 160 km per day.

5.4.2 Depth Sounders

A number of agencies have developed laser profilers for hydrographic applications. These systems make use of the fact that the Nd:YAG laser's fundamental frequency of 1064 nm can be frequency doubled to the green wavelength of 532 nm. The infrared beam is reflected by the water. The green beam does penetrate the water (unless at a right angle to it) and is reflected at the sea floor. The difference of the two distances gives the depth of the water.

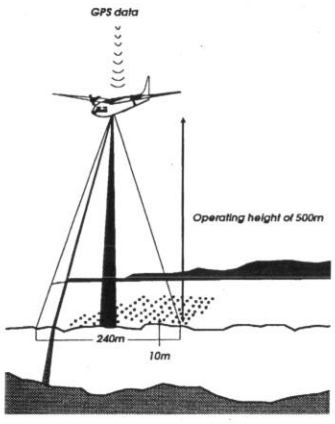

Figure 5.12: Principle of the Laser Airborne Depths Sounder (LADS) of the Royal Australian Navy.

A Scanning Hydrographic Operational Airborne Lidar Survey (SHOALS) system was developed by Optech in Canada for the US Army Corps of Engineers. It has a normal operating altitude of 200 m. The width of the swath of soundings is about 120 m, with 200 soundings per second. Maximum depths are 25 to 30 m in moderately clear waters. This can be

doubled at night. The off-nadir scan angle is 15 to 25 degrees. The rotation rate can be varied between 0 and 5 Hz. The depth accuracy was estimated as ±0.3 m and the horizontal accuracy with 4 to 5 m.

A similar system was developed by BHP Engineering and Vision Systems for the Australian Navy. The Australian Laser Airborne Depth Sounder (LADS) is in operation with the Hydrographic service of the Royal Australian Navy. It is installed on board of a Fokker F27-200 Frienship aircraft and operates at altitudes of about 500 m. It can map the sea floor at a rate of 50 km^2 per hour. As the Fig. 5.12 shows, the swath is 240 m wide and individual soundings are spaced at 10 m intervals. Depths of 50 m can be measured. The aircraft flies at a speed of 270 km/h and can stay 7 hours in the air. Like the SHOALS system, it uses a Nd:YAG laser at two frequencies, with a pulse rate of 168 Hz, a pulse power of 1 MW and a pulse length of 5 ns. The return pulses are digitised at 2 ns intervals, which gives a resolution of 0.2 m in height. The positional accuracy is given as ±15 m; it includes the errors of the GPS positioning and the inaccuracy of the platform stabilisation. The laser platform is stabilised for roll, pitch and yaw (azimuth) with input from an inertial measurement system. Orientation data are also provided by a fluxgate compass. Data are stored on tape and post-processed on the ground, immediately after the return of the aircraft.

5.5 Single Beam Laser Trackers for Metrology

At one time, there were triple-beam and single-beam laser tracking interferometers on the market. Because of the more universal appeal and wider usage, only the latter type is discussed here. The single-beam laser tracking interferometers, of the types shown in Fig. 5.13, consist of a single laser interferometer, the beam of which is deflected in three-dimensions (about two axes, one vertical and the other horizontal) by a tilting and rotating mirror. This tracker has angular encoders fitted to both angular servo motors and, thus, delivers directions and zenith angle information very much like electronic theodolites. Together with the (slope) distances, three-dimensional coordinates can be computed for the target points. A feed-back loop ensures that the laser beam is kept on the (moving) reflector.

Figure 5.14 shows the measured quantities (on the right) and the electro-optical components of one device (on the left). The left part of Fig. 5.14 shows the interferometer and the servo loops for the servo mirror. The "Detector" near the "Interferometer's Beam Splitter" records the interference fringes between the transmitted and the returned laser beam. Whenever the reflector moves, constructive and destructive interference alternates. The number of bright fringes is counted by the "Position Electronics" and processed into the change of distance per time interval. A second beam splitter (between the "Interferometer's Beam Splitter" and the "Servo Mirror") deviates 15% of the returned laser light onto the "Position Sensor".

The latter is a position sensitive diode, which measures the position of the light spot. If the light moves out of the centre, the appropriate servo motors are switched on until the light spot is centred again. This correction mechanism occurs at a rate of 1 kHz in the case of the CMS3000 (Ruland 1993).

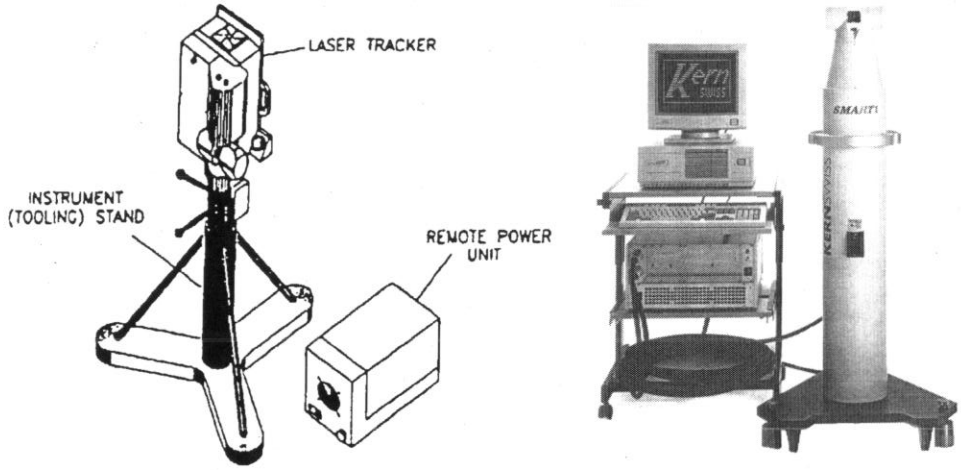

Figure 5.13: Chesapeake CMS3000 "Coordinate Measuring System" (on left, after Ruland 1993) and Leica "Smart 310" 3-D Laser Tracker (on right, after Kern/Leica 1990)

The interferometer of the laser tracker measures only changes in distance, not the absolute distance. To refer the distance to the tracker and its coordinate system, the reflector has to be placed on a reference mounting on the tracker or, alternatively, on two target points with a known distance in between (baseline). Another property of the laser interferometers (see Rüeger 1990 1996 for reference) is that the change of distance between two positions of the reflector can only be measured if the beam is constantly pointed to the reflector and if no beam interruptions occur. In the case of a beam interruption, the measurements have to start again from the reference point(s).

The Kern (now Leica) SMART 310 is one of the systems shown in Fig. 5.13. Its tracking range is ±240° horizontally and ±45° vertically. The working range is specified as 0.2 m to 25 m. The maximum tracking speed (at 2 m to 5 m from the tracker) is 2 m/s across the beam (horizontally and vertically) and 0.6 m/s along the beam. The resolution of the angular encoders is 0.2 mgon or 0.7". This corresponds to 0.03 mm per 10 m. The distance resolution is specified as ±0.16 μm. The coordinate accuracy in the object space depends on the tracking speed. It varies between ±20 ppm and ±50 ppm or ±20 μm/m to ±50 μm/m (three times standard deviation). The data are collected at a rate of 1000 points per second. The tracker weighs 30 kg and the control unit (under the personal computer in Figure 5.8) 15.5 kg.

The reflectors are mounted in precision fittings (usually a stainless steel sphere) for the attachment to reference and target points. This permits a centring accuracy that is compatible with the overall accuracy of the system. The reflectors are either of the corner cube type (like in EDM) or of the cat's-eye variety. The latter allows larger incidence angles.

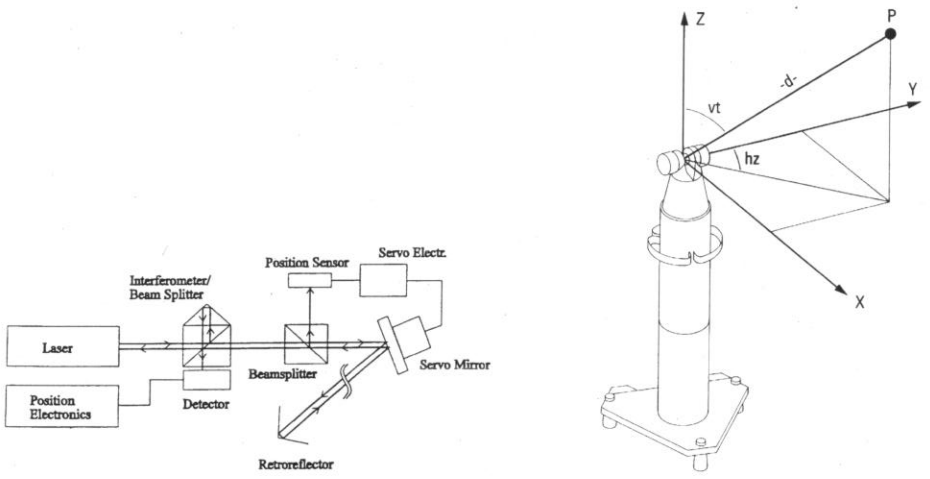

Figure 5.14: Block diagram of the servo-controlled tracking system of the Chesapeake CMS3000 Laser Tracker (after Ruland 1993) and the basic optical-mechanical lay-out of the Leica "Smart 310" 3-D Laser Tracker (after Leica 1993)

The performance of the Chesapeake CMS3000 laser tracker was evaluated comprehensively by Ruland (1993). Ruland recommends that all measurements are taken in "two faces" (for the same reasons as with theodolites) and that measurements are taken at different reflector orientations (about the reflector axis). The latter procedure will reduce the errors due to the eccentricities between the reflectors and their mounting spheres.

Since 1997, the two major suppliers of single beam laser trackers offer special models that feature an 'absolute distance meter' (ADM) besides the usual laser interferometer ('relative distance meter'). The absolute distance meters referred to here are nothing else than high precision electronic distance measurement (EDM) instruments. The Leica LTD-500 3D-Laser Tracking System (a further development of the SMART 310 shown in Fig. 5.14) uses a distance meter that operates at an infrared wavelength of 780 nm, has an accuracy of ±0.025 mm (1 σ), a resolution of 1 μm and a range of 2 - 35 m. The firm SMX supplies the Tracker 4500 with ADM. Its EDM section uses a HeNe gas laser, has a resolution of 0.5 μm, an accuracy of ±20 μm at close range and an accuracy of ±1.1 ppm at 'long' range (to 35 m).

The single-axis laser trackers are used for robot calibration, 'teach-in' of

manufacturing robots, automatic tracking of robots, dynamic measurements of large objects, digitising of surfaces, inspection of antennas, quality control on master-gauges, jigs and tools in mechanical engineering, alignment and assembly of machines and for the calibration of coordinate measuring machines (CMM) and numerically controlled (NC) machine tools, to name just a few examples. The 3-D laser trackers compete with the multi-theodolite 3-D measurement systems. The trackers require that the measuring points are, temporarily, marked with a reflector. If the interferometer is being used, the reflector must be moved between all measurement points without beam interruptions. Clearly, they are most appropriate in applications where the item to be measured can move the reflector automatically, under computer control.

5.6 Reflectorless Single Station Laser Measurement Systems

The previously discussed single beam laser tracking interferometers and the single beam laser trackers with absolute distance measurement require that reflectors be used to mark the points on an object. The Coherent Laser Radar (CLR) MV100B by Metric Vision, and the Leica Laser Radar LR200 now allow to scan quickly and precisely large surfaces without reflectors. Since no reflectors need to be attached to the measured objects, sensitive and non-accessible surfaces can be measured. The Leica system measures three points per second in the most accurate ('metrology') mode. In the 'pseudo vision' mode, measuring rates of up to 1000 points per second are possible. Different models are available for maximum ranges of 8 m, 24 m and 60 m.

Figure 5.15: Leica Laser Radar System LR200 (after Leica 2002), similar to Metric Vision MV100B Coherent Laser Radar (CLR)

Leica specifies the coordinate accuracy (1 σ) for 'tooling ball targets' (highly polished perfect steel spheres), as ±0.05 mm for distances below 10 m and ±5 ppm for distances longer than 10 m. Like with all other reflectorless measuring systems (refer to Sections 4.1.8, 4.1.9, 5.1, 5.2), the quality of the data will depend on the type, reflectance, roughness and orientation of the surfaces. The usefulness of such a system depends on the sophistication of

the software used to convert the measured data ('point clouds') into CAD plans and files and into coordinates of specially marked points (e.g. with tooling ball targets).

The distance meter of the Leica LR200 operates at a wavelength of 1.55 μm. A visible pointing laser is also available. According to Slotwinski et al. (1989) the distance meter uses a frequency modulated continuous wave (FMCW) laser, where the optical frequency of the laser diode is changed in a saw-tooth ('chirp') pattern by thermal tuning. The distance is derived from the difference in the frequencies of the transmitted and received IR wavelengths.

5.7 Exercises

5.1 Discuss the pros and cons of two methods of checking the alignment between the beam of a reflectorless EDM instrument and the line of sight of the telescope.

5.2 Discuss the different behaviours of reflectorless phase measuring and pulse distance meters, when measuring to two targets at the same time.

5.3 Explain how to determine the horizontal and vertical beams width of an infrared reflectorless distance meter.

5.4 Discuss the pros and cons of motorised precision levelling in comparison with precision levelling on foot.

5.5 Your firm is tendering for the coordination of the centre line of a two-lane road between two cities, 500 km apart. You are evaluating a laser profiling system.
(a) Discuss the pros and cons of this system for this particular application.
(b) What accuracy could be achieved?
(c) What surveying infrastructure would you have to put in place?
(d) Approximately, how long would the actual field survey take with the laser profiler?

5.6 (a) Determine how many soundings (at 10 m spacing) are made by the Australian Laser Airborne Depth Sounder in one second of time if flying at 75 m/s and at a height of 500 m above sea level.
(b) Hydrographic survey ships, in comparison, travel at a speed of, say, 10 m/s but take continuous soundings to the sea floor. How much longer does a survey by ship take, if it is assumed that the hydrographic survey vessel runs longitudinal profiles at 10 m spacing?
(c) If the same area were mapped by LADS and by ship (as discussed in

(b)), which survey would provide more information on the sea floor?

5.7 Discuss the pros and cons of a 3-D laser tracking interferometer, in comparison with a multi-theodolite 3-D measuring system, for
(a) the dimensional measurement of a steel structure of 1 x 1 x 1 m,
(b) the calibration of the movements of a manufacturing robot.

5.8 What are the similarities of (and differences between) laser scanners and reflectorless single station laser measurement systems?

References

Ailisto, H., Kostamovaara, J., Lammasniemi, J., Myllylä, R. 1996. Lidar Measures Up. Photonics Spectra, March 1996, 96-100.

Angus-Leppan, P. V. 1984. Refraction in Geodetic Levelling. In: Brunner, F. K. (ed.), Geodetic Refraction - Effects of Electromagnetic Wave Propagation Through the Atmosphere, Springer-Verlag, Berlin, 163-180.

Bannister, A., Raymond, S., Baker, R. 1992. Surveying. 6th edition. Longman Scientific & Technical, Harlow, England, ISBN 0-470-21845-2, 482 + XII pages

Becker, J.-M. 1979. Heutige Messverfahren beim Nivellement – Erfahrungen mit dem motorisierten Nivellement in Sweden (Current Measurement Procedures in Levelling – Experiences with the Motorised Levelling in Sweden). In: Vorträge zum Seminar Präzisionsnivellement, 7 Dec 1978, Aachen, Germany. Veröffentlichung des Geodätischen Instituts der Rheinisch-Westfälischen Technischen Hochschule Aachen, No. 26, 2-18

Becker, J.-M., Andersson, B., Ericksson, P.-O., Nordquist, A. A new Generation of Levelling Instruments: NA2000 and NA3000. In: Papers, Commission 5, 20th FIG Congress, Melbourne, Australia, 5-12 March 1994, TS509.1/1 - TS509.1/11

BEI. 1987. Optical Encoder Design Guide. Doc. No. 924-08027-002, BEI Motion Systems Company, Industrial Encoder Division, 7230 Hollister Avenue, Goleta California 93117-2819, USA, 15 pages.

Buchmann, P., Scherer, M. 1994. Building Surveys with a Computer Controlled 3D-Laser Scanner. Der Vermessungs-Ingenieur, 45(5): 210-215 (in German)

Bureau of Meteorology. 1990. The Aneroid Barometer ... and how to use it. Information leaflet, 2 pages.

Carr, B. 1992. Using Laser Technology for Forestry and Engineering Applications. The COMPILER, 10(4): 5-15.

Cooper, M. A. R. 1982. Modern Theodolites and Levels. 2nd edition. Granada, London, ISBN 0-246-11502-5, 258 + XI pages

Deumlich, F. 1982. Surveying Instruments. Walter de Gruyter, Berlin-New York, ISBN 3-11-007765-5, 316 pages

Feist, W., Gürtler, K., Marold, T., Rosenkranz, H. 1995. Die neuen Digitalnivelliere DiNi10 und DiNi20 (The new Digital Levels DiNi10 and DiNi20). Vermessungswesen - Raumordnung (VR), 57: 65-89 (in German)

Finlayson, D. M. 1973. Isomagnetic Maps of the Australian Region for Epoch 1970.0. Report 159, Bureau of Mineral Resources, Geology and Geophysics. Australian Government Publishing Service, Canberra.

George, J. 1984. Large Area Photodiode yields Pinpoint Accuracy. Eureka – Innovative Engineering Design, July/August 1984, reprint, 3 pages.

Geotronics AB. 1994. Geodimeter System 600. Publ. No. 571 710 351, 8 pages.

Geotronics AB. 1989. Geodimeter 140 SMS Surveying Robot – Slope Monitoring System Description. Publ. No. Geo - 0024, 17 pages

Haag, R., Bayer, G., Zimmermann, M., Scherrer, R. 1997. Surveying with the automatic Fine-Pointing of the Leica TCA1800. Vermessung-Photogrammetrie-Kulturtechnik (VPK), 95(7): 466-471 (in German)

Hennes, M., Witte, B. 1991. Genauigkeitsuntersuchungen an elektronischen Tachymetern und Theodoliten der Baureihe E von Zeiss (Investigation of the Accuracy of Electronic Tacheometers and Theodolites of the E-Series by Zeiss). Vermessungswesen - Raumordnung (VR), 53(1): 30-45

Höglund, R. 1994. Practical Use of an One Man Total Station. Proc., Commission 5, 20th FIG Congress, Melbourne, Australia, 5-12 March 1994, TS502.1/1 - TS502.1/9

Ibeo. 1991. Ladar: 2D, 2D Linear, 3D. IBEO Ingnieurbüro für Elektronik und Optik, Fahrenkrön 125, D-2000 Hamburg 71, Germany, 4 pages

Ibeo. 1986. Survey Instruments - Laser Technology - Sensors and Systems: Sensors for Industrial Applications. IBEO Ingnieurbüro für Elektronik und Optik, Fahrenkrön 125, D-2000 Hamburg 71, Germany, 28 pages

Ingensand, H. 2001. Systematic Influences on Practical Measurements with (Electronic) Tacheometers and Digital Levels. In: Heister, H., Staiger, R. (eds.) Quality Management in Geodetic Metrology, 54th DVW Seminar, Fulda, 19/20 November 2001, Schriftenreihe des DVW, Vol. 42/2001, Verlag Konrad Wittwer, Stuttgart, pp. 120-135

Ingensand, H. 1993. Wild NA2000 - NA3000: Technical Paper Digital Levels. Leica AG, CH-9435 Heerbrugg Switzerland, Publ. No. G1 220e-V.93, 14 pages.

Ingensand, H. 1990. Das Wild NA2000 - Das erste Digitale Nivellier der Welt. Allgemeine Vermessungs-Nachrichten (AVN), 97(6): 201-210 (in German)

Kahmen, H., Faig, W. 1988. Surveying. Walter de Gruyter, Berlin-New York, 578 +xvii pages, ISBN 3-11-008303-5

Kern/Leica. 1990. Smart 310 – Measuring Movements. Publication 206e – 4.90 FA/8TE, Kern & Co. Ltd. (now Leica AG, Photogrammetry and Metrology, CH-5035 Unterentfelden, Switzerland)

Kogoj, D. 2001. Performance of Electronic Distance Meters in Reflectorless Distance Measurement. Allgemeine Vermessungs-Nachrichten (AVN), 108(5): 186-190 (in German)

Köhler, M. 1994. Some Theoretical Foundations for Reflectorless Measurements with the Zeiss Tacheometer Rec Elta RL. Der Vermessungsingenieur, 45(5): 216-221 (in German)

Lardelli, A. 1988. ECDS2 – A Mobile 3D-Measuring System – The New Standard for Metrology and Quality Control. Publ. No. 261e - 11.88, Kern & Co Ltd (now: Leica AG, Photogrammetry and Metrology, CH-5035 Unterentfelden, Switzerland)

Laser Alignment Inc. 1986. Laser Beacon 5000 Series for Construction and Machine Control. Publ. No. LAI 2002 (1-22-86), Laser Alignment Inc., 2850 Thornhills S.E., Grand Rapids Michigan 49546, USA, 6 pages

Lechner, W., Sudau, A., Wanzke, H. 1987. Motorisiertes Nivellement mit Digitalbarometern (Motorised Levelling with Digital Barometers). Zeitschrift für Vermessungswesen (ZfV), 112(8): 385-396

Leica. 2002. Leica Laser Radar System LR2002 - Non-contact 3D laser metrology advances factory automation. Publ. No. 727 644en, 1.2002, 4 pages.

Leica. 2001. RL-EDM Measurements. TPS News, 11/2001.

Leica. 1996. Wild NA2002 - NA3003: Technical Report, Digital Levels. Publ. No. G1 - 220 - 0en - IV.96 - VD, 14 pages

Leica. 1995. Leica Vector. Publication No. A1-300-0en-I.95-RVA, 4 pages.

Leica. 1993. Smart 310 – 3D Laser Tracker. Publication U1 206 e – V.93, Leica AG, Photogrammetry and Metrology, CH-5035 Unterentfelden, Switzerland

Leica. 1992. Mobile 3-D Metrology for Industry – Measurably Better. Publ. U1 241e - XI.92, Leica AG, Photogrammetry and Metrology, CH-5035 Unterentfelden, Switzerland

Leica Instruments. Pocket Laser Level – Perfect Dimensional Control. Leica Instruments Pty Ltd, 45 Epping Road, North Ryde NSW 2113, Australia, 4 pages.

Liechti, D. D., Harvey, B. R. 2002. An Investigation into the effects of Reflecting Surface Material Properties on Terrestrial Laser Scanner Measurements. Geomatics Research Australia, No. 76, 1-22.

Maurer, W., Schnädelbach, K. 1995. Laserinterferometry - Ten Years Experience in Calibrating Invar Levelling Staffs. Proc., First Int. Symp. Appl. Laser Techniques in Geodesy and Mine Surveying, Ljubljana, September 1995, 9 pages

Meier-Hirmer, B. Meier-Hirmer, R. 1996. Investigations of the Zeiss Tacheometer Rec Elta RL for Measurements to Structured Targets. Allgemeine Vermessungs-Nachrichten (AVN), 103(6): 233-240 (In German)

Moll, J. 1993. Low-Volume Roads Survey Laser. Publ. No. 9377 1202-SDTDC, Forest Service, Technology and Development Program, US Department of Agriculture, Washington DC 20250, February 1993, 11 pages

Möser, M. 2000. Close Range Distance Measurements. Zeitschrift für Vermessungswesen (ZfV), 125(11): 377-381

Noack, G. 1989. Problems with the Levelling of Rotating Laser Levels for Area Levelling of High Accuracy. Vermessungstechnik (VT), 37(2): 59-61 (in German)

Pallett, E. H. J. 1972. Aircraft Instruments – Principles and Applications. Pitman Publishing, London, ISBN 0-273-31747-4.

Pascoe, R. W., Rüeger, J. M. 1989. Testing a Precise Hand-Held Digital Barometer. The Australian Surveyor, 34(5): 502-513

Pike, J. M., Bargen, D. W. 1976. The NCAR Digital Barometer. Bulletin of the American Meteorological Society, 57(9): 1106-1111

Pike, J. M., Brock, F. V., Semmer, S. R. 1983. Integrated Sensors for PAM II. Paper 17.5, 5th Symposium on Meteorological Observations and Instrumentation, Toronto, Canada, pp. 326-333

Rizos, C. 1997. Principles and Practice of GPS Surveying. Monograph No. 17, School of Surveying and Spatial Information Systems, University of New South Wales, Sydney, Australia, 565 pages.

Rüeger, J. M. 2000. The Topcon DL-101C Digital Level. The Australian Surveyor, 45(2): 62-70 (Trans Tasman Surveyor, 1(3): 62-70).

Rüeger, J. M. 1996. Electronic Distance Measurement – An Introduction. 4th ed., Springer-Verlag, Berlin-Heidelberg-New York, xvii + 266 pages, ISBN 3-540-61159-2

Rüeger, J. M. 1995. EDM-Height Traversing Refraction Correction and Experiences. The Australian Surveyor, 40(4): 48-56.

Rüeger, J. M. 1995b. Surveying Practice, Education, Textbooks and Instrument Design in the Light of Changing Instrumentation. The Australian Surveyor, 40(3): 197-204

Rüeger, J. M. 1990. Electronic Distance Measurement – An Introduction. 3rd ed., Springer-Verlag, Berlin-Heidelberg-New York, xvii + 266 pages, ISBN 3-540-51523-2

Rüeger, J. M. 1978. Misalignment of EDM Reflectors and its Effects. The Australian Surveyor, 29(1): 28-36

Rüeger, J. M., Brunner, F. K. 1981. Practical Results of EDM-Height Traversing. The Australian Surveyor, 30(6): 363-372.

Ruland, R. E. 1993. The Chesapeake Laser Tracker in Industrial Metrology. Proceedings of the Third International Workshop on Accelerator Alignment, European Laboratory for Particle Physics (CERN), Geneva, Switzerland, 28 September to 1 October 1993, I/101–I/118

Schauerte, W. 1993. Digitalnivelliere des Typs Leica NA 3000 und ihr Einsatz beim Präzisionsnivellement (Digital Levels of the Type Leica NA3000 and their Use for Precise Levelling). BDVI-Forum, 19(3): 125-138

Schauerte, W. 1995. Effects of Special Errors on NA-3000 Measurements. BDVI-Forum, 21(1): 17-28 (in German)

Schwarz, W. 1985. Zur Ermittlung der integralen Temperatur der Atmosphäre mit Ultraschall für Refraktionsbestimmungen im Nahbereich (On the Evaluation of the Integral Temperature of the Atmosphere with Ultrasound for the Determination of Refraction on Close Range). No. 38 of the Veröffentlichungen des Geodätischen Instituts der Rheinisch-Westfälischen Technischen Hochschule Aachen, Germany, 136 pages (ISSN 0515-0574)

Slotwinski, A. R., Goodwin, F. E., Simonson, D. L. 1989. Utilizing GaAlAs Laser Diodes as a Source for Frequency Modulated Continuous Wave (FMCW) Coherent Laser Radars. In: Figueroa, L. (ed), Proc., Laser Diode Technology and Applications, 18-20 January 1989, Los Angeles, California, SPIE, Vol. 1043: 245-251

Sudau, A. 1994. Untersuchungen zur Leistungsfähigkeit elektronischer Druckaufnehmer für präzise barometrische Höhenmessungen (Investigations into the Performance of Electronic Pressure Sensors for Precise Barometric Heighting). Series C (Dissertations), No. 434, German Geodetic Commission, C. H. Beck'sche Verlagsbuchhandlung, München, 142 pages

Topcon Corporation. 1994. Auto Tracking Total Station AP-L1. Publ. No. 94-08-36W TE.TS 16-1, 8 pages

Vincueria, I., Tudanca, M., Aroca, C., Lopez, E., Sanchez, M. C., Sanchez, P. 1994. Flux-Gate Sensor Based on Planar Technology. IEEE Transactions on Magnetics, 30(6): 5042-5045

Walcher, H. 1985. Winkel- und Wegmessung im Maschinenbau (Angle and Distance Measurement in Mechanical Engineering). 2nd ed. VDI-Verlag GmbH, Düsseldorf, 218 pages

Whitaker, S., Call, D. B. 1986. Intelligent Pressure Transducers. Paper, Symposium, Instrumentation Society of America, Houston, Texas, October 1986, 8 pages

Whitaker, S., Call, D.B. 1987. A New Hand-Held Barometer/Altimeter Offers Portable Accuracy. Paper 24.1, Extended Abstracts, Sixth Symposium on Meteorological Observations and Instrumentation, American Meteorological Society (AMS), New Orleans, 12-16 January 1987, pp. 4487-451

Witte, B., Yang, J. 1994. Das Hand-Lasermeter DISTO der Firma Leica (The Hand-Held Laser Meter DISTO by Leica). Vermessungswesen und Raumordnung (VR), 56(4+5): 284-289

Woschitz, H. 2003. System Calibration of Digital Levels: Calibration Facility, Procedures and Results. PhD Thesis, Dept of Engineering Geodesy and Measuring Systems, Technical University, Graz, Austria, 142 pages

Wüller, H. 1988. Entwicklung und Untersuchung eines Rotations-Nivellierinstrumentes und einer photoelektrischen Nivellierlatte zur Automatisierung des geometrischen Nivellements (Development and Evaluation of a Rotating Laser Level and of a Photo-Electric Levelling Staff for the Automation of Geodetic Levelling). No. 41 of the Veröffentlichungen des Geodätischen Instituts der Rheinisch-Westfälischen Technischen Hochschule Aachen, Germany, 138 pages (ISSN 0515-0574)

Zeiske, K. 1999. TPS1100 Professional Series – A new Electronic Tacheometer Generation from Leica. Vermessungswesen und Raumordnung (VR), 61(2): 82-90 (in German)

Subject Index

3D imaging sensor 133

angle-angle-distance devices 8
  use of 13
automatic focussing 86
automatic levels 29
automatic pointing 87
automatic monitoring system 71
automatic power off 112
automatic searching 86

bar code levelling instruments 27
bar code levels 27
  accuracy 37
  errors 41
bar code staffs 39
  errors 40, 46
barometer 15
  digital 15
  electronic 15
batteries 29, 112

calibration
  computer assisted 31, 89
capacitive pressure sensor 17
cellular phones 112
Chesapeake CMS3000 141, 142
circles 30
  absolute 80
  incremental 79
  quasi-absolute 80
circle graduation errors 106
    interpolation errors 107
    periodic errors 106
  circle reading 81, 91

Accutape-S 6
altimeter 15, 137
  coarse measurement 92
  diametrical 81
  direction of rotation 95
  fine measurement 93
  graduation errors 106
clinometer 12
communication with computer 31, 85
compensator 30, 53, 82
compensation error 53, 103
computer interface 31
computing
  on-board 31, 84
corrections
  of instrument errors 31, 112
Criterion 8

data recording 31, 83
depth sounders 139
diametrical circle reading 81
digital barometer 15
digital levelling instruments 27
digital levels 32
  errors 41
direction measurement 113
dislevelment 100

electronic barometer 15
  heighting with 20
  performance 19
  working principles 15
electronic data recording 30
electronic distance measurement (levelling) 30

electronic level sensor 82
properties 82, 102
electronic pocket tape 5
electro-optical sensor 7
ultrasound sensor 6
electronic staff reading (levelling) 30
electronic theodolites 65
circles 79
features 78
levelling 110
use of 109, 111
electronic tacheometers 65, 66
features 78
levelling 110
motorised 68
reflectorless 76, 121
scanning 77
tracking 76
use of 109, 112
electro-optical level sensors 95
errors in levelling with digital levels 40
earth curvature 57
exercises 22, 59, 118, 144

fluxgate compass 10
focussing
automatic 86

graduation errors
circles 106
Geodimeter 600 71
Gyromat 2000 68
gyro-theodolites 67

hand-held equipment 5
high definition surveying system 133

Inductosyn 79
instrument calibration 89
instrument errors 31
interface 85
interpolation error 107
invar bar code staffs 40

Kern E2 98

ladar 77, 132, 143
laser altimeter 137
laser levels 48
calibration 54, 56
computing heights, earth curvature and refraction 57
errors of 53, 54, 55, 56
laser measurement system 143
laser profiling 137
laser scanners 132
laser theodolites 75
laser trackers 140
Leica Automatic Polar System (APS) 85
Leica invar bar code staff 40
Leica normal bar code staff 39
Leica DISTO 6
Leica DNA03 32
Leica HDS3000 133
Leica Laser Radar System LR200 143
Leica Locator 8
Leica NA2000 32
Leica NA3003 42, 44
Leica Smart310 141, 142
Leica TCA1800 72, 88
Leica TCRM 127
Leica TPS1100 96, 97
level sensor
electro-optical 95, 97, 98
levelling
electronic distance measurement 30
electronic theodolites 110
electronic tacheometers 110
errors 40
motorised 134
levelling equipment 27
automatic levels 29
barcode levels 27
digital levels 27
levelling staffs 30
lidar 77, 132, 143
line of sight 47

measurements to corners 129
measuring units 110
Mensi GS100 133
Mensi GS200 133
MetricVision MV100B 143
metrology 140, 143
mobile phones 112
motorised electronic tacheometer 68
motorised electronic video theodolites 73
motorised levelling 134

Nikon DTM-1 91, 92, 93, 94, 96, 97
Nikon DTM-720 66
Nikon DTM-750 109

on-board computing 84
one-person-survey-system 70
periodic errors 107
personal computers
communication 31, 85

phase measuring distance meters 127
phones
cellular 112
mobile 112
piezo-restistive pressure sensor 18
plumbing
buildings 118
shafts and wells 117
pointing
automatic 86
power off facility 112
power supply 29, 84
precise levelling
errors 40
pressure sensors 15
capacitive 17
piezo-resistive 18
vibration 15
profiling 137
pulse distance meters 125

radar 77, 132, 143
real-time corrections 31, 112
recording
data 83
reflectorless distance measurement 76, 121, 122
beam size and shape 123
measurements to corners 129
multiple targets 125
target material and colour 128
target orientation 128
use of 130
reflectorless electronic tacheometers 76, 121, 130
refraction 57
Riegl LMS-Z21 133
rotating laser levels 49

scale factor error 103
searching,
automatic 86
setting error 104
random component 104
systematic component 105
single beam laser trackers 140
Sokkia SDL30 29
staff 30
staff reading 30
electronic 30

tacheometers 65
electronic 65
motorised 73
scanning 77
tracking 76
Theis Telamat 51, 52
theodolites 65
digital 65
electronic 65
gyro 67
laser 75
motorised 68
video 73
Topcon AP-L1 71
Topcon DL-101C 43, 44
Topcon DL-102 28
Topcon ETL-1 90
Topcon GTS-6 110
Topcon GTS-701 66
tracking electronic tacheometers 76
two-way radios 112

ultrasound 6
ultrasound distance meter 6
umbrellas 111
use of
digital levels 40
electronic theodolites and tacheometers 109
reflectorless EDM 130

vertical axis systems 90
vertical circle compensator 82
vertical circle index error 105
vertical circle index correction 105
vibration pressure sensor 15
video theodolites 73

walkie-talkies 112
Wild NA2000 32, 33, 34, 35, 36, 42
Wild TC1600 81
Wild TM3000D 72
Wild TM3000L 74
Wild TM3000V 74

Zeiss DiNi 10 28
Zeiss Elta6 107
Zeiss ETh3 108
Zeiss Reg Elta RL 126, 129
Zeiss Ni002 135
zenith angle measurement 116

Publications from the

SCHOOL OF SURVEYING AND SPATIAL INFORMATION SYSTEMS
(formerly: SCHOOL OF GEOMATIC ENGINEERING)
THE UNIVERSITY OF NEW SOUTH WALES
ABN 57 195 873 179

To order, write or fax to:
Publications Officer, School of Surveying and Spatial Information Systems,
The University of New South Wales, UNSW SYDNEY NSW 2052, AUSTRALIA
Email: survsis@unsw.edu.au Fax: +61 - 2 - 9313 - 7493

NOTE ON MAIL ORDERS: ALL ORDERS MUST BE PREPAID.
NO REQUESTS FOR RETURNS ARE ACCEPTED.
CREDIT CARDS ARE ACCEPTED. CONDITIONS APPLY. SEE ORDER FORM FOR DETAILS.
WHEN PAYING BY *CHEQUE*, THE CHEQUES MUST BE PAYABLE TO 'SCHOOL OF SURVEYING & SIS, UNSW',
IN AUSTRALIAN DOLLARS AND DRAWN ON AN AUSTRALIAN BANK.

MONOGRAPHS

Australian prices include GST #. Overseas prices include delivery by UNSW's air-lifted mail service (~2-4 weeks to Europe and North America) #. Rates for air mail through Australia Post on application.

 # For all (local and overseas) **orders, add $11.00 for processing and handling** (once per order).

(Prices effective Oct 2010)

		Price # Australia (incl. GST)	**Price #** Overseas
M1.	R. S. Mather, "The Theory and Geodetic Use of some Common Projections", (3rd edition), 125 pp, reprint 1998, ISBN 0-85839-007-8	$ 16.50	$ 15.00
M2.	R. S. Mather, "The Analysis of the Earth's Gravity Field", 172 pp, 1971 (no ISBN)	$ 8.80	$ 8.00
M8.	A. H. W. Kearsley, "Geodetic Surveying", 96 pp, revised reprint 1988, ISBN 0-85839-036-1	$ 13.20	$ 12.00
M11.	W. F. Caspary, "Concepts of Network and Deformation Analysis", 183 pp, 3rd corrected impression, 2000, ISBN 0-85839-044-2	$ 27.50	$ 25.00
M12.	F. K. Brunner, "Atmospheric Effects on Geodetic Space Measurements", 110 pp, 1988, ISBN 0-85839-048-5	$ 17.60	$ 16.00
M13.	B. R. Harvey, "Practical Least Squares and Statistics for Surveyors", (3rd revised and extended edition), 341 pp, 2006, Reprint 2009, ISBN 0-7334-2339-6	$ 40.00	$ 36.36
M14.	E. G. Masters and J. R. Pollard (Eds.), "Land Information Management", 269 pp, 1991, ISBN 0-85839-061-2	$ 22.00	$ 20.00
M15/1	E. G. Masters and J. R. Pollard (Eds.), "Land Information Management - Geographic Information Systems - Advance Remote Sensing Vol. 1", 295 pp, 1993, ISBN 0-85939-064-7	$ 33.00	$ 30.00
M15/2	E. G. Masters and J. R. Pollard (Eds.), "Land Information Management - Geographic Information Systems - Advance Remote Sensing Vol. 2", 376 pp, 1993, ISBN 0-85839-065-5	$ 33.00	$ 30.00
M16.	A. Stolz, "An Introduction to Geodesy", 2nd extended edition, 148 pp, 2001, Reprint 2009, ISBN 0-7334-1736-1	$ 24.20	$ 22.00
M18.	J. M. Rüeger, "Electronic Surveying Instruments – A Review of Principles, Problems and Procedures", 1st ed., 166 pp, 2003, Reprint 2010 ISBN 0-7334-2083-4	$ 25.30	$ 23.00

UNISURV REPORTS - S SERIES

(Prices effective Oct 2010)

Australian Prices *:	S8 - S20	$11.00 #	S29 onwards	$33.00 #
Overseas Prices **:	S8 - S20	$10.00 #	S29 onwards	$30.00 #

* Australian prices include GST. #

** Overseas prices include delivery by UNSW's air-lifted mail service (~2-4 weeks to Europe and North America). # Rates for air mail through Australia Post on application.

 # For all (local and overseas) **orders, add $11.00 for processing and handling.**

S17. C. Rizos, "The Role of the Gravity Field in Sea Surface Topography Studies", Unisurv S17, 299 pp, 1980, ISBN 0-85839-029-9

S19. R. Coleman, "A Geodetic Basis for Recovering Ocean Dynamic Information from Satellite Altimetry", Unisurv S19, 332 pp, 1981, ISBN 0-85839-029-9

S36. A. R. Marshall, "Network Design and Optimisation in Close Range Photogrammetry", Unisurv S36, 249 pp, 1989, ISBN 0-85839-054-X

S37. W. Jaroondhampinij, "A Model of Computerised Parcel-Based Land Information System for the Department of Lands, Thailand", Unisurv S37, 281 pp, 1989, ISBN 0-85839-055-8

S39. C. Bosloper, "Multipath and GPS Short Periodic Components of the Time Variation of the Differential Dispersive Delay", Unisurv S39, 214 pp, 1990, ISBN 0-85839-057-4

S40. J. M. Nolan, "Development of a Navigational System Utilising the Global Positioning System in a Real Time, Differential Mode", Unisurv S40, 163 pp, 1990, ISBN 0-85839-058-2

S41. R. T. Macleod, "The Resolution of Mean Sea Level Anomalies along the NSW Coastline Using the Global Positioning System", Unisurv S41, 278 pp, 1990, ISBN 0-85839-060-4

S42. D. A. Kinlyside, "Densification Surveys in New South Wales - Coping with Distortions", Unisurv S42, 209 pp, 1992, ISBN 0-85839-062-0

S43. A. H. W. Kearsley (ed.), Z. Ahmad, B. R. Harvey and A. Kasenda, "Contributions to Geoid Evaluations and GPS Heighting", Unisurv S43, 209 pp, 1993, ISBN 0-85839-063-9

S44. P. Tregoning, "GPS Measurements in the Australian and Indonesian Regions (1989-1993)", Unisurv S44, 134 + xiii pp, 1996, ISBN 0-85839-068-X

S45. W.-X. Fu, "A Study of GPS and Other Navigation Systems for High Precision Navigation and Attitude Determinations", Unisurv S45, 332 pp, 1996, ISBN 085839-069-8

S46. P. Morgan et al, "A Zero Order GPS Network for the Australia Region", Unisurv S46, 187 + xii pp, 1996, ISBN 0-85839-070-1

S47. Y. Huang, "A Digital Photogrammetry System for Industrial Monitoring", Unisurv S47, 145 + xiv pp, 1997, ISBN 0-85839-072-8

S48. K. Mobbs, "Tectonic Interpretation of the Papua New Guinea Region from Repeat Satellite Measurements", Unisurv S48, 256 + xv pp, 1997, ISBN 0-85839-073-6

S50. M. D. Subari, "Low-cost GPS Systems for Intermediate Surveying and Mapping Accuracy Applications", Unisurv S50, 179 + xiii pp, 1997, ISBN 0-85839-075-2

S51. L.-S. Lin, "Real-Time Estimation of Ionospheric Delay Using GPS Measurements", Unisurv S51, 199 + xix pp, 1997, ISBN 0-7334-1664-0

S53. D. B. Lemon, "The Nature and Management of Positional Relationships within a Local Government Geographic Information System", Unisurv S53, 273 + xvi pp, 1997, ISBN 0-7334-1678-0

S54. C. Ticehurst, "Development of Models for Monitoring the Urban Environment Using Radar Remote Sensing", Unisurv S54, 282 + xix pp, 1998, ISBN 0-7334-1679-9

S55. S. S. Boey, "A Model for Establishing the Legal Traceability of GPS Measurements for Cadastral Surveying in Australia", Unisurv S55, 186 + xi pp, 1999, ISBN 0-7334-0685-X

S56. P. Morgan and M. Pearse, "A First-Order Network for New Zealand", Unisurv S56, 134 + x pp, 1999, ISBN 0-7334-0685-8

S57. P. N. Tiangco, "A Multi-Parameter Radar Approach to Stand Structure and Forest Biomass Estimation", Unisurv S57, 319 + xxii pp, 2000, ISBN 0-7334-0786-2

S58. M. A. Syafi'i, "Object–Relational Database Management Systems (ORDBMS) for Managing Marine Spatial Data: ADCP Data Case Study", Unisurv S58, 123 + ix pp, 2000, ISBN 0-7334-1704-3

S59. X.-Q. Lu, "Strategies for Improving the Determination of Displacements of Sea Surface Temperature Patterns Using Consecutive AVHRR Thermal Images", Unisurv S59, 209 + xiii pp, 2000, ISBN 0-7334-1721-3

S60. G. Dickson, "GPS-Controlled Photography: The Design, Development and Evaluation of an Operational System Utilising Long-Range Kinematic GPS", Unisurv S60, 417 + x pp, 2000, ISBN 0-7334-1725-6

S61. J. Wang, "Modelling and Quality Control for Precise GPS and GLONASS Satellite Positioning", Unisurv S61, 171 + x pp, 2001, ISBN 0-7334-1766-3

S62. Y. Wang, "Knowledge-Based Road Extraction from Aerial Images", Unisurv S62, 178 + xi pp, 2001, ISBN 0-7334-1767-1

S63. L. Ge, "Development and Testing of Augmentations of Continuously-Operating GPS Networks to Improve their Spatial and Temporal Resolution", Unisurv S63, 230 + xvi pp, 2001, ISBN 0-7334-1841-4

S64. H.-Y. Chen, "A Study on Real-Time Medium-Range Carrier-Phase-Based GPS Multiple Reference Stations", Unisurv S64, 182 + xxiv pp, 2001, ISBN 0-7334-1842-2

S65. G. Y. K. Shea, "A Web-Based Approach to the Integration of Diverse Data Sources for GIS", Unisurv S65, 233 + xv pp, 2001, ISBN 0-7334-1845-7

S66. M. Mirbagheri, "Analysis of Interferometric SAR for Topographic Mapping", Unisurv S66, 135 + xvii pp, 2001, ISBN 0-7334-1856-2

S67. P. Wang, "Applying Two-Dimensional Kalman Filtering Techniques to Digital Elevation Models for Terrain Surface Modelling", Unisurv S67, 175 + xi pp, 2001, ISBN 0-7334-1857-0

S69. C. Satirapod, "Improving the GPS Data Processing Algorithm for Precise Static Relative Positioning", Unisurv S69, 131 + viii pp, 2002, ISBN 0-7334-1901-1

S70. R. Mason, "Developing Australian Spatial Data Policies – Existing Practices and Future Strategies", Unisurv S70, 258 + xv pp, 2002, ISBN 0-7334-1941-0

S71. C. Ogaja, "A Framework in Support of Structural Monitoring by Real Time Kinematic GPS and Multisensor Data", Unisurv S71, 191 + xiii pp, 2002, ISBN 0-7334-1958-5

S72. L. Dai, "Augmentation of GPS with GLONASS and Pseudolite Signals for Carrier Phase Based Kinematic Positioning", Unisurv S72, 188 + viii pp, 2002, ISBN 0-7334-1975-5

S73. C. Roberts, "A continuous Low-Cost GPS-Based Volcano Deformation Monitoring System in Indonesia", Unisurv S73, 271 + xvi pp, 2002, ISBN 0-7334-1976-3

S74. V. Janssen, "A Mixed-Mode GPS Network Processing Approach for Volcano Deformation Monitoring", Unisurv S74, 199 + viii pp, 2003, ISBN 0-7334-2059-1

S75. Y. H. Lu, "Automatic Building Extraction for 3D Terrain Reconstruction Using Image Interpretation Techniques", Unisurv S75, 175 + xii pp, 2004, ISBN 0-7334-2141-5

S76. Y. K. Lee, "Integration of GPS/Pseudolites/INS for High Precision Kinematic Positioning and Navigation", Unisurv S76, 200 + xiv pp, 2004, ISBN 0-7334-2149-0

Note: Since 1 January 2005, the School's PhD and MEng theses are nor longer published in this series. See www.ssis.unsw.edu.au for information on post 2004 theses.

School of Surveying and Spatial Information Systems
The University of New South Wales

ABN 57 195 873 179

ORDER FORM

To order, mail or fax this form to: Publications Officer, School of Surveying and Spatial Information Systems, The University of New South Wales, UNSW SYDNEY NSW 2052, AUSTRALIA Fax: +61 - 2 - 9313 - 7493

Name and postal address of ordering person/organisation:

_____

_____

_____

_____

_____

Email : _____ Fax : _____

Day time phone number : _____ Date : _____

Note: All orders must be prepaid. No requests for returns are accepted.

I/We order herewith:

_____ $ _____

_____ $ _____

_____ $ _____

Postage and Handling (from 1 July 2004) $ **11.00**

Total $ _____

Payment Details:

☐ A cheque, drawn on an Australian Bank, in Australian Dollars and payable to 'School of Surveying & SIS, UNSW' is enclosed

☐ Please debit my credit card: ☐ Mastercard ☐ Visa

Name on Card: _____ Signature: _____

Card No: ☐☐☐☐☐☐☐☐☐☐☐☐☐☐☐☐ Expiry Date : _____